UNIVERSITÀ DEGLI STUDI DI PALERMO

Dottorato di Ricerca in Ingegneria dell'Innovazione Tecnologica
Dipartimento di Ingegneria.
ING-IND/27

STUDY OF ELECTROCHEMICAL PROCESSES FOR THE CONVERSION OF CARBON DIOXIDE TO ADDED-VALUE PRODUCTS

IL DOTTORE
Ing. FEDERICA PROIETTO

IL COORDINATORE
Prof. SALVATORE GAGLIO

IL TUTOR
Prof. Ing. ONOFRIO SCIALDONE

IL CO TUTOR
Prof. Ing. ALESSANDRO GALIA

CICLO XXXII
ANNO CONSEGUIMENTO TITOLO 2020

"La Meraviglia è il principio della conoscenza."

Wonder is the seed of knowledge and discovery.

"Life is not about waiting for the storm to pass.
It's about learning to dance in the rain!"

"La scelta di un giovane dipende dalla sua inclinazione,
ma anche dalla fortuna di incontrare un grande Maestro."

The choice of a young person depends on her inclination,
but also on the luckiness of meeting a great Teacher.
Rita Levi Montalcini

References Figures

3) Book Cover “L’abbraccio” of David Grossman

Contents

Abstract

Abstract

In this work, the electrochemical conversion of carbon dioxide to added value products, i.e. formic acid and carbon monoxide, was investigated in detail with the aim to improve the performances of the process in terms of current density, faradaic efficiency, concentration of the liquid product, in the case of formic acid, and stability with the time. In order to overcome one of the main hurdles of the CO_2 reduction in water, i.e. its low solubility at atmospheric pressure, a particular attention was devoted to the synthesis of formic acid and carbon monoxide, respectively, at Sn and Ag cathode in aqueous electrolyte using cheaper and simple undivided pressurized system.

The electrochemical conversion of CO_2 is considered one of the more appealing strategies to contribute to the reduction of CO_2 emission in atmosphere and to obtain products with higher economic value; however, its commercial implementation has been hindered until now due the technological challenges. ***Chapter 1***, in particular, is dedicated to the description of advantages and mainly challenges of the process to be suitable from the applicative standpoint. In addition, the electrochemical conversion of CO_2 in water solution as well as the key factors of the process are presented.

In the last years, increasing attention has been devoted to the CO_2 electrochemical conversion into formic acid/formate in water. In ***Chapter 2***, the current status of the formic acid industry and the current literature of the electrochemical conversion of CO_2 to formic acid are discussed. In particular, since the most interested results were achieved at tin-based cathodes, the chapter is focused on these electrode systems, taking in account the strategies to reduce the overpotentials, to limit mass transport issues and to study the stability with the time.

Among the wide range of chemical products produced by CO_2 electrochemical reduction in water solvent, the highest faradaic efficiencies and current densities are commonly reported for formate/formic acid and CO ($2e^-$ reduction products). Hence, in ***Chapter 3*** the current status of CO production is discussed as well as the main operative parameters, i.e.

electrolyte composition and electrodes configuration, that affect the electrochemical conversion of CO_2 into CO at Ag based electrodes.

One of the main hurdles of the CO_2 electrochemical conversion in water solutions is its low solubility. According to the Henry's law, the higher is the CO_2 pressure, the higher is the CO_2 bulk concentrations in water. Hence, ***Chapter 4*** is devoted to the study of the effect of the pressure on the electrochemical conversion of CO_2 for formic acid and carbon monoxide generation with particular attention at tin and silver based electrodes.

All reagents and electrodes used, electrochemical apparatuses as well as the analytics apparatuses and methods are reported and described in ***Chapter 5***.

In ***Chapter 6***, electrochemical conversion of CO_2 to formic acid is investigated using a simple and cheap Sn foil cathode in aqueous electrolyte of Na_2SO_4 and an undivided cell under pressurized conditions. In order to optimize the process, the effect of various operating parameters, including pressure, current density, mixing rate, was evaluated by both polarization and electrolyses on the performances of the process, in terms of formic acid concentration and its faradaic efficiency. The scale-up of the system was carried out as well as the development of a theoretical model based on pressurized CO_2 reduction to formic acid and its anodic oxidation, that allowed to describe and predict the effect of several operative parameters, including the effect of the electrochemical cell. Eventually, the stability of the scaled-up system using a filter-press cell with a continuous recirculation of the pressurized solution was studied for more than 40 hours.
Carbon monoxide is one of the main appealing C-derivate products of CO_2 reduction. To date, promising results on the CO_2 electrochemical conversion to CO were achieved by the utilization of Ag-based Gas Diffusion Electrode (GDE) by different research; however, due to the problems and costs of GDEs, it would be interesting to evaluate, as a possible alternative, the utilization of simpler cathodes under pressurized conditions. Hence, in ***Chapter 7,*** electrochemical conversion of CO_2 to CO was studied at simple silver electrodes with the aim to evaluate the effect of pressure (1 – 30 bar), nature of the supporting electrolyte (K_2SO_4, KCl, $KHCO_3$ and KOH) and the utilization of electrodes

with high active surface under pressurized conditions on the performances of the process using an aqueous solution and an undivided and simple cell in order to avoid the penalties given by the presence of the separator. Eventually, the stability of the CO production was studied at relatively high pressure (15 bars) using different electrolytes for 10 hours.

Furthermore, according to the literature, the utilization of GDE allows to achieve very high current densities. Hence, during a research stage at the *Chemical and Biomolecular Engineering Department*, *University of Illinois at Urbana-Champaign*, Illinois, *USA*, under the supervision of Dr. Paul J. A. Kenis, the effect of different operative parameters, including nature of the supporting electrolyte, catalyst cathode loading, electrolyte flow rate and concentration, on the performances of the CO_2 reduction to CO was investigated using an electrolyzer flow cell equipped with an Ag based gas diffusion electrode

Chapter 1

Electrochemical processes for CO_2 conversion to added-value products

1. Electrochemical processes for CO_2 conversion to added-value products

The electrochemical conversion of CO_2 is considered one of the more appealing strategies to contribute to reduce the CO_2 emission in the atmosphere and to obtain products with higher economic value. This chapter is dedicated to the description of the advantages and the mainly challenges of the process to be suitable from the applicative standpoint. In addition, the electrochemical conversion of CO_2 in water solution as well as the key factors of the process will be presented.

1.1 Electrochemical conversion of CO_2

The electrochemical conversion of CO_2 was first investigated in 1870, but its commercial implementation has been hindered until now due to the technological challenges. However, in the last few years, significant steps forward have been done and some technologies are approaching demonstration phase [1,2]. Recently, Bushuyev et al. [3] have discussed the current state of emerging technologies for the catalytic conversion of carbon dioxide into various chemical products, keeping in consideration the economics of the process. They visualized at least six potentially disruptive CO_2 catalytic conversion technologies (i.e. electrocatalysis, photocatalysis, biohybrid, nanoporous confinement, etc..), envisioning a timeline for their implementation on a large scale and getting the conclusion that the closest technologies to commercialisation with start-up and entrenched companies (i.e. Opus-12, Dioxide Material, and Carbon Recycling International) are based on CO_2 electrochemical conversion (*Figure 1.1*).

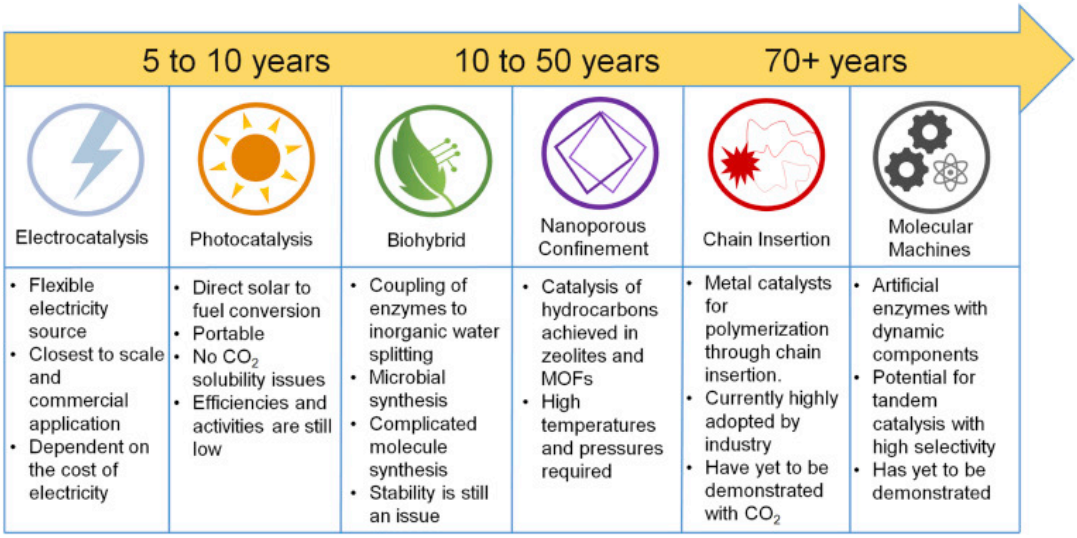

Figure 1.1 Proposed timeline of CO_2 utilization methods [3]. Reproduced from Joule, 2, O. S. Bushuyev, P. De Luna, C. T. Dinh, L. Tao, G. Saur, J. Van de Lagemaat, S. O. Kelley, E. H. Sargent, What Should We Make with CO_2 and How Can We Make It?, 825 - 832, Copyright (2018), with permission from Elsevier.

The CO_2 electrochemical conversion has engaged attention due to some unique advantages [4,5]:

- the process requires mild conditions and it is easily controllable;
- the products can be selectively controlled by changing the operative conditions of the electrolysis (such as working potential, temperature, supporting electrolyte, solvent, pH, etc…)[6,7];
- by improving and engineering the electrocatalysis, it is possible to minimize the by-products;
- the process could utilize the excess electric energy from intermittent renewable sources to transform CO_2 into carbon-based chemical, storing electric energy in the form of chemical energy [3,8,9], optimistically, without any additional electric power sources based on fossil fuels [10,11];
- recently, it has been highlighted that coupling the CO_2 reduction (i.e. cathodic process) with, for example, the purification of wastewater or the synthesis of chlorine (i.e. as suitable anodic process) can drastically improve the economics of the overall process [12,13].

Moreover, from the economic and environmental point of view, the production of fuels and/or chemicals from carbon dioxide conversion is rather appealing. This process is expected to have smaller environmental impact than the current industrial process, and, in particular, the realization on a large scale of CO and HCOOH seems more feasible than other products, such as CH_3OH, C_2H_4, CH_4, from a purely economic perspective [8,14–16].

Despite various merits of the process, the state-of-the-art systems are not able to meet yet the necessity of the large-scale industry. The electrochemical conversion of carbon dioxide can be carried out in the well-known water electrolyzes cells (or fuel cell) that are also alternative technologies for storing electric energy [17]. Indeed, there are several conceptual and technological characteristics that link together the CO_2 reduction and the water splitting process. However, the carbon dioxide molecule is difficult to convert due to the highest oxidation state of the C-atom making it very stable and inert; even if both are cathodic process with a similar reduction potential, the hydrogen evolution reaction (HER) is characterized by a simple kinetics on a various material making this process easier. Indeed, to date, the water-splitting technologies are more advanced than that the CO_2 electroconversion ones, demonstrated by the higher number of projects up to megawatt-scale based on the H_2O electrolysis than the few ones in the kilo-watt based on CO_2 reduction.

1.2 Electrochemical conversion of CO_2 in water solution

CO_2 molecules can be electrochemically introduced in the backbone of several chemicals and/or fuels thanks to multi-electrons transfer reduction. In the electrochemical conversion of CO_2, thanks to an applied cell potential, the electrons flow from the anode side, where is involved mainly the oxygen evolution reaction, or another suitable process that can add value to the overall system, through the external circuit to the cathode surface where they can combine with CO_2 molecules to yield various products, such as carbon monoxide,

methane, ethane, methanol, formic acid or formate, and/or with proton/water in acid/basic solution to form hydrogen [1].

In *Table 1.1* are reported the possible CO_2 reduction reactions at the cathode surface followed by the equilibrium electrode potentials in aqueous solution at 25°C, 1 atm, and pH = 0 [2,4,18–20].

Table 1.1 Cathodic reaction in the electrochemical conversion of CO_2 and corresponding equilibrium potential [2,4,18–20].

Eq.	Thermodynamic reduction reactions	E° / V vs SHE
1.1	$CO_2 + e^- \rightleftarrows CO_2^{-\bullet}$	-1.9
1.2	$CO_{2(g)} + 2H_2O_{(l)} + 2e^- \rightleftarrows HCOO^-_{(aq)} + OH^-$	-1.078
1.3	$CO_{2(g)} + H_2O_{(l)} + 2e^- \rightleftarrows CO_{(g)} + 2OH^-$	-0.934
1.4	$CO_{2(g)} + 3H_2O_{(l)} + 4e^- \rightleftarrows CH_2O_{(l)} + 4OH^-$	-0.898
1.5	$CO_{2(g)} + 5H_2O_{(l)} + 6e^- \rightleftarrows CH_3OH_{(l)} + 6OH^-$	-0.812
1.6	$2CO_{2(g)} + 8H_2O_{(l)} + 12e^- \rightleftarrows CH_2CH_{2(g)} + 12OH^-$	-0.764
1.7	$2CO_{2(g)} + 9H_2O_{(l)} + 12e^- \rightleftarrows CH_3CH_2OH_{(l)} + 12OH^-$	-0.744
1.8	$CO_{2(g)} + 6H_2O_{(l)} + 8e^- \rightleftarrows CH_{4(g)} + 8OH^-$	-0.659
1.9	$CO_{2(g)} + 2H_2O_{(l)} + 4e^- \rightleftarrows C_{(s)} + 4OH^-$	-0.627
1.10	$2CO_{2(g)} + 2e^- \rightleftarrows C_2O^{2-}_{4\,(aq)}$	-0.590
1.11	$2CO_{2(g)} + 2H^+ + 2e^- \rightleftarrows H_2C_2O_{4(aq)}$	-0.500
1.12	$CO_{2(g)} + 2H^+ + 2e^- \rightleftarrows HCOOH_{(l)}$	-0.250
1.13	$CO_{2(g)} + 2H^+ + 2e^- \rightleftarrows CO_{(g)} + H_2O_{(l)}$	-0.106
1.14	$2H^+ + 2e^- \rightleftarrows H_{2(g)}$	0
1.15	$CO_{2(g)} + 6H^+ + 6e^- \rightleftarrows CH_3OH_{(l)} + H_2O_{(l)}$	0.016
1.16	$2CO_{2(g)} + 12H^+ + 12e^- \rightleftarrows CH_2CH_{2(g)} + 4H_2O_{(l)}$	0.064
1.17	$2CO_{2(g)} + 12H^+ + 12e^- \rightleftarrows CH_3CH_2OH_{(l)} + 3H_2O_{(l)}$	0.084
1.18	$CO_{2(g)} + 8H^+ + 8e^- \rightleftarrows CH_{4(g)} + 2H_2O_{(l)}$	0.169
1.19	$CO_{2(g)} + 4H^+ + 4e^- \rightleftarrows C_{(s)} + 2H_2O_{(l)}$	0.210

In the wide range of chemicals reported in *Table 1.1*, the main products achieved by the CO_2 reduction are strictly linked to the nature of the electrodes; indeed, four distinct classes of metal catalyst have been recognized working in aqueous solution: (i) Pb, Hg, In, Sn, Cd, Ti metals in which the main product is formate/formic acid; (ii) Au, Ag, Zn, Pd, Ga metals

that mainly form carbon monoxide; (iii) Pt, Ni, Fe, Ti metals that mainly produce H_2; and, (iv) metals that form significant amounts of hydrocarbons such as methane and ethylene (Cu) [2,21]. This classification still remains the main known one, but nowadays there are more and more kinds of complex catalysts and materials that are under investigation.

In water solution, the electrochemical conversion of CO_2 requires high overpotential. The pathway for the CO_2 reduction is likely to involve an initial adsorption of carbon dioxide and a subsequent reduction of the absorbed CO_2 to the corresponding radical anions $CO_2^{-\bullet}$ that occurs at -1.9 V vs SHE (see *Eq. 1.1* - *Table 1.1*), highest equilibrium electrode potential. Furthermore, the equilibrium potentials of most of the reactions reported in *Table 1.1* are less negative compared to the hydrogen evolution one from water, showing that the main competitive reaction to the CO_2 reduction is the production of hydrogen, aggravated by the fact that the hydrogen evolution reaction is characterized by a simple kinetics on a various material. According to this consideration about the equilibrium electrode potential, it is clear the necessity to exploit electrodes/catalysts to decrease the activation energy of the reaction, allow or even accelerate the CO_2 conversion reaction and suppress the hydrogen evolution reaction, since the electrocatalytic effect is one of the key factors in the productivity of the CO_2 reduction process [1].

1.2.1 Key factors of the process

In terms of key factors, there are independent and dependent factors from the operating conditions.
In particular, thermodynamic potential and the electrolyser design are included in the independent agents. From the electrochemical point of view, the thermodynamic of CO_2 can be evaluated using the *Eq. 1.20* [22].

$$E^n = -\,{}^{\Delta G}/_{nF} \qquad (1.20)$$

where E^n is the Nernst potential (equilibrium potential) (V), n is the number of electrons involved per electrolysis reaction, and F is the Faraday constant (96'485 C mol^{-1}). It was shown that the free energy required to the CO_2 reduction is inversely proportional to the number of electrons involved in the reduction and the equilibrium potential decrease by increasing the number of electrons involved (*Figure 1.2*).

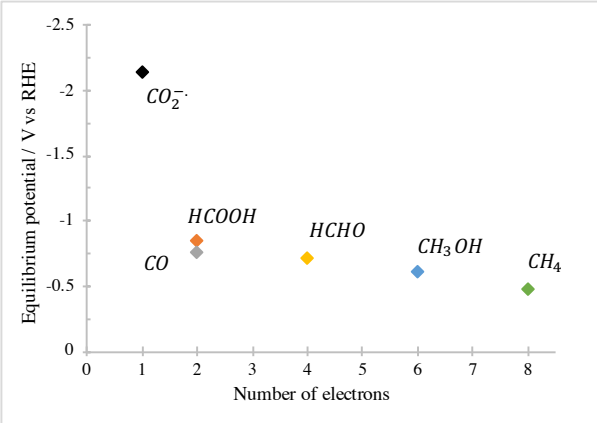

Figure 1.2 Equilibrium potential (pH = 7) vs number of electrons involved in the reduction of CO_2.

The design of the electrochemical cell can be considered one of the main factors on the large-scale industry, even if it is less important for laboratory-scale studies. There are no consolidated configurations of the cell for CO_2 reduction; in the literature, most of these are characterized by the presence of two compartment (cathodic and anodic one) divided by the presence of a separator, that is usually an ionic exchange membrane; typical design can be seen in *Figure 1.3*.

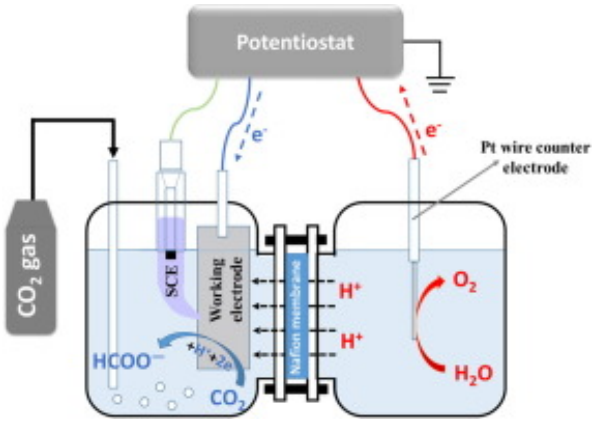

Figure 1.3 Typical divided cell design for CO_2 electrochemical conversion [23]. Reproduced from Chemical Engineering Journal, 293, C. Zhao, J. Wang, Electrochemical reduction of CO_2 to formate in aqueous solution using electro-deposited Sn catalysts, 161-170, Copyright (2016), with permission from Elsevier.

Conversely, other relevant factors depend on the operating conditions; from the electrochemical standpoint, these factors depend on the anodic and cathodic process, i.e. that includes the kinetic agents, mass transport limitation and the dissipation of energy from the Joule effect. These factors can be summarized with the overvoltage terms added to the theoretical minimum cell voltage (given by the Nernst equation), as the following equation:

$$E = E^n + \eta^{act} + \eta^{ohm} + \eta^{mt} \qquad (1.21)$$

where E is the cell voltage, E^n corresponds to the reversible potential (listed in *Table 1.2*) and η^{act}, η^{ohm} and η^{mt} are, respectively, the overpotentials associated to kinetic activation of the redox reaction, of the presence of ohmic resistances (voltage losses caused by the finite ionic conductivity of the electrolyte solution) and of the limited mass transport in the cathode and anode surface.

Table 1.2 Standard Nernst (E^n) potentials values at standard conditions and 25°C of the cell reaction [24].

Entry	Overall reaction	E^n / V
1	$H_2O \rightleftharpoons H_2 + ½O_2$	1.23
2	$CO_2 + H_2O \rightleftharpoons HCOOH + ½O_2$	1.48
3	$CO_2 \rightleftharpoons CO + ½O_2$	1.33
4	$CO_2 + 2H_2O \rightleftharpoons CH_4 + 2O_2$	1.06
5	$2CO_2 + 2H_2O \rightleftharpoons C_2H_4 + 3O_2$	1.15

To clarify this concept, Martín et al. [17] gave an imaginary current-voltage curve (see *Figure 1.4*) for the reduction of CO_2 to CO and O_2 evolution as anode process, showing the different contributions of the single factor by varying the current density. At fixed value of current density, the total overpotentials is given by the sum of the E^n and the other contributions just explained (see *Eq. 1.21*). In particular, the magnitude of the kinetic limitation, of ohmic resistances and of the mass transport phenomena become, respectively, more relevant by increasing the current density. At the higher cell potential, the current density is constant due to the pure mass transport limitations.

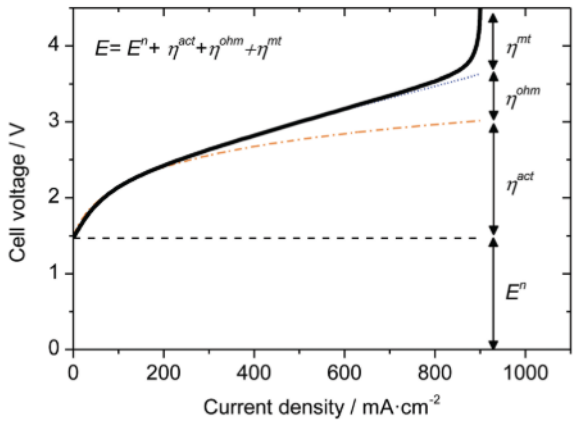

Figure 1.4 Imaginary curve of overvoltage contributions vs current density [17]. Reproduced from Green Chemistry, 17, A.J. Martín, G.O. Larrazábal, J. Pérez-Ramírez, Towards sustainable fuels and chemicals through the electrochemical reduction of CO_2: Lessons from water electrolysis, 5114-5130, Copyright (2015), with permission from Royal Society of Chemistry.

1.3 Key figures of merit of the process

The performances of the process are described by the utilization of several key figures of merit which are relevant to assist in determining the economic feasibility of the process. In order to realize a process that could be a competitive alternative to produce chemicals and/or fuels from the CO_2 electrochemical conversion, there is a necessity to improve each of the following figure of merits: i) current density, j, (i.e. a measure of the rate of the reaction); ii) faradaic efficiency, FE[1], (i.e. a measure of the faradic selectivity towards the target product); iii) energy efficiency, EE[2], (i.e. a measure of the overall energy utilization toward the desired product); iv) the stability of the catalyst and, more in general, of the process; and v) the overall costs, including material consumption costs, capital cost and electricity cost.

1.4 Challenges of the process

The electrochemical conversion of CO_2 remains a challenging process because of the:

- high cost for CO_2 capture and separation;
- high energy consumption during the process, depending on the target products and mainly affected by high overpotentials; several studies have shown that the only reducible species is the CO_2, and no other equilibrium, derivates or its associated form, thus confirming that high overpotentials (higher than 1 V) are necessary for the formation of the anion radical CO_2^- (which occurs at -1.9V vs SHE, see *Eq. 1.1*), which usually leads to relatively low EE [1,2];
- high catalytic cost and low catalyst stability; for example, during the process, some

[1] The faradaic efficiency of the products is evaluated based on the followed equation: $FE = \frac{z\,F\,n}{Q}$ where z in the number of electrons exchanged, F faraday constant, n mole number of product and Q total charge passed.

[2] In the electrochemical process, the energy efficiency is given by the following equation: $EE = \frac{E^n}{E^n + \eta} * FE$ where E^n is the standard potential (*Table 1.2*) and η is the overpotential.

phenomena may reduce the area of the electrodes, limiting a further catalysis process and/or speeding up the cathodic degradation. It was shown that the main actors in this field is the deposition of inert intermediates or poisonous by-product (leads to the degradation and/or inactivation of the reaction sites) and the generation of gas bubbles on the surface, mostly, due to the hydrogen evolution reaction [2,25];

- low solubility of CO_2 at both ambient pressure and temperature in aqueous electrolyte (ca. 0.033 M), resulting in low CO_2 conversion rate (limited by mass-transport limitations) and in low productivity or/and low energetic efficiencies;
- low selectivity or high selectivity linked to a low productivity;
- the small market for some products which could not be attractive to investors;
- small industrial participation;
- it is difficult to predict the performances of the specific electrocatalysis due to the absence of consolidate fundamental theories and optimized experimental set-up. Furthermore, electrochemical systems and operative condition are really varied which makes difficult the evaluation and comparison of different experimental cases.

In order to be economically suitable for the scale up the CO_2 electrochemical conversion process must allow to reach, at least, moderate energetic efficiency (typically of about 55-75%), high selectivity towards to the target product with quite high current density (close to 500-1100 mA cm^{-2}), and good stability with the time; performances should be close to the commercial water electrolyser ones [9,26–29].

Furthermore, several researchers point out that, among the wide CO_2 electrochemical products previously listed, the electrochemical production of formic acid and carbon monoxide from CO_2 is straightforward, environmental friendly and cheaper than their current production process [9,19,30,31]. For example, it was shown that the electrochemical cost for CO and HCOOH production (of about 300 and 200 $/ton for CO and HCOOH, respectively) is lower than the traditional manufactories price (of about 900

and 1100 $/ton for CO and HCOOH, respectively), while the electrochemical cost for other light hydrocarbons can be 20 times higher than the current market price (i.e. of about 4250 vs 200 $/ton for CH_4, 1000 vs 400 $/ton for CH_3OH, 3500 vs 500 $/ton for ethylene) [9,32].

Hence, in the following chapters, a particular attention will be devoted on the studies of the electrochemical conversion of CO_2 to formic acid and carbon monoxide in aqueous electrolyte (***Chapters 2-4***).

Chapter 2
Synthesis of formic acid

2. Synthesis of formic acid

In the last years, increasing attention has been devoted to the CO_2 electrochemical conversion into formic acid/formate in water. In this chapter, the current status of the formic acid industry and the current literature of the electrochemical conversion of CO_2 to formic acid will be presented. In particular, since the most interested results were achieved at tin-based cathodes, the chapter is focused on these electrode systems.

2.1 Current status of formic acid industry

Formic acid is the simplest carboxylic acid, containing a single carbon. It is low flammable, rapidly biodegradable, and extremely stable liquid under ambient conditions ($pK_a = 3.74$), thus, its handling, transportation and storage are quite feasible under common infrastructure conditions [19].

HCOOH is commercialized in water solution at 85%wt. and, currently, its global demand is about 0.95 10^6 ton/year. The global formic acid market is projected to exhibit a CARG (*Compound Annual Growth Rate*) of about 4.5% from 2019 to 2024, due to the growing demands, mainly, in the agriculture field. As the smallest, most dense and most powerful carboxylic acid thanks to its unique chemical and physical properties, formic acid is characterized by wide usage field. HCOOH is a prominent intermediary in the pharmaceutical and chemical industry; in particular, it is mainly used in industrial feed as antibacterial agent (promoted by the banning in the utilization of antibiotics), in the cotton and food disinfection, in the natural rubber production, and in the formation of acid baths for the dyeing processes of fibers and leathers [8,19,33]. Moreover, HCOOH is the unique EU-certified chemicals that has been received the triple European permission to be used for both human and animal food (as preservatives, silage additives and hygiene condition enhancers). Additionally, it has been proven that formate treatment for slippery roads is more effective and environmentally friendly than traditional salts treatments (already demonstrated in countries such as Switzerland and Austria).

Among the many encourage factors, the price of HCOOH (1300 $/ton with an estimation of an annual increase of about 2% [33]) was much higher than other chemicals (i.e. CH_3OH: 400 $/ton) and it is also considered a carrier for storage and transport of H_2 for industrial application, for addition to the natural gas pipeline network and in fuel cells. Indeed, formic acid is characterized by a hydrogen content of about 4.4% wt, corresponding to 100 MPa of compressed H_2; i.e., at standard temperature and pressure, HCOOH stores 580 times more H_2 than the same volume of hydrogen gas [34]. Furthermore, as a H_2 storage medium, HCOOH could be used in chemical reaction, as example, in the hydrogenation of olefins or glycerol or in the conversion of hemicellulose sugar without the necessity to be converted in molecular H_2 [35,36]. However, its application as fuel is limited by its lower energy density than the other CO_2 derived products (i.e. 2.1 kWh L^{-1} vs 43.3 kWh L^{-1} of HCOOH and CH_3OH, respectively) [19,37,38].

Furthermore, in spite of the wide application fields of the formic acid, its real utilization is currently limited by the high cost for its production for large usage as fuel or chemical. To date, methylformate hydrolysis, hydrocarbon oxidation, formide hydrolysis and alkali formates acidolysis are the traditional ways for the synthesis of HCOOH; these commercial routes are neither straightforward nor environment friendly [39]. In addition, these conventional process suffer of slow reaction rate, undesirable by-products, high cost of investment, and of the high energy requirements (in the separation stage) as well as a discernible dependence on fossil fuel [40].

In this framework, the electrochemical conversion of CO_2 could be a simple and straightforward alternative with a smaller environmental impact than the current production processes. The engineering and economic feasibility of large-scale electrochemical reduction of carbon dioxide to formate salts and formic acid at tin cathodes was evaluated by many authors [8,24,41] that concluded that this process could be operationally profitable due to the great business value of the formic acid.
As an example, the OCO company, established in 2016 by the incorporation of the Det Norske Veritas GL with the Brix-Berg LLC, recognizes a high applicative potential in the production of formic acid by CO_2 electrocatalytic conversion (EF ~ 78%) with the aim to

reduce the cost of the HCOOH production to less than 200 $/ton in 10 years, using just CO_2, water and renewable energy. Furthermore, they point out that the production of formic acid from CO_2 can reduces also the CO_2 emission of the manufacturing plant, so it become more profitable for companies to capture and reuse, rather than emit, CO_2.

2.2 CO_2 electrochemical conversion to formic acid

The literature on the CO_2 electrochemical conversion is very extensive but the topic still attracts much interest. In the last years, a particular attention was devoted to the CO_2 reduction process with the aim to investigate several operative parameters on the HCOOH production in order to reach simultaneously i) high faradaic selectivity towards formic acid (high EF), ii) high CO_2 reduction rate (high *j*), iii) elevate concentration of HCOOH in water solution (avoiding the costs of subsequent steps of separation and concentration of it), and iv) good stability with the time. In detail, different strategy has been studied for this purpose, as discussed in the following sections.

Table 2.1 (see *p. 40*) shows the main results currently present in literature about the electrochemical conversion of CO_2 to formic acid under several operative conditions. From the electrochemical point of view, it is well-know that the selectivity towards formic acid depends strongly on the nature of the electrode and on the adopted operative condition, such as applied potential, electrolyte, pH value, mixing rate, temperature and pressure. In aqueous electrolyte, under proper conditions, formic acid can be formed in neutral or acidic solution (*Eq. 2.1*), whereas formate ions are the main products in weak alkaline medium (*Eq. 2.2*).

$$CO_2 + 2H^+ + 2e^- \rightleftarrows HCOOH \quad (2.1)$$

$$CO_2 + H_2O + 2e^- \rightleftarrows HCOO^- + OH^- \quad (2.2)$$

Among the first data, the formation of HCOOH was showed in 1994 by Hori and coworkers [42] at In, Cd, Tl, Hg, Pb and Sn electrodes using a 0.1 M $KHCO_3$ saturated CO_2 aqueous electrolyte at 5 mA cm^{-2}. They demonstrated the possibility to produce formic acid using numerous non-precious flat electrodes. Among these electrodes, Pb and Sn have aroused more interest from the researcher's community due to their higher selectivity towards the formic acid generation under several operative conditions (*Table 2.1, entries 1-8*) [42–45]. More recently, from the kinetic standpoint, Feaster and colleagues [46] have studied the CO_2 electrochemical conversion to formate on various polycrystalline cathodes, i.e. Sn, Zn, Cu, Ag, Ni, by confuting experiments with theoretical investigation to understand the reaction mechanism and key intermediates for formate production. According to their work, Sn cathode is highly selective towards formic acid than the other ones, because, according to their volcano plot, Sn appears near the top showing its optimal binging energy for the key intermediate (*OCHO-) to produce formate, highlighting a good adsorption and easy desorption of the intermediates on the surface [2,46]. Furthermore, the utilization of these electrodes (i.e. Sn, Zn, Cu, Ag, Ni) in large scale for formate production was evaluated by many authors that concluded that only for the Sn based catalyst there is an interesting engineering and economic feasibility, thanks its good selectivity to HCOOH, catalytic power, low-cost, non-noble and eco-friendly characteristics [8,24,42,47].
However, as better described in ***Chapter 1***, the electrochemical conversion of CO_2 in aqueous solution is likely to be limited largely by the high overpotentials (favors the hydrogen evolution), the low solubility of CO_2 in water solution and the insufficient long-term analysis of the process.

2.3 Electrochemical conversion at tin-based electrodes

2.3.1 High cell potentials

The electrochemical conversion of CO_2 to formate/formic acid occurs at relatively high negative potentials to achieve high values of FE_{HCOOH}; it was shown that the optimum

potential for the HCOOH generation at Sn plate cathode is close to -1.8 V vs SCE [8,34,48], due to the high overpotentials needed for the formation of the $CO_2^{-\bullet}$ (*Table 1.1, Eq. 1.1*), usually linked at high cell potentials, reducing the energy efficiency of the process. Furthermore, at these negative potential values, the hydrogen generation reaction take place unavoidably at Sn electrode, thus reducing the selectivity of the process. To be suitable in the applicative standpoint, many researchers had focused their work on the engineering and implementation of new system and electrocatalysts to reduce the overpotentials.

In particular, engineering of the electrolyte, in terms of supporting electrolyte nature and/or its concentration, could be an interesting way to increase the overall energy efficiency (key factor to evaluate the economic viability of a process), reducing the required overpotentials to drive the process.

In an attempt to decrease the overall cell voltage, the minimization of the inter-electrodic gap between anode and cathode, the removal of the separator among them and the incrementation on the electrolyte conductivity can reduce the drop voltage due to the solution, $\Delta\emptyset_{solution}$, *Eq. 2.3* [10,49,50]:

$$\Delta\emptyset_{solution} = \Delta\emptyset_{ohmic} + \Delta\emptyset_{diffusion} = f(x, \kappa^{-1}) + f\ (D_i, c_i, \kappa^{-1}) \qquad (2.3)$$

where x is the position, κ the electrolyte conductivity, D_i the diffusion coefficient, c_i the concentration of the i-th species. Several studies have shown that an increase of the concentration of the supporting electrolyte allows to enhance the electrolyte conductivity, thus reducing remarkably the cell potential. For instance, Kopljar et al. [50] highlighted how the electrolyte concentration can significantly improve the EE of the CO_2 reduction at Sn electrode; indeed, an enhancement of the concentration gave rise to a reduction of the cell voltage of about 2 V (from 5 to 3 V at 0.1 and 1 M $KHCO_3$, respectively), due to the larger conductivity (9.7 vs 75 mS cm^{-1} for 0.1 vs 1M $KHCO_3$, respectively). In addition, they showed that the nature of the supporting electrolyte does not affect the selectivity of the process (FE_{HCOOH} ~ 80%), but has a strong effect on the energy efficiency of the process (EE: 14 vs 26% using 1 M $KHCO_3$ and KOH, respectively) due to the reduction of the cell potential (of about 3.5 vs 2.5V for 1 M $KHCO_3$ and KOH respectively) (*Table 2.1, entries*

9 and 10). Furthermore, Wu and coworker [51] have investigated the effect of the electrolyte on the performances of the CO_2 electrochemical reduction to formate at Sn foil cathode by using different supporting electrolyte, i.e. $KHCO_3$, K_2SO_4, KCl, Na_2SO_4, Cs_2SO_4, $NaHCO_3$, $CsHCO_3$ in undivided cell. They have shown that sulfate-based electrolytes were characterized by higher conductivity than the bicarbonate ones (respectively, 30.8 vs 62.5 mS/cm for 0.5 M $NaHCO_3$ vs Na_2SO_4 and 39.6 vs 80.7 mS/cm for 0.5 M $KHCO_3$ vs K_2SO_4) and, even if the enhancement of concentration for both kind of electrolyte determined an increase of the conductivity (reducing the cell potential) and of the formate production rate, there was a no or a negative effect on the FE_{HCOOH} with the electrolyte concentration (*Figure 2.2*). The lowest production rates and faradaic efficiencies for formate were observed with Cs based electrolyte (*Figure 2.2*).

More in general, considering the faradaic efficiency of HCOOH along with energy efficiency, the utilization of Na^+ and SO_4^{2-} as supporting electrolyte would be more favorable than the others ones; while HCO_3^- and K^+ favor a higher formate production rate; indeed, FE_{HCOOH} as high as ~90% using 0.5 M Na_2SO_4 at a -1.7 V vs SCE was reported (*Table 2.1, entry 11*), while formate production rate of formate over 3 μmol min^{-1} cm^{-2} at a potential of -2.0 V vs SCE maintaining a FE of about 63% was reached using 0.5 M $KHCO_3$ saturated CO_2 aqueous solution after 1 h. (*Table 2.1, entry 12*).

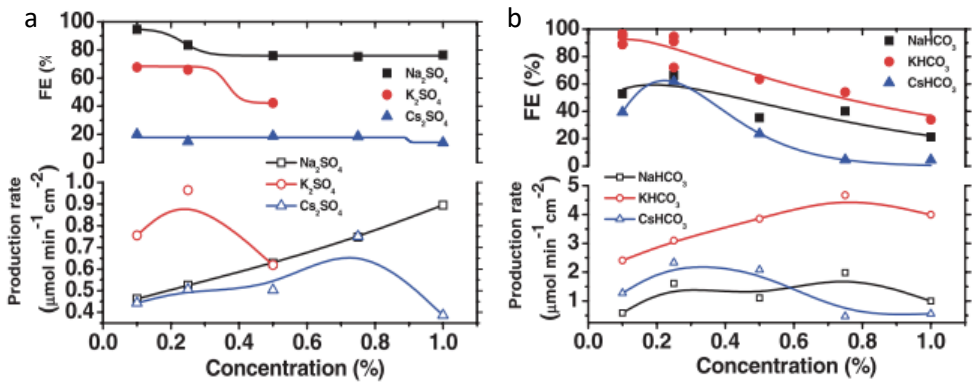

Figure 2.2. Faradaic efficiency and formate production rate vs concentration of different electrolyte at -2 V vs. SCE: (a) Na_2SO_4, K_2SO_4, Cs_2SO_4; (b) $NaHCO_3$, $KHCO_3$, $CsHCO_3$ [51]. Reproduced from Journal of the Electrochemical Society, 159, J. Wu, F.G. Risalvato, F. Ke, P.J. Pellechia, X. Zhou, Electrochemical Reduction of Carbon Dioxide I. Effects of the Electrolyte on the Selectivity and Activity with Sn Electrode, 353 – 359, Copyright (2012), with the permission from IOP Publishing, Ldt.

From the electrochemical design point of view, the utilization of the membrane is to transport the majority charge carriers (carbonate and bicarbonate ions) and avoid the crossover of the CO_2 reduction products. In the effort to reduce the cell voltage drop, Singh et al. [10] have focused their attention on the presence of the separator showing that its absence allows reducing the polarization losses. In addition, they demonstrated that the utilization of a cation exchange membrane (CEM) causes higher polarization losses compared to those for an anion exchange membrane or the absence of a membrane; indeed, using a CEM the anions (i.e. majority charge carriers) will be stucked and cations will be forced to move towards cathode causing electrodialysis and extremely high polarization losses. Unluckily, most work on CO_2 electrochemical conversion is carried out by using a Nafion membrane (a proton exchange membrane) (see *Table 2.1; Set-up column*).

Eventually, most studies have shown that the overall efficiency of the electrochemical conversion of carbon dioxide is limited by the overpotentials for the catalysts needed to favor the main reactions: CO_2 reduction and O_2 evolution. In literature, it was discussed extensively the effect of catalyst, including single metals, alloys, oxides, sulfides, and their hybrids with carbon nanomaterials or metal oxide, on the overpotentials for CO_2 reduction. It was widely reported that the utilization of tin oxide based electrode (SnO_x) can reduce CO_2 to HCOOH with higher FE and moderate reduction rate at relatively low overpotentials (*Table 2.1, entries 13,14,16-19*). Indeed, several authors [4,52–60] have shown that SnO_x takes part in the CO_2 reduction pathway by supplying chemical functionality that stabilizes the incipient negative charge on CO_2 or by mediating the electron transfer directly, thus reducing the overpotentials required to drive the reaction. For instance, Daiyan and coworker [53] engineered SnO_x/Sn interface cathode that exhibited a low onset potential for HCOOH production (-0.59 V vs NHE), which it is among the lowest of Sn based catalyst; it was recorded a FE close to 77% with a stable current density of 4.8 mA cm^{-2} at -1.09 V vs RHE using a $KHCO_3$ CO_2-saturated aqueous solution (*Table 2.1, entry 13*). Recently, Rasul et al. [54] showed that the utilization of tin oxide allows to increase the FE_{HCOOH} more than two time at low potentials (FE_{HCOOH} of about 18 vs 45% for Sn vs SnO_x, respectively, at -0.8 V vs RHE) than at relatively high

potentials (FE_{HCOOH} of about 70 vs 80% for Sn vs SnO_x, respectively, at -1.2 V vs RHE) using CO_2 saturated 0.1 M $KHCO_3$ electrolyte (*Table 2.1, entries 14 and 15*).
In addition, few authors have proposed that doping the SnO_x electrode can help to improve the performances of the electrocatalysis and results in lower overpotentials for CO_2 electrochemical conversion than the undoped SnO_x [2,4,54,61,62]. For example, Hu and colleagues [61] found that the utilization of Cu and S co-doped SnO_2 material showed higher electrocatalytic activity than that undoped one characterized by overpotentials as low as 130 mV, increasing 7 times more the current density up to 5.5 mA cm^{-2} at -1.2 V vs Ag/AgCl (*Table 2.1, entry 19*).
However, to date, the stability of any oxide phase electrode under operando condition is still an issue to be tackled, aggravated to the low reduction rate associated with electrocatalysis on oxide layer (low *j*) [59,63]; Dutta and coworkers [63] found that , for relatively high negative potentials, the oxide layer is reduced to metallic Sn leading to significant degradation in efficiency of the CO_2 reduction process to formate.

To lower the overpotentials by maintaining good selectivity, researchers have focused on the development of new alloys of Sn electrode, such as Au-Sn nanoparticles [64] (*Table 2.1, entry 20*), activated carbon (AC)-supported Pd–Sn alloy NP electrocatalyst with varied Pd/Sn composition, Zn-Sn [65,66], In-Sn [66,67] (*Table 2.1, entry 21*) or in the implementation of different metallic electrode, such us Pd [68], Ru-Pd, Pd-Pt [69], that allow to reach high FE for HCOOH working at potential lower than the Sn catalyst up to 0.5V.

Despite these good results, the fabrication of tin oxide electrodes or/and hybrid/alloy catalysts (time-consuming preparation process), their low reduction rate and the utilization of expensive catalyst (i.e. Pd-electrode) limits their development for the large-scale application.

2.3.2 Mass transport limitation

As previously mentioned, to be suitable from the applicative standpoint, the CO_2 electrolyser cell should reach high current densities (ca. 100 - 500 mA cm^{-2}) like the ones used with the water electrolyser [17]. However, in aqueous electrolyte, the main hurdle of the electrochemical conversion of carbon dioxide is its low solubility (ca 33 mM) and relatively low diffusivity (ca 1.94 10^{-9} m^2 s^{-1}), resulting in a low CO_2 reduction rate (limited by the mass transfer), low faradaic efficiency and/or low productivity. Under the standard condition of pressure and temperature, the limiting current density[3] (j_{lim}) of the CO_2 electrochemical conversion does not exceed 30 mA cm^{-2} on flat electrode [17,70,71]; at higher j than the j_{lim}, CO_2 transfer to the active sites becomes rate-determining and the main process usually converts to the hydrogen evolution.
In order to overcome this issue and improve CO_2 transfer, many researchers have devoted their attention to the engineering and implementation of a new catalysts and/or new configuration systems. In this frame, main studies have been focused on the utilization of *i)* high surface electrode, *ii)* the well-known gas diffusion electrodes[4] (GDEs), and *iii)* pressurized CO_2 (which is discussed in detail in ***Chapter 4***).

Several authors have shown that the implementation of high surface electrode, such us Sn dendrite (*Table 2.1, entry 22*) [72,73], Sn rod (*entry 23*) [73], Sn rectangular sheet rod, Sn foam (*entry 24*) [66], porous Sn-film (*entry 25*) [74], nanoporous Sn/SnO_x (*entry 26*) [75], can allow to reach higher CO_2 reduction rate by maintaining a good selectivity of formic acid due to the numerous active sites than the polycrystalline cathode. For example, Won et al. [72] have shown that, in the high overpotentials region, the utilization of a Sn dendrite

[3] The limiting current density is defined as followed: $j_{lim} = z * F * \frac{D}{\delta} * c^b_{CO_2}$
where z is the number of the electron involved in the carbon dioxide reduction, F faraday constant (96485 C mol^{-1}), D Diffusive coefficient, δstagnat layer, $c^b_{CO_2}$ is the bulk carbon dioxide concentration.

[4] The gas diffusion electrodes are porous electrodes characterized by a carbon matrix wherein the catalyst is dispersed. Carbon dioxide can be fed in the gas phase from one side while the electrolyte penetrates into the pore network from the other. Consequently, the triple-phase boundary between gas, electrolyte and catalyst where reaction takes place forms in the interior of the electrode enhancing the electroactive area.

electrodes (synthesized by electrodeposition) determines current densities at least six times higher than the ones achieved from the Sn foil (i.e. 2 vs 12 $mAcm^{-2}$ for Sn foil vs Sn dendrite, respectively, using 0.1M $KHCO_3$ aqueous electrolyte at -1V vs RHE), thus showing that the enlarged surface area and high porosity of the dendrite electrode affects the performances of the process, improving the reduction rate. From the kinetic standpoint, they concluded that high surface electrode facilities the electrochemical reduction of CO_2 owing to the electrodeposition which reduce the charge transfer resistance (R_{CT}) (~ 390 vs 82 Ω for the Sn foil and Sn dendrite, respectively). In addition, in terms of CO_2 reduction products, the higher surface area allowed to increase the FE_{HCOOH} from of about 25 to 40% by changing from Sn foil to Sn dendrite at -1.06 V vs RHE after 1 h using CO_2-saturated aqueous solution of 0.1 M $KHCO_3$. Promising results using high area electrode were showed also from Kelsall and his group [76] that developing a tinned graphite felt cathode for scale up increase the CO_2 reduction rate up to 100 mA cm^{-2} with FE_{HCOOH} of about 60% for 10 min, in order to minimize as more as possible the electrode deactivation (*Table 2.1, entry 27*).

Another strategy to reduce the mass transfer limitations due to the low CO_2 solubility in water based electrolyte and increase the total current density for CO_2 reduction is the utilization of the GDEs, which allows to enhance the three phase boundary area where the reaction takes place [30,31,77–81]. As an example, Del Castillo et al. [78] have achieved a 70% of FE and formate concentration of about 54 mM at 150 mA cm^{-2} by CO_2 electro-reduction in a divided filter-press type cell equipped with Sn-GDE (*Table 2.1, entry 28*). They were able to reach higher *j* (200 mA cm^{-2}) coupled with quite high concentration of HCOOH of about 0.35 M, but resulting in losses of selectivity of the process (FE_{HCOOH} ~ 43) (*Table 2.1, entry 29*). In addition, the same researcher group [79] have demonstrated that the metal loading and particle size plays a relevant role on the performances of the CO_2 reduction: indeed, smaller Sn nanoparticles achieved high FE for formate production overcoming the mass transfer limitation of CO_2 onto the surface (*Table 2.1, entry 30*).
More recently, data recorded by Kopljar [30,50] and Sen [59] and their coworkers have shown that the implementation of Sn or SnO_2 nanoparticles catalyst deposited on gas

diffusion layer can allow to reach *j* and FE_{HCOOH} up to 200 mA cm^{-2} and 70%, respectively (*Table 2.1, entries 31 and 32*).

More in general, several works have focused their attention on the implementation of GDEs obtained from different preparation procedures that allows to increase the CO_2 reduction rate, the faradaic selectivity as well as the concentration of formic acid; in *Table 2.1 entries 9,10,30-37* relevant results achieved by different authors were highlighted [8,70,82–84].

However, even if the implementation of GDEs gave promising results in terms of CO_2 conversion rate, selectivity towards to the target products and productivity, more in general, their application is still likely to be limited by: i) loss of the catalyst possibly due to the low adhesion of the Nafion solution as a binder of the catalyst to the support; ii) low stability with the time; iii) high overall costs; iv) time consuming preparation procedure less suitable for the large scale application; and, vi) salt deposition on the gas diffusion layer determining blocking of CO_2 access in the GDE. Furthermore, a crucial factor, using a GDE-type cell, is the pressure balance between the gas and liquid compartments in order to avoid that the gas can go through the gas diffusion layer, not allowing the essential three-phases contact (among the solid catalyst, liquid electrolyte and gas reagent), or flooding of the gas compartment due to the electrolyte [80,85].

2.3.3 Long term analysis

For practical applications, one of the main bottlenecks in the development of the CO_2 electrochemical conversion is the stability and the long term analysis, that combined with all the previous issues above discussed, make the scale up of process really challenging. It was highlighted that the performances of the process strongly depend on the time passed; various authors have shown that the FE of the process decreased with the time [24,34,51,81,86].

As you can appreciate in *Table 2.1*, there are just few examples of electrolyses that were carried out for more than 10 h; most studies were performed for less than 2 h.

Among the first authors focused on stability, Wu and coworker [51] have evaluated the stability of the CO_2 electrochemical reduction at Sn foil cathode using Na_2SO_4 or $KHCO_3$ saturated CO_2 electrolyte for 48 h (*Figure 2.3 -Table 2.1, entries 11 and 12*). For both electrolytes, they showed a fast degradation in the first 10 h of the process; indeed, it was shown a reduction of the FE_{HCOOH} higher than 40 and 70% within 9 and 48 h, respectively, at relatively high potentials (i.e. -1.7 and -2 V vs SCE for Na_2SO_4 and $KHCO_3$, respectively), mainly due to the deposition of metal ions (Zn) onto the surface of the electrodes, inhibiting the CO_2 reduction into formate. This degradation phenomena was also observed, for example, by Hori [87] and Anawati [48] confirming that the metallic impurities play a relevant role in the deactivation of the electrodes (i.e. due to Fe^{2+} or Zn^{2+} present in the electrolyte at Cu cathode [87] or the surface penetration by alkali metal at Sn electrode [48]).

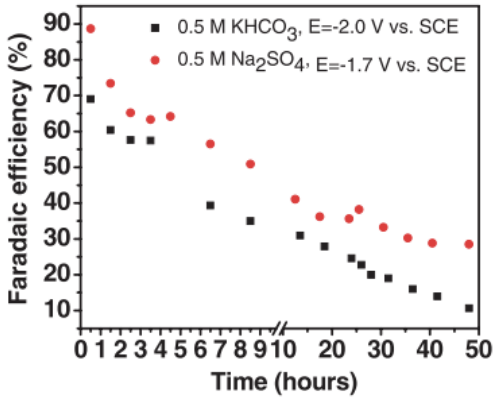

Figure 2.3 Effect of the time on CO_2 reduction using Na_2SO_4 and $KHCO_3$ saturated aqueous solution [51]. Reproduced from Journal of the Electrochemical Society, 159, J. Wu, F.G. Risalvato, F. Ke, P.J. Pellechia, X. Zhou, Electrochemical Reduction of Carbon Dioxide I. Effects of the Electrolyte on the Selectivity and Activity with Sn Electrode, 353 – 359, Copyright (2012), with the permission from IOP Publishing, Ldt.

More recently, long term electrolyses were performed from Fu and colleagues [81] (*Figure 2.4 - Table 2.1, entry 38*) at SnO_2 cathode using a H-type cell for 28 h. They showed a rapid reduction of the formic acid generation already within the first 5 h of the CO_2

electrochemical conversion and imputed this phenomenon due to the deposition of the fluoride ions on the surface of the electrode can be the cause of the reduction of the selectivity of the process hindered the reduction of CO_2 to formate on the surface.

These studies aforementioned show that the stability of the CO_2 reduction process to formic acid is strictly linked to the impurities present in the electrolyte solution; however, the impurities could not be the only actors and alone to explain the degradation of the electrode performance. Indeed, several authors have shown that another cause of the reduction in performances of the process is due to the pulverization of the catalyst. For example, electrolyses were performed over long term operation (60 h) with a high purity electrolyte (0.1 M $KHCO_3$) (*Table 2.1, entry 39*) by Wu et al. [86]; under adopted condition, it was recorded a fast reduction of the selectivity towards formate within the first 10 h (*Figure 2.5a*) by maintaining a constant CO_2 reduction rate of about 17 mA cm^{-2} (*Figure 2.5b*). These authors have attributed the loss of the selectivity to a hydrogen diffusion into the bulk of the electrode solid surface, inducing stress and fractures of the Sn cathode.

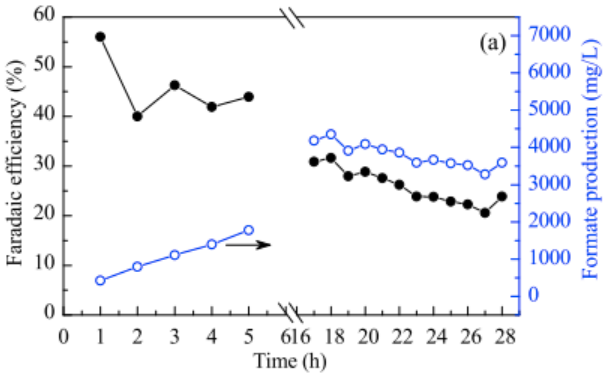

Figure 2.4 Stability electrolyses performed at SnO_x cathode for 48h: faradaic efficiency (●) and formate production (○) [81]. Reproduced from Chinese Journal of Catalysis, 159, Y. Fu, Y. Li, X. Zhang, Y. Liu, X. Zhou, J. Qiao, Electrochemical CO_2 reduction to formic acid on crystalline SnO_2 nanosphere catalyst with high selectivity and stability, 1081 - 1088, Copyright (2016), with the permission from Elsevier.

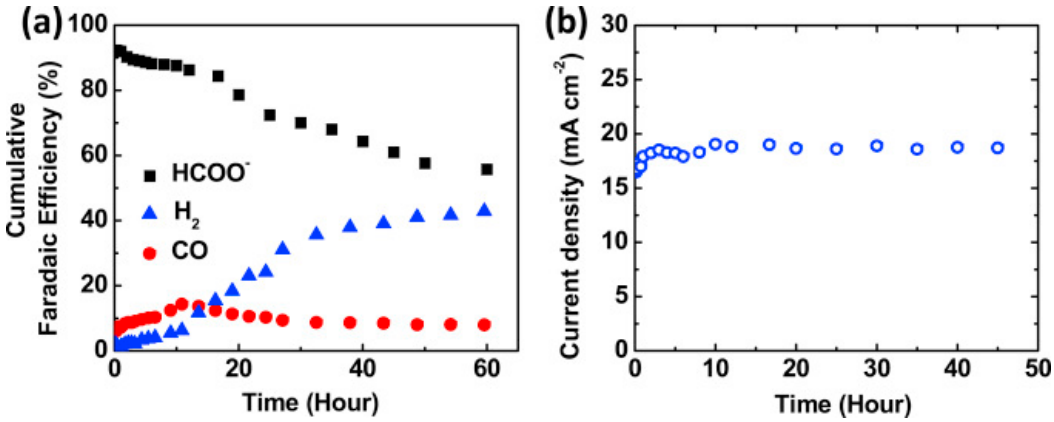

Figure 2.5 (a) Cumulative faradaic efficiencies and (b) current density vs. time of electrolysis performed with high purity 0.1 M $KHCO_3$ at -2V cell potential [86]. Reproduced from Nano Energy, 159, J. Wu, S.G. Sun, X.D. Zhou, Origin of the performance degradation and implementation of stable tin electrodes for the conversion of CO_2 to fuels, 225 - 229, Copyright (2016), with the permission from Elsevier.

Moreover, the reason of the decay of the performances of the CO_2 reduction with the time can be also due to the accumulation of a product of the CO_2 reduction in the electrolyte causing a remarkable decrease in the selectivity; for undivided cell, the main issue is the anodic oxidation of formic acid produced at cathode surface. Lv [7] recorded a reduction of about 60% on the selectivity for formate production in 40 h (*Figure 2.6 – Table 2.1, entry 40*); they assumed that the main reason for efficiency decreasing with the time for undivided cell was the oxidation of formate; the higher is the formate concentration in the electrolyte, the higher is the formate oxidation rate. This phenomenon was also recently highlighted by Scialdone et al. [34]; *Figure 2.7* reports the formation of formic acid and the relative FE achieved at Sn cathode at 11.6 mA cm^{-2} in divided and undivided cells, respectively; from the comparison of the performances, a strong decrease of FE with the time was observed in electrolyses carried out in the undivided cell than that divided one, because of the acceleration of the anodic oxidation of formic acid.

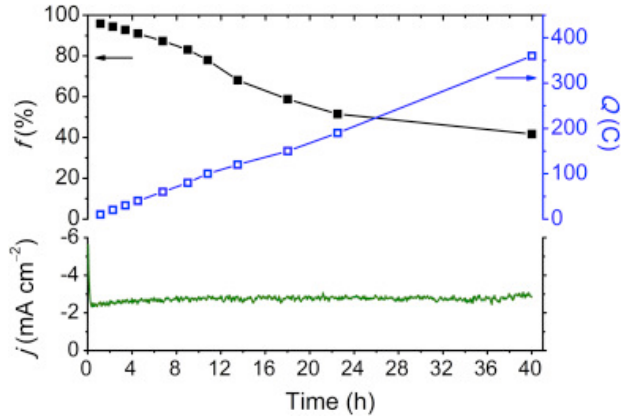

Figure 2.6 Stability of the CO_2 reduction at Sn cathode using undivided cell at -1.8 V vs Ag/AgCl in 0.1M $KHCO_3$ electrolyte [7]. Reproduced from Journal of Power Sources, 253, W. Lv, R. Zhang, P. Gao, L. Lei, Studies on the faradaic efficiency for electrochemical reduction of carbon dioxide to formate on tin electrode, 276 - 281, Copyright (2014), with permission from Elsevier.

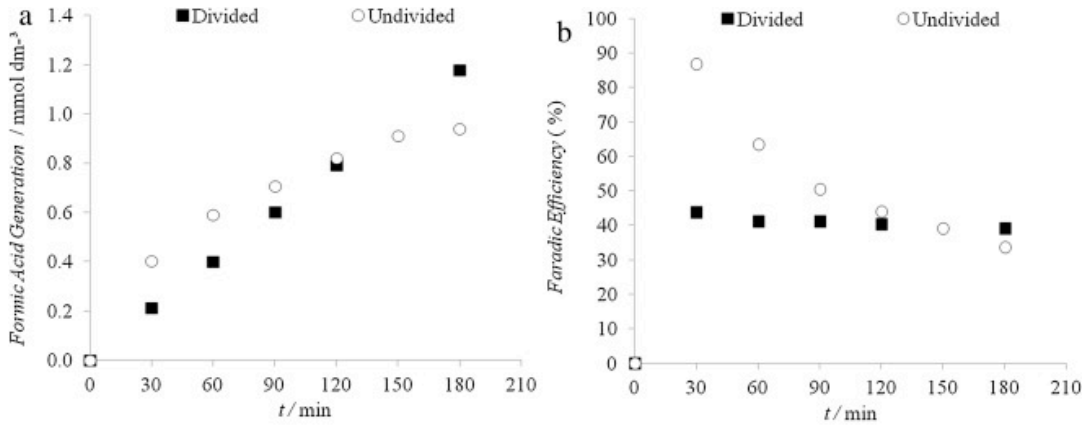

Figure 2.7 Comparison of the utilization of divided and undivided cell on the (a) formic acid concentration and (b) faradaic efficiency during the time [34]. Reproduced from Electrochimica Acta, 199, O. Scialdone, A. Galia, G. Lo Nero, F. Proietto, S. Sabatino, B. Schiavo, Electrochemical reduction of carbon dioxide to formic acid at a tin cathode in divided and undivided cells: Effect of carbon dioxide pressure and other operating parameters, 332 – 341, Copyright (2016), with permission from Elsevier.

To date, there are really few examples in literature in which the process is stable with the time for more than 10 h. For practical applications, good stability is crucial as well as high CO_2 reduction rate. It worth to mention the works of Agarwal [8] (*Table 2.1, entry 34*), Won [72] (*entry 41*), and Wu [86] (*entry 42*). All of these authors have tested the electrochemical conversion of CO_2 into formate/formic acid under different condition, but the common point linking these results is that, even if the process seems stable with the time coupled with a quite good faradaic efficiency over all the duration of the electrolyses (*Figures 2.7-2.9*), the current densities remain fairly constant at really low values that are not promising for the applicative scale.

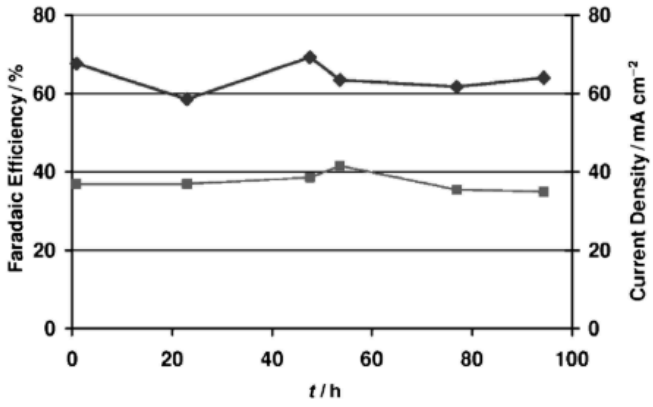

Figure 2.7 Stability of electrodeposited Sn cathode at -2 V vs SCE in a CO_2 saturated 2 M KCl electrolyte [8]. Reproduced from ChemSusChem, 4, A.S. Agarwal, Y. Zhai, D. Hill, N. Sridhar, The electrochemical reduction of carbon dioxide to formate/formic acid: Engineering and economic feasibility, 1301 – 1310, Copyright (2011), with permission from John Wiley and Sons.

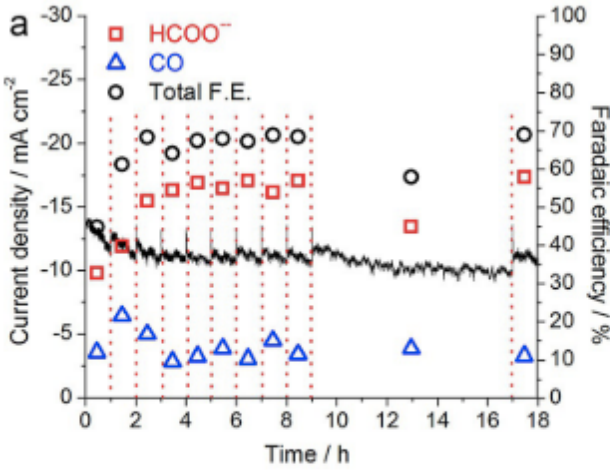

Figure 2.8 Stability of heat-treated Sn dendrite electrode at -1.06 V in a CO_2 saturated 0.1 M $KHCO_3$ electrolyte [72]. Reproduced from ChemSusChem, 8, D.H. Won, C.H. Choi, J. Chung, M.W. Chung, E.H. Kim, S.I. Woo, Rational Design of a Hierarchical Tin Dendrite Electrode for Efficient Electrochemical Reduction of CO_2, 3092 – 3098, Copyright (2015), with permission from John Wiley and Sons.

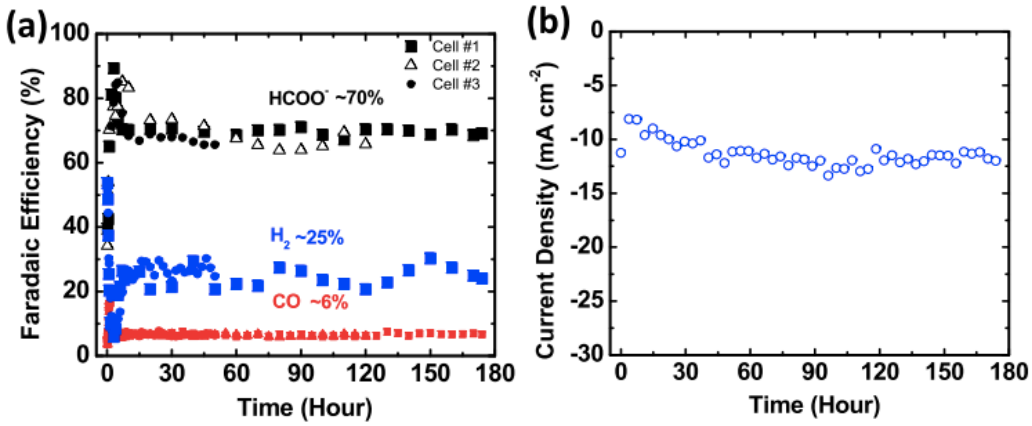

Figure 2.9 Stability of SnO_2 GDE at 2 V in a CO_2 saturated 0.1 M $KHCO_3$ electrolyte [86]. Reproduced from Nano Energy, 159, J. Wu, S.G. Sun, X.D. Zhou, Origin of the performance degradation and implementation of stable tin electrodes for the conversion of CO_2 to fuels, 225 - 229, Copyright (2016), with the permission from Elsevier.

Since, as previously mentioned, the modified-Sn-electrode gave rise an improvement of the performances, some studies have focused their attention on their stability with the time, showing that also for this kind of electrodes there is a good stability of the process but these data were achieved only at really low CO_2 reduction rate. For example, Hu et al. [61] have

achieved a catalyst stability ((Cu,S)-doped SnO_2) for CO_2 reduction for more than 33 h (*Table 2.1, entry 19*) at ~ 6 mA cm^{-2} with a FE of formate of about 59%.

It is worth to mention the work of Kaczur [88] and their coworker from the Carbon Dioxide company. They have developed a new imidazolium-based anion exchange membrane functionalized with stylene and vinylbenzyl chrolide-based polymers, called "Sustainion®" (characterized by high conductivity). The utilization of this membrane allowed to carry out CO_2 reduction in a three-compartment cell at 140 mA cm^{-2} coupled with an FE_{HCOOH} of about 94% for more than 140 h (*Table 2.1, entry 43*), thus demonstrating that the CO_2 reduction process can be a valid approach to reuse the CO_2 with high performances. Indeed, this solution allowed to achieve high concentration of formic acid up to 2M, the highest reported in literature, to the best of our knowledges. However, this solution is likely to present high costs due the utilization of three compartments, an ionic resin media and two membranes, which are still in the development stage in order to improve their mechanical and ionic conductivity properties.

In conclusion, to be suitable for the large-scale industry, it is necessary to reach simultaneously high j, FE and stability as well as high concentration of HCOOH. *Figure 2.10* reports the results of a large number of publications in term of j, FE and time for all the electrolyses reported in *Table 2.1*. It is clear that, to date, we are far to reach this goal (*Figure 2.10*); indeed, most studies are characterized by high FE_{HCOOH} in a wide range of CO_2 reduction rate (~ 5 - 400 mA cm^{-2}) but there is no long test analysis on the performances of the process (time < 4 h); conversely, the few stability analysis reported in literature are coupled with quite high FE_{HCOOH}, but at really low conversion rate (< 20 mA cm^{-2}) which is no appealing for the applicative scale. An exception is given by the results reported by Kaczur [88] that report high j (140 mA cm^{-2}), FE (85%) and time (140 h). However, as above mentioned, the utilization of two membranes and three compartments make this process less suitable from an applicative point of view.

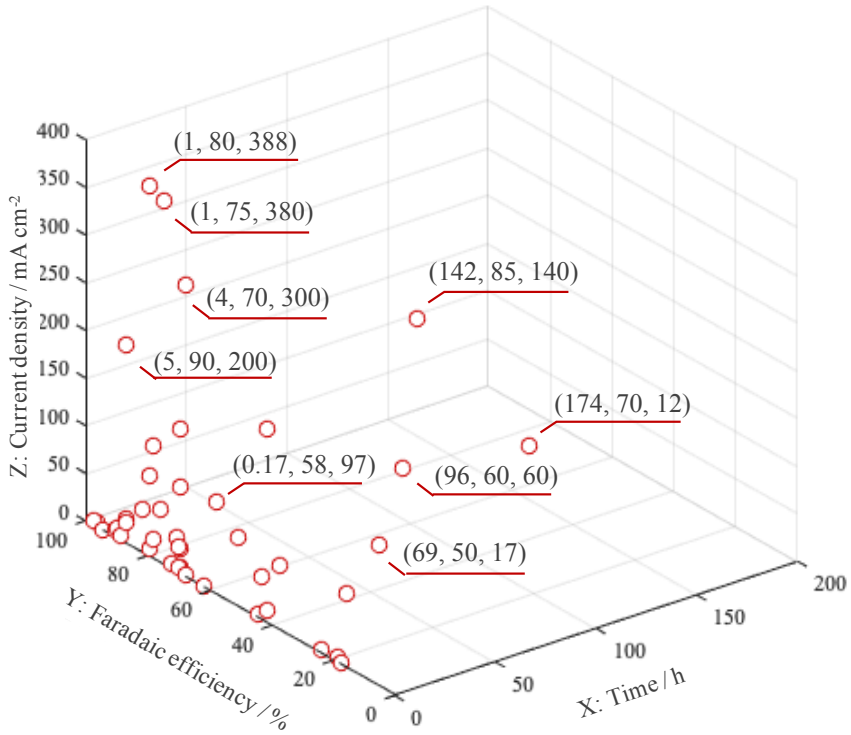

Figure 2.10 3D-scatter points representation of data achieved in literature in terms of current density, FE_{HCOOH} and duration of the test for all the electrolyses reported in Table 2.1.

Table 2.1 Summary of CO_2 electrochemical conversion into formic acid in water electrolyte.[a]

Entry	*Set-up [Cell design / Membrane]*	*Working Electrode*	*Electrolyte solution (catholyte)*	*Current density (mA cm^{-2})*	*Working or cell potential (V)*	*Formate/Formic Acid concentration (mM)*	*FE formic acid / formate (%)*	*Time*	*[Ref.] – years*
1	H-type cell / Selemion CEM	Pb plate	0.1 M $KHCO_3$	5	-1.63 V vs SHE	NA	97.4	5 min	[42] - 1994
2	H-type cell / Selemion CEM	Sn plate	0.1 M $KHCO_3$	5	-1.48 V vs SHE	NA	88.4	5 min	[42] - 1994
3	H-type cell / Selemion CEM	Pb plate	- $KHCO_3$	NA	-2.2 V vs SCE	NA	16.5	NA	[43] - 1990
4	H-type cell / Selemion CEM	Sn plate	- $KHCO_3$	NA	-2.2 V vs SCE	NA	28.5	NA	[43] - 1990
5	H-type cell / Selemion CEM	Pb plate	1 M $KHCO_3$	5	-1.62 V vs SCE	NA	72.5-88.8	30 min	[44] - 1985
6	H-type cell / Selemion CEM	Sn plate	1M $KHCO_3$	5	-1.4 V vs SCE	NA	65-79.9	30 min	[44] - 1985
7	Undivided fixed-bed reactor	Pb granulare	0.5 M $KHCO_3$	1.41	-1.8 V vs SCE	12.66[c]	65	30 min	[45] -2003
				1.49		16.46[c]	20	2 h	
8	Undivided fixed-bed reactor	Sn granulate	0.5 M $KHCO_3$	0.8	-1.8 V vs SCE	17.51[c]	68	30 min	[45] - 2003
				0.16		5.15[c]	25	2 h	
9	Microstructured flow cell	Sn GDE	1 M $KHCO_3$	83	Cell potential 3.48 V ($E_{iR\text{-}comp.}$ 1.3 V)	259.38[c]	80	1 h	[50] - 2016
10	Microstructured flow cell	Sn GDE	1 M KOH	116	Cell potential 2.50 V ($E_{iR\text{-}comp.}$ 1.3 V)	386.48[c]	79	1 h	[50] - 2016
11	Undivided conventional three electrode cell	Sn plate	0.5 M Na_2SO_4	NA	-1.7 V vs SCE	NA	90	1 h	[51] - 2012
							55	9 h	
							30	48 h	

Entry	*Set-up [Cell design / Membrane]*	*Working Electrode*	*Electrolyte solution (catholyte)*	*Current density (mA cm^{-2})*	*Working or cell potential (V)*	*Formate/Formic Acid concentration (mM)*	*FE formic acid / formate (%)*	*Time*	*[Ref.] – years*
12	Undivided conventional three electrode cell	Sn plate	0.5 M $KHCO_3$	NA	-2.0 V vs SCE	NA	63.5	1 h	[51] - 2012
							35	9 h	
							10	48 h	
13	Two compartment cell / glass frit separator	SnOx/Sn	0.1 M $KHCO_3$	4.8	-1.09 V vs RHE	NA	77	12 h	[53]-2017
14	H-type cell / CEM Fumapem® F-950	SnOx	0.1 M $KHCO_3$	~ 1.3	-0.8 V vs RHE	NA	45	1 h	[54] - 2019
15	H-type cell / CEM Fumapem® F-950	Sn	0.1 M $KHCO_3$	~ 1.3	-0.8 V vs RHE	NA	18	1 h	[54] - 2019
				~ 4.5	- 1.2 Vvs RHE		70		
				~ 6	- 1.2 Vvs RHE		80		
16	Two compartment cell / Selemion AMW	SnO_2 pourous nanowires	0.1 M $KHCO_3$	~ 6	- 0.8 V vs RHE	NA	80	15 h	[55]-2017
17	Two compartment cell / NA	NP-SnOx/graphene	0.1 M $NaHCO_3$	10.2	-1.8 V vs SCE	NA	93.6	18h	[60]- 2014
18	H-type cell / CEM Fumapem® F-950	Pb-Sb-Sn-SnOx	0.1 M $KHCO_3$	8.3	-1.4	NA	91	2 h	[54] - 2019
19	H-type cell / Nafion	(Cu,S) co-doped SnO_2	0.5M $NaHCO_3$	5.5	-0.75 V vs Ag/AgCl	NA	58.5	33 h	[61] - 2018
20	Two compartment cell / Nafion 117	Au-Sn NP	0.1 M $KHCO_3$	11	-1.1 V vs RHE	NA	42	1 h	[64]- 2019
21	H type cell / Nafion 117	In-Sn	0.1 M $KHCO_3$	15	-1.2 V vs RHE	NA	~ 90	22 h	[67] - 2017
22	Two compartment cell / Selemion AMV	Sn dendride	0.1 M $KHCO_3$	NA	-1.4 V vs RHE	NA	60	1 h	[72] - 2015
23	Undivided glass cell	Sn rod	NA	~ 0.15	-1.6 V vs Ag/AgCl	0.4 mmol	94.5	30 min	[73] - 2018

Entry	*Set-up [Cell design / Membrane]*	*Working Electrode*	*Electrolyte solution (catholyte)*	*Current density (mA cm^{-2})*	*Working or cell potential (V)*	*Formate/Formic Acid concentration (mM)*	*FE formic acid / formate (%)*	*Time*	*[Ref.] – years*
24	H-type cell / Nafio® NRE-212	Sn foam	0.1 M $NaHCO_3$	NA	- 1 V vs RHE	0.41	40.7	1 h	[66] - 2018
25	Undivided glass cell	Porous Sn-film	0.1 M $KHCO_3$	5	-1.8 V vs Ag/AgCl	4.75	91.5	2 h	[74] – 2015
26	H-type cell / Nafio® 117	Nanoporous Sn	0.5 M $NaHCO_3$	16	-1.1 V vs RHE	24	80	3 h	[75] - 2018
27	PEM	Tinned graphite felt	0.5M NaOH +1M $NaClO_4$	97	-1.6 V vs	NA	58	10 min	[76] - 2015
28	Divided filter-press cell / Nafion® 117 membrane	Sn GDE – 0.75 mg_{Sn} cm^{-2}	0.45M $KHCO_3$ + 0.5M KCl	150	-1.5 V vs Ag/AgCl	54*	70	90 min	[78] - 2017
29	Divided filter-press cell / Nafion® 117 membrane	Sn-GDE	0.45M $KHCO_3$ + 0.5M KCl	200	-1.8 V vs Ag/AgCl	~ 350*	42.3	90 min	[78] - 2017
30	Divided filter-press cell / Nafion® 117 membrane	Sn GDE (NP 150 nm)	0.45M $KHCO_3$ + 0.5M KCl	90	-1.3 V vs Ag/AgCl	32.6	70	90 min	[79] - 2017
31	Semi-batch two compartment cell / Nafio 117	Sn-GDE	0.1 M $KHCO_3$,	200	-1.6 V vs RHE	NA	82	5 h	[30] - 2014
32	Two compartment flow cell /Nafion 212	SnO_2 GDE	0.5M Na_2CO_3 + 0.5 M Na_2SO_4	380	-1.8 V vs Ag/AgCl	NA	75	1 h	[59] - 2019
33	Three compartment cell / Nafion 117 membrane	Sn-coated GDE / GDL Pulsed Electrodeposition	0.5M Na_2CO_3 + 0.5 M Na_2SO_4	388	- 1.6 V vs Ag/AgCl	NA	80	1h	[82] – 2017

Entry	*Set-up [Cell design / Membrane]*	*Working Electrode*	*Electrolyte solution (catholyte)*	*Current density (mA cm^{-2})*	*Working or cell potential (V)*	*Formate/Formic Acid concentration (mM)*	*FE formic acid / formate (%)*	*Time*	*[Ref.] – years*
34	Flow-through reactor / Nafion 117 membrane	NP-Sn-GDE electrodeposited on carbon fiber paper	2 M KCl	~ 60	- 2 V vs SCE	NA	~ 60	96 h	[8] - 2011
35	Gas flow cell	Sn Nafion-coated GDE	0.5 M $NaHCO_3$	27	-1.6 V vs NHE	NA	70	15 min	[83] - 2013
36	Three compartment cell	Sn-GDE with PTFE	0.5 M $KHCO_3$	22	-1.8 V vs Ag/AgCl	NA	87	30 min	[84] - 2015
37	Filter-press flow cell	GDE-Sn	0.5 M $KHCO_3$ + 2 M KCl	300	NA	NA	70	4 h	[70] - 2008
38	H – type cell / Nafion	SnO_2	0.5 M $KHCO_3$	NA	NA	9	56	1 h	[81]- 2016
							24	28 h	
39	Three compartment cell / Nafion 212	Sn-GDE	0.1 M $KHCO_3$	17	Cell potential 2 V	NA	90	5 h	[86] - 2016
							70	30 h	
							50	60 h	
40	Undivided glass cell three- electrode system	Sn plate	0.1M $KHCO_3$	~ 2.5	-1.8 V vs Ag/AgCl	~ 1.1*	97	1 h	[7] - 2014
						~ 18.9*	41.7	40 h	
41	Two compartment cell / Selemion AMV	Heat-treated Sn dendrite	0.1 M $KHCO_3$	~ 12	-1.06 V vs RHE	NA	~ 55	18 h	[72] - 2015
42	Three compartment cell / Nafion 212	SnO_2-GDE	0.1 M $KHCO_3$	~ 12	Cell potential 2 V	NA	~ 70	174 h	[86] - 2016
43	Three compartment flow cell / Nafion® 324 etc	Sn-GDE[b]	DI Water	140	Cell potential 3.6 V	~ 2 M	~ 85 (average value)	142 h	[88] - 2018

[a]Electolyses were perfomed at ambient pressure and temperature.

[b]GDE, Nanoparticle Sn, Sn Loading: 5 mg cm^{-2} 5 wt% PTFE, 5 wt% carbon black, 5wt% imidazolium-based Sustainion® 37-50 ionomer

*Evaluated by the authors according to the data contains in the related paper. NA: not available in the related paper

Chapter 3

Conversion to carbon monoxide

3. Conversion to carbon monoxide

Among the wide range of chemical products produced by the CO_2 electrochemical reduction in water solvent, the highest faradaic efficiencies and current densities are commonly reported for formate/formic acid and CO ($2e^-$ reduction products). Hence, in the following chapter, the current status of CO production will be discussed as well as the main operative parameters, i.e. electrolyte composition and electrodes configuration, that affect the electrochemical conversion of CO_2 into CO at Ag based electrodes.

3.1 Current status of CO production

From the chemical standpoint, CO is colorless, odorless and tasteless flammable gas, but it is highly toxic and it has to be handled carefully. Carbon monoxide is probably one of the main C_1-building blocks and a key carbon intermediate used in large industrial processes, such as the synthesis of hydrocarbons by the Fischer-Tropsch process, the acetic acid by the Monsanto/Cativa process or the purification of nickel via Mond process [4,89]. In particular, pure CO is primarily required for the production of phosgene, acrylic acid, dymethil formamide, polyurethane, polycarbonate, and many other copolymers; while over 90% of CO is used in the form of syngas for the production ammonia, hydrogen and methanol. Hence, the CO has large market compatibility and a wide range of applications in bulk chemicals manufacturing, medicine, and so on, playing an important role in a country's economy.
Hence, considerable efforts were conducted to find a careful way of accessing CO from non-toxic compounds in order to bypass the issues related to the handling of this useful gas [89].

In this context, the electrochemical via for the CO production could be a valid strategy to both reuse waste-CO_2 obtaining an added-value product and develop a new and safer alternative in- or ex- situ CO generation to be integrated with a follow-up CO utilization

for organic synthesis, overcoming the transportation issues linked to the CO usage as reagent [89]. Recently, Jensen and colleagues [90] have shown the first example of applying electrochemistry for a scalable reduction of CO_2 to CO coupled to following carbonylative transformations. They reported that a user-friendly electrochemical device allows for the generation of biologically active compounds and simultaneously avoids the concerns of working with CO, which is generated inside the electrochemical reaction chamber and only in near-stoichiometric amounts with respect to the ensuing carbonylation reaction, even if still at low current densities.

Furthermore, it worth to mention that the CO generation from CO_2 electrochemical conversion is supported by the facile separation of gas products from aqueous electrolyte, avoiding any separation costs.

For the future industrial usage of the electrochemical reduction of CO_2 to CO, the current density has to reach at least 100 mA cm^{-2}, cell potentials need to drop below 3V and the FE for CO should be as high as possible at least 70% coupled with long term stability [9,26–29]. However, the implementation in the largescale industry is still challenging since the limitations of the electrochemical conversion process makes hard to reach this goal.

3.2 CO_2 electrochemical conversion to CO

Electrochemical conversion of CO_2 to CO has been widely studied; in aqueous electrolytes, several catalysts are known to selectively lead to the production of CO, i.e. Ag, Zn, Au, Cu [42]. These kinds of catalysts are able to bind the $CO_2^{-\bullet}$ intermediate, but cannot reduce CO, thereby producing CO at different levels of selectivity. Furthermore, Hori et al. have pointed out that the carbon monoxide formation in aqueous electrolyte from CO_2 takes place at lower overpotentials than formate (i.e. ~ -1.3 V vs NHE at Au, Ag, Zn, Pd, Ga vs ~ - 1.6 V vs NHE at Pb, Hg, In, Sn, Cd for CO and $HCOO^-$ production, respectively, at 5 mA cm^{-2}), independently for the used working electrode.
In this context, it was reported that Ag and Au based electrodes allow to achieve quite high faradaic efficiencies in CO (FE_{CO}) in short electrolyses and they are characterized by relatively low overpotential values for the hydrogen evolution reaction (HER) allowing to obtain both CO and H_2 (syngas), highly interesting for applicative scale. Furthermore, although the Au based cathode gave slightly higher selectivity towards CO, among the noble metals, the Ag electrode could be considered one of the hopeful materials for the scale-up of the CO_2 reduction process due to its lower market cost (i.e. silver price ~ 0.66 €/gr, gold ~ 47 €/gr and platinum ~ 39 €/gr) and good faradaic efficiency [26].

3.3 Electrochemical conversion of CO_2 at silver-based electrodes

In 1994, the formation of CO from CO_2 reduction was investigated using conventional plate electrodes; Hori et al. [42] reported FE_{CO} values of 81% at 5 mA cm^{-2} (-1.37 V vs NHE) on Ag foils in CO_2 saturated electrolyte of 0.1 M $KHCO_3$ using an H-type cell. Conversely, more recently, at Ag foil, Sun et al. [91] have reported a poor CO selectivity (from less than 5 to about 40%) with a current density lower than 1 mA cm^{-2} (partial current density for CO production from 0.01 to 0.3 mA cm^{-2}) while the duration of the experiment was not reported. As another example, Hsieh et al. [92] reported for an Ag foil a faradic efficiency

lower than 20% for a current density lower than 1 mA cm^{-2}. Hence, in last years, many researchers have focused their attention on the engineering of better electrodes, catalysts, electrolyte composition, configuration of electrolyser [6,19,20] and the utilization of pressure conditions (discussed in ***Chapter 4***) in order to improve the performances of the process for CO generation in terms of higher productivity, stability as well as FE_{CO}. However, it is worth to highlight that although many works present in literature reported high FEs towards CO (> 90%), these are often associated with a low production rate or a short term electrolyses; indeed, there are neither results nor a discussion about the long-term results or stability of the catalyst in most of the reported experiments in literature.

3.3.1 Effect of supporting electrolyte

Among all the operative key factors aforementioned, the electrolyte plays an important role on the performances of the cathodic reduction of CO_2 to CO generation; indeed, the effect of the nature of the supporting electrolyte on the process at Ag based cathodes was evaluated by several authors [49,93,94].

A remarkably effect of the cation size of the salt used in the electrolyte on the CO_2 reduction at Ag electrodes was reported by Thorson et al. [93]. In particular, they have shown that larger cations ($Cs^+ > Rb^+ > K^+ > Na^+$) suppress the hydrogen evolution reduction and favor the CO production. Furthermore, in some recent works, the effect of alkaline electrolytes has shown to favor CO production. Verma and co-authors [49] have studied that effect of the anion of the supporting electrolyte on the reduction of CO_2 on Ag based GDEs using KOH, KCl and $KHCO_3$. These authors showed that the presence of HO^- allows to reduce the onset potential for CO (i.e. -0.3 vs -0.7 V vs RHE for KOH and KCl, respectively), increasing the EE and the FE_{CO}. They attributed the better performances achieved with KOH to different potential reasons and in particular on the fact that smaller ions, such as HO^-, are likely to interact with the surface only by electrostatic forces while larger ones, i.e. Cl^-, is likely to be specifically adsorbed on the Ag surface (*Figure 3.1*), thus potentially destabilizing the rate limiting $CO_2^{-\bullet}$ species and, consequently, limiting the CO_2 reduction.

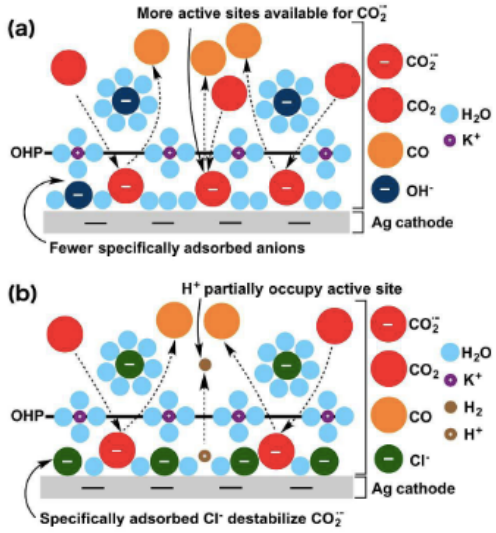

Figure 3.1 Schematic illustrations of the role of supporting electrolyte on the CO_2 reduction to CO at Ag cathode using (a) KOH or (b) KCl [49]. Reproduced from Physical Chemistry Chemical Physics, 18, S. Verma, X. Lu, S. Ma, R.I. Masel, P.J.A. Kenis, The effect of electrolyte composition on the electroreduction of CO_2 to CO on Ag based gas diffusion electrodes, 7075 - 7084, Copyright (2016), with the permission from Royal Society of Chemistry.

Furthermore, the presence of HO^- gives rise to a higher pH, thus limiting the hydrogen evolution. Indeed, it has been shown that, in acid/neutral media, the higher concentration of protons favor the reduction of H^+ with respect to that of CO_2 on the active sites of the electrode surface, resulting in low FE for CO [95]. Indeed, as shown in *Figure 3.2*, alkaline media gives rise to higher performances of the process in terms of both FE_{CO} and partial current density of CO; in particular, Kim et al. [95] showed that an increase of the pH from 4 to 14 allows to improve drastically the selectivity of the CO generation up to 98% at -3V (see *Figure 3.2*).

It is reported that the utilization of 3 M KOH, as electrolyte solution (pH ~ 14), allowed to reach very high current densities (i.e. - 440 $mA \cdot cm^{-2}$), coupled with appreciable value of EE (i.e. 42%), with respect to that achieved with other considered electrolytes [49]. However, these studies were carried out for a short time and it is crucial to understand the performances of this supporting electrolyte during long term electrolyses.

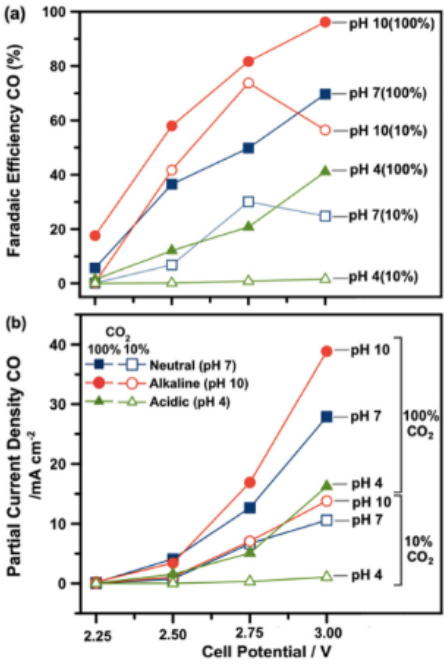

Figure 3.2 Faradaic efficiency for CO (a) and partial current density for CO (b) as a function of the cell potential for different pH value for different concentrations of carbon dioxide in the feed (10 or 100%) [95]. Reproduced from Electrochimica Acta, 166, B. Kim, S. Ma, H.R. Molly Jhong, P.J.A. Kenis, Influence of dilute feed and pH on electrochemical reduction of CO_2 to CO on Ag in a continuous flow electrolyzer, 271 – 276, Copyright (2015), with permission from Elsevier.

3.3.2 Silver based electrodes with high surfaces

Recently, the engineering of the electrodes has aroused large interest in order to both reduce the overpotentials needed to drive the reaction and increase the CO_2 reduction rate.

Several works have shown that the implementation of electrodes with high active surface allows operating at higher current densities than the plate electrode improving the performances of the process [96–102]. For example, Lu [98] and Ma [103] and their co-workers have synthesized, respectively, a nanoporous, np-Ag, and an oxide-derived nanostructured, OD-Ag, silver catalyst (i.e. both structures characterized by a larger area for catalytic reaction than the polycrystalline one) which allow, at low overpotentials, to achieve a current density, at least, 20 times higher than the one reached at plate Ag and to increase drastically the FE_{CO} from less than 4% using a plate silver to 80 or 92% using OD-

Ag or np-Ag electrode, respectively, in a CO_2-saturated aqueous $KHCO_3$ electrolyte, thanks to the high number of active sites for CO_2 reduction (*Figure 3.3*). In particular, it was demonstrated that electrodes with high active surface for low potentials are characterized by a lower value of the Tafel slope (i.e. 58 and 77 mV dec^{-1} for np-Ag and OD-Ag, respectively) than the polycrystalline silver electrode (~130 mV dec^{-1}), that indicates a fast initial electron transfer to a CO_2 molecule speeding up the reduction rate; however, at relatively high potentials, the Tafel slope increases, thus showing that, also for this kind of electrodes, the CO_2 electrochemical conversion could be limited by a mass transport of CO_2 to the surface of the electrode [98,103–105]. The utilization of high active surface can also help to avoid the mass transfer limitations of CO_2 to the cathode surface at least at relatively low potentials; however, mass transport limitations still persist at higher potentials, implying not very high current densities, making the process less appealing from the applicative point of view. Moreover, it is difficult to discuss about the implementation of these electrodes in large scale due to the absence of long-term analyses (experiments performed for ≤ 5 h), although they allowed reaching high selectivity towards CO (> 80%) and maintaining stable current density.

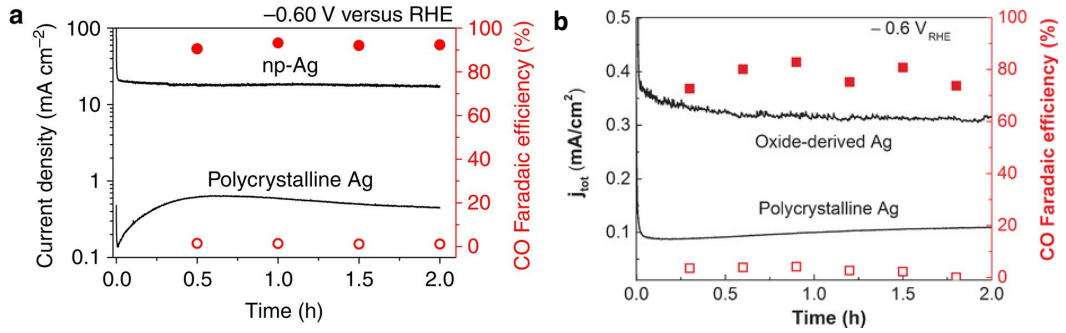

Figure 3.3 Electrochemical conversion of CO_2 performed at (a) np-Ag [98] and OD-Ag [103] electrode: comparison with the polycrystalline one. Total current density versus time on left axis and CO Faradaic efficiency versus time on right axis. (a) Reproduced from Nature Communiations, 5, B. Q. Lu, J. Rosen, Y. Zhou, G.S. Hutchings, Y.C. Kimmel, J.G. Chen, F. Jiao, A selective and efficient electrocatalyst for carbon dioxide reduction, 3242, Copyright (2014), with permission from Springer Nature. (b) Reproduced from Angewandte Chemie International Edition, 55, B. M. Ma, B.J. Trześniewski, J. Xie, W.A. Smith, Selective and Efficient Reduction of Carbon Dioxide to Carbon Monoxide on Oxide-Derived Nanostructured Silver Electrocatalysts, 9748 - 9752, Copyright (2016), with permission from John Wiley and Sons.

The nanoparticles utilization of noble metals supported on different materials could be a valid alternative to reduce the cost of such electrode; indeed, it is largely under investigation a way to stabilize small nanoparticles on different support materials, increasing catalysts dispersion and utilization, enhancing electron conductivity and mass transport.

In this framework, the utilization of GDEs electrochemical technologies for the CO generation allowed to achieve really promising results at atmospheric pressure in H_2O-based electrolyte [3,13,29–31]. Ma et al. [96] have shown that it is possible to achieve a current density up to 350 mA cm^{-2} with high faradaic efficiency (FE_{CO} ~ 95%) and an energy efficiency of CO (EE_{CO}) of about 45% working with an Ag-GDE at 3V in alkaline media (1M KOH) for a short time. In addition, under adopted conditions, the utilization of an Ag-GDE can guarantee a quite high conversion ratio up to 32% per pass maintaining a FE_{CO} close to 80% at current density of about 50 mA cm^{-2} [95]. Although the implementation of GDEs gives also really promising results in term of FE_{CO}, current density and productivity of CO [3,11,33,34], these GDE technologies are still challenging due to the low stability with the time, catalyst losses, time consuming preparation procedure and the presence of deposition salts inside the fibers of the porous layer which limits the three phases contact [80,85], as already described in detail in ***Section 2.3.2***.

Nevertheless, quite good results on the long term stability of the CO_2 reduction to CO were achieved by Jeanty and co-worker [85]. Stable conversion of CO_2 on Ag gas diffusion electrode at 150 mA cm^{-2} over several hundred hours on 100 cm^2 can be observed even if it is coupled in loss of selectivity towards CO (FE_{CO} ~50%) and high cell voltage of about 8V.

Chapter 4

Effect of CO_2 pressure

4. Effect of CO_2 pressure

One of the main hurdles of the CO_2 electrochemical conversion in water solutions is its low solubility. According to the Henry's Law, the higher is the CO_2 pressure, the higher is the CO_2 bulk concentration in water. Hence, this chapter will be devoted to the study of the effect of the pressure on the electrochemical conversion of CO_2 for formic acid and carbon monoxide generation with particular attention at tin and silver based electrode.

4.1 Effect of pressure on CO_2 electrochemical conversion

To date, the effect of the CO_2 pressure on its electrochemical conversion was poorly investigated, even if the pressure can affect both the electrochemical performances and industrial integration with up- and downstream processes. Additionally, there are relatively few systematic studies on pressurized flow cells whereas most works on pressurized conditions were performed in H-type cells, limiting their eligibility and evaluation for the scale-up on the applicative scale.

In this context, few authors are focusing their attention on the utilization of pressurized CO_2 as a strategy to cope with mass transfer limitations in water solution improving the performances of the process. Indeed, an enhancement of the pressure give rise to: i) higher concentration of CO_2, according to Henry's Law (*Figure 4.1*) (the CO_2 solubility in water at room temperature increases almost proportionally with the CO_2 pressure) [106]; ii) the possibility to work at higher temperatures (because at atmospheric pressure higher temperature leads to lower CO_2 solubility); and iii) direct utilization of the pressurized products stream (i.e. syngas) as a feedstock to other conventional process under pressure [107].

More in detail, higher concentration of CO_2 increases the limiting current density (j_{lim}), allowing to work at higher current densities than that used at atmospheric one and favors

the CO_2 reduction with respect to the water reduction on the cathode surface. Furthermore, it was found that the CO_2 can be reduced at less negative potentials under high pressure conditions, rising the energy efficiency of the overall process. In addition, Giovanelli et al. [108] have reported that technical obstacles related to the high pressure system can be easily overcome and that the combination of electrochemistry with high pressure condition gave useful information of thermodynamics and kinetics for a wide range of redox reactions as well as a higher comprehension of the processes under non-classical conditions with a potential implementation in industrial field. Nevertheless, in spite of the fact that pressurized systems are widely adopted for both chemical and electrochemical processes under applicative scale, the effect of the pressure is not often reported in the literature since most of the academic labs involved in this research field do not adopt high pressure technologies.

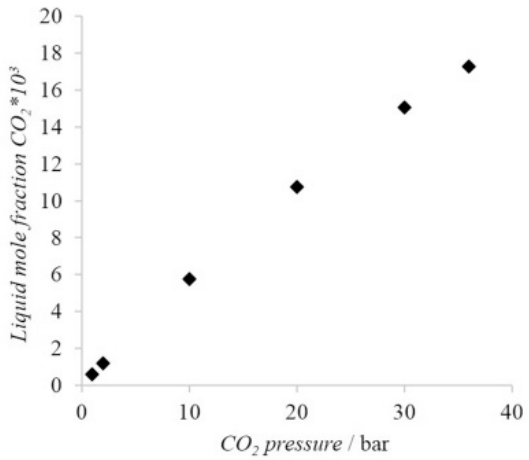

Figure 4.1 CO_2 solubility in water vs CO_2 absolute pressure (T= 25°C) [109]. Reproduced from Electrochimica Acta, 277, F. Proietto, B. Schiavo, A. Galia, O. Scialdone, Electrochemical conversion of CO_2 to HCOOH at tin cathode in a pressurized undivided filter-press cell, 30 – 40, Copyright (2018), with permission from Elsevier.

First studies on the utilization of pressurized CO_2 in the frame of the electrochemical conversion of CO_2 were reported by the research team of Sakata [110–115] and Mizuno [116], between 1993 and 1997. These studies have shown an enhancement of the process performances, in terms of both the total FE of CO_2 reduction (FE_{CO_2}) and FE of the target-

products, by increasing the CO_2 pressure; in particular, the selectivity towards the target-product was remarkably increased at all the electrodes under investigation (i.e. Ag, Au, Pb, In, Sn, Zn, Pb, Cu, glassy carbon) compared with that obtained at atmospheric pressure as well as the FE_{CO_2}. In order to study the pressure effect, the electrolyses were carried out using divided or undivided stainless-steel cells able to work at high pressure, as schematically shown in *Figure 4.2* and *4.3*.

As examples, Sakata et al. have shown that an enhancement of the pressure from 1 to 40 bar drastically increases the FE of formic acid from of about 15% to 89% at In electrodes under galvanostatic condition (~ 200 mA cm^{-2}) in 0.5 M $KHCO_3$ aqueous electrolyte [113] and the FE of CH_4 up to 55% at Cu electrode under galvanostatic condition (~ 160 ma cm^{-2}) in 0.1 M $KHCO_3$ aqueous electrolyte [112] for a total charge passed of about 300 C.

It is worth to mention that, to date, these studies at high pressure reported among the highest current densities and reduction efficiencies of CO_2 ever published in the literature, in spite of the fairly vintage years of these works.

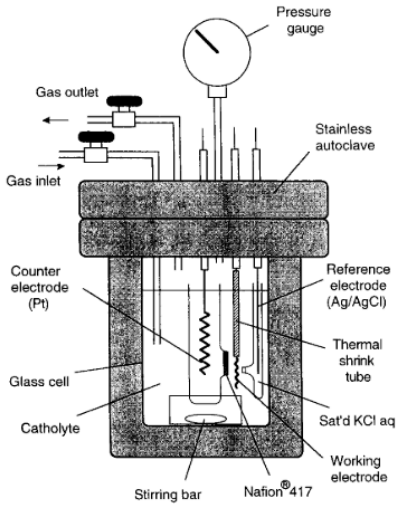

Figure 4.2 Autoclave electrochemical cell for CO_2 electrochemical conversion at high pressure [110]. Reproduced from Journal of Electroanalytical Chemistry, 391, K. Hara, A. Kudo, T. Sakata, Electrochemical Reduction of Carbon Dioxide under High Pressure on Various Electrodes in an Aqueous Electrolyte, 141 – 147, Copyright (1995), with permission from Elsevier.

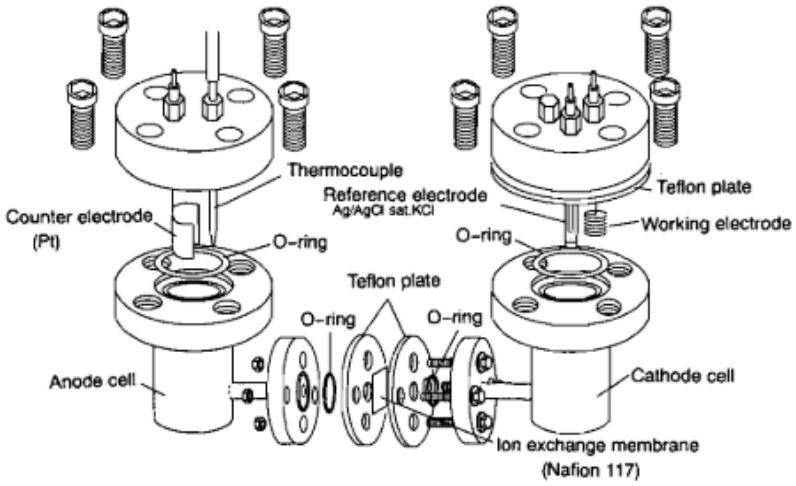

Figure 4.3 Stainless H-type cell for electrochemical conversion of high-pressure CO_2 [116]. Reproduced from Energy Sources, Part B: Economics, Planning, and Policy, 17, T. Mizuno, K. Ohta, A. Sasaki, T. Akai, M. Hirano, A. Kawabe, Effect of Temperature on Electrochemical Reduction of High-Pressure CO_2 with In, Sn, and Pb Electrodes, 503 – 508, Copyright (1995), with permission from Taylor & Francis.

Additionally, the same authors have shown that the utilization of the pressure can drive the reaction towards different target products on specific electrodes; indeed, some catalysts, which are known to be selective for the H_2 evolution at 1 bar (characterized by low overpotentials for the HER), such us Fe, Co, Ni, Pt, can drastically change the main product of the CO_2 reduction under pressurized CO_2. Kudo and coworker [115] have investigated the conversion of CO_2 via electrochemical process at Ni wire electrode, showing that with an increase of CO_2 pressure allows to remarkably favor the CO_2 reduction minimizing the hydrogen evolution (*Figure 4.4*).

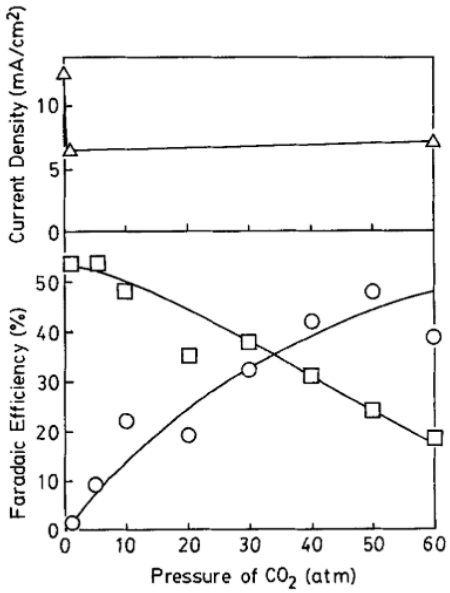

Figure 4.4 Effect of CO_2 pressure on the FE of CO_2 reduction in water electrolyte at -1.8 V vs Ag/AgCl on a Ni electrode. (○) Total FE of CO_2 reduction, (□) FE of H_2 and (Δ) current density [115]. Reproduced from Journal of the Electrochemical Society, 140, A. Kudo, S. Nakagawa, A. Tsuneto, T. Sakata, Electrochemical Reduction of High Pressure CO_2 on Ni Electrodes, 1541 – 1545, Copyright (1993), with permission from IOP Publishing, Ltd.

Since CO_2 reduction allowed to reach moderate high current densities and faradaic efficiencies on a variety of electrodes, to date, it could be considered one of the most promising methods for achieving a commercial electrochemical process; hence, in following sections, a particular attention will be devoted to the electrochemical conversion of CO_2 under high pressure conditions for the production of formic acid and carbon monoxide at tin and silver based electrodes, respectively.

4.1.1 Synthesis of HCOOH at tin based electrodes

In the late 90s, the electrochemical conversion of CO_2 at Sn electrode under pressurized conditions was reported by Hara [110] and Mizuno [116] and their colleagues. These authors demonstrated that the utilization of the pressure can be one of the key factors to increase the selectivity of the process toward formic acid, over to 92%, and to be able to

work at high CO_2 reduction rate (more than 150 mA cm^{-2}) at Sn plate electrode (*Table 4.1, entry 1*).

In the years following the 90s, few relevant efforts were made towards optimizing the utilization of pressurized CO_2 for its electrochemical conversion. Among them, in order to reach higher current density and FE, Köleli and coworkers [117,118] have studied the utilization of pressure for the HCOOH generation at Sn granules using an undivided fixed-bed reactor for the first time (*Figure 4.5*), with the aim to increase the surface area as much as possible.

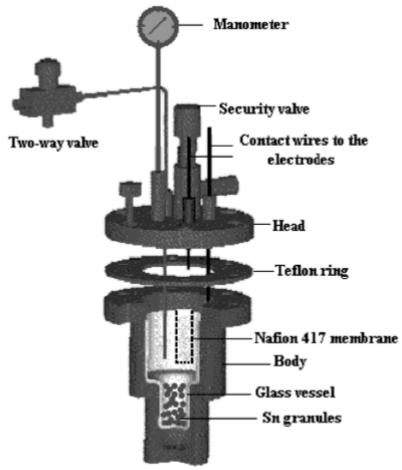

Figure 4.5 Electrochemical fixed-bed reactor equipped with Sn granules electrode [117]. Reproduced from Fresenius Environmental Bulletin, 12, F. Köleli, T. Yesilkaynak, D. Balum, High pressure-high temperature CO_2 electro-reduction on Sn granules in a fixed-bed reactor, 1202 – 1206, Copyright (2003).

They have shown that the CO_2 reduction process, performed on Sn granules in 0.2M K_2CO_3 CO_2-saturated aqueous electrolyte, drastically depends on the applied pressure. At all the fixed working applied potential, an increase of the pressure gave rise to both higher faradaic efficiency (*Figure 4.6a*) and current density (*Figure 4.6b*), improving the performances of the process. In particular, they reached an enhancement in selectivity for formic acid from 47% to 90% and in CO_2 reduction rate from less than 0.5 up to 1.4 mA cm^{-2} at 1 and 50 bars, respectively, at -1.9V vs SCE after 30 minutes of electrolyses (*Table 4.1, entries 2*

and 3). In addition, they observed that, for all the adopted CO_2 pressure, as the electrode potential shifts to more negative potential, the HER became predominant with respect to the CO_2 reduction, decreasing the FE_{HCOOH} (*Figure 4.6a*). In spite of the higher selectivity reported, these data are obtained at a low current density; furthermore, it is worth to note that the process under these adopted operative conditions is characterized by a low stability with the time, indeed they indicated that an increase of the electrolyses time over to 30 minutes caused a loss in selectivity of the process towards formic acid.

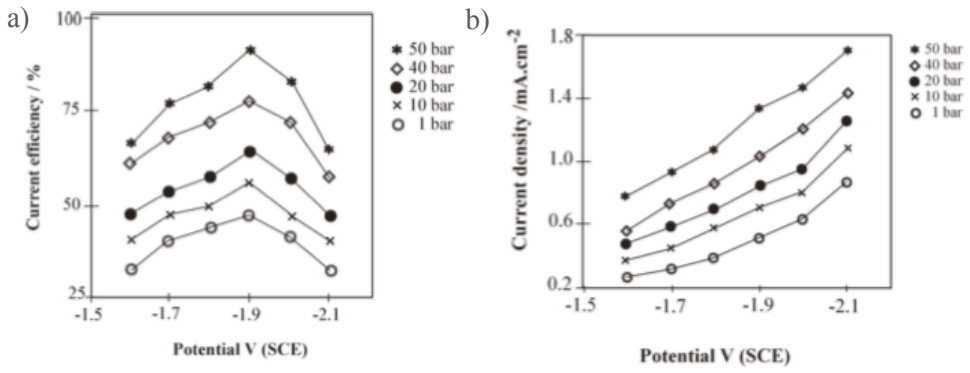

Figure 4.6 Effect of the pressure on the CO_2 reduction process at Sn granules cathode using a fixed-bed reactor. Plot of current efficiency of HCOOH (a) and current density (b) vs the applied potential at different value of CO_2 pressure [117]. Reproduced from Fresenius Environmental Bulletin, 12, F. Köleli, T. Yesilkaynak, D. Balum, High pressure-high temperature CO2 electro-reduction on Sn granules in a fixed-bed reactor,1202 – 1206, Copyright (2003).

The utilization of Sn granules at slightly high pressures that the atmospheric one, ca 6 bar, was also investigated by Oloman et al. [16]. By operating in the continuous flow-by ‘‘trickle-bed’’ mode with co-current upward 2-phase flow of the catholyte liquid and CO_2 gas in divided cell, they reported a notable and unprecedented result of formate concentration of about 1 M at 310 mA cm^{-2} (*Table 4.1, entry 4*) tested for 100 min; despite this interesting result, there is no further study on it. Furthermore, under these particular conditions, the process was characterized by a slightly high energetic consumption of about 340 kWh $kmol^{-1}$ of formate and the system is affected by high pressure drop along the reactor bed (outlet P_{CO_2} ~ 1 atm).

Among the few studies presents in literature, in 2015, the effect of the pressure on the CO_2 reduction to formic acid at Sn plate electrode has been investigated by Scialdone et al. [34]. They highlighted a remarkably effect of the CO_2 pressure on the performances of the process, carrying out a systematic study at both atmospheric and high CO_2 pressure using a simple and cheap undivided stainless-steel cell (which allows to avoid the penalty given by the presence of the separator). They showed that, at fixed value of current density, the final FE of formic acid increases coupled with a drastic enhancement of the final formic acid concentration by enhancing the pressure. However, high increase of the pressure, at constant values of the current density, did not result in an appreciable variation on the performances of the process in terms of both final concentration and FE of formic acid, that reached a plateau value. More in detail, as shown in *Figure 4.7*, an increase of the pressure from 1 to 5 bars gave rise to an enhancement of the HCOOH concentration from 30 to 46 mM with a correspondent increase of the FE from 27 to 41%, respectively, at about 12 mA cm^{-2} in 0.1 M Na_2SO_4 aqueous electrolyte for 6 h (*Table 4.1, entries 5 and 6*). Conversely, a further increase of the pressure up to 10 bars did not affect the performances of the process (*Table 4.1, entry 7*). Authors pointed out that, under these conditions, the process was not under CO_2 mass transport control to the cathode surface (due to the high concentration of CO_2 in solution, $j_{applied} << j_{lim}$ at $P_{CO_2} \neq 1\ bar$), but it could be limited by subsequent stages of CO_2 adsorption or reduction of the adsorbed CO_2. Further studies of the same authors showed a combined effect of current density and CO_2 pressure; in particular, the utilization of relatively high CO_2 pressure (30 bar) at higher current density of about 90 mA cm^{-2} allowed to achieve high concentrations of formic acid up to 460 mM with a 55% of FE (*Table 4.1, entry 8*).

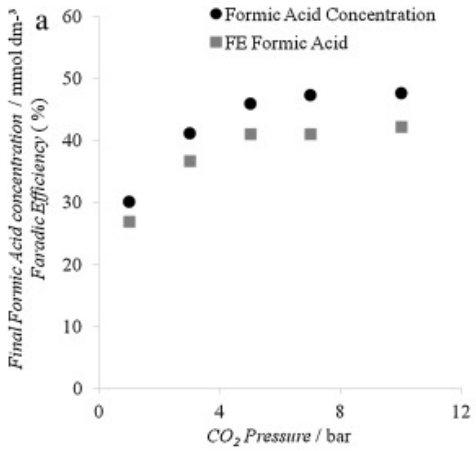

Figure 4.7 Effect of the CO_2 pressure on both the formic acid concentration and the FE_{HCOOH} in 0.1M Na_2SO_4 aqueous electrolyte at 11.6 mA cm^{-2} after 6h [34]. Reproduced from Electrochimica Acta, 199, O. Scialdone, A. Galia, G. Lo Nero, F. Proietto, S. Sabatino, B. Schiavo, Electrochemical reduction of carbon dioxide to formic acid at a tin cathode in divided and undivided cells: Effect of carbon dioxide pressure and other operating parameters, 332 – 341, Copyright (2016), with permission from Elsevier.

More recently, in 2019, Ramdin et al. [119] have performed the electrochemical conversion of CO_2 to formic acid/formate on a Sn-based electrode using a divided pressurized semi-continuous batch cell equipped with a bipolar membranes[5] (BPMs) or a CEMs for 20 minutes. Their results show that an increase of the pressure up to 50 bars at 3.5V of cell potential allows to drive the CO_2 reduction at about 30 mA cm^{-2} in 0.5 M $KHCO_3$ aqueous electrolyte with a selectivity of formate close to 80% and a formate concentration of about 200 mM (*Table 4.1, entry 9*). A further increase of the cell potential (up to 4V) allows working at higher current density (up to 100 mA cm^{-2}) and achieving a higher concentration of formate (440 mM) but at the expense of the selectivity of the process (FE_{HCOOH} drop to 65%) (*Table 4.1, entry 10*). Furthermore, the remarkably discover of these researchers was a BMP able to maintain a different compartment pH between the anodic and the cathodic compartment at high pressure of CO_2 and to limit the crossover of the liquid product which is crucial for the economics of a large-scale CO_2 electrolysis process.

[5] In two compartment electrochemical cell, the bipolar membrane drives both protons (H+) and hydroxylic ions (OH–) toward the anode and cathode, respectively, enabling a constant pH for higher stability [119].

More in general, in spite of the several disadvantages in the utilization of common membrane in an electrochemical cell (i.e. high price, complex fabrication, product crossover, pH imbalance, low stability, etc…[119]), this work has shown the possibility to perform the CO_2 reduction at high pressure of CO_2 up to 50 bar in a divided cell, opening the pathway to the possibility to couple the CO_2 reduction with a suitable anodic process at high pressure, increasing the overall economic of the process from the applicative standpoint, even if the stability was not investigated.

For the sake of comparison, *Figure 4.8* reports the current results achieved in literature on CO_2 reduction to formic acid under pressurized condition (data are represented by closed symbols and are taken from *Table 4.1*) and some key results obtained at atm pressure (data are represented by open symbols and are taken from *Table 2.1*, ***Section 2.3***), limiting the time view range up to 80 hours. It is clear that the utilization of the pressure allows reaching quite good values of both *j* and FE_{HCOOH}; however, most of the works under pressurized condition do not report the stability study.

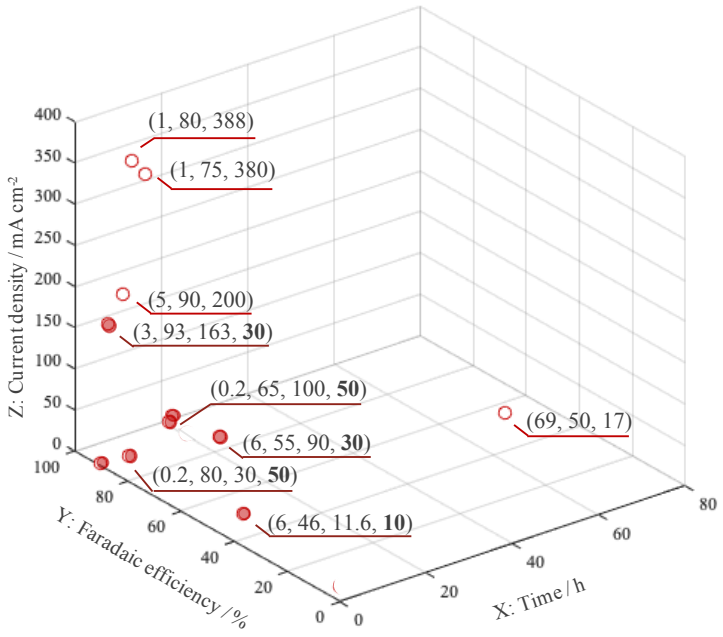

Figure 4.8 3D-scatter points representation of data achieved in literature in terms of current density, FE_{HCOOH} and duration of the test for all the electrolyses under pressurized conditions (closed symbols) reported in Table 4.1 and some key results obtained at atm pressure (open symbol) reported in Table 3.1.

Table 4.1 Summary of CO_2 electrochemical conversion into formic acid in water solution at high CO_2 pressure.[a]

Entry	*Set-up [Cell design / Membrane]*	*Working Electrode*	*Electrolyte solution*	*Current density (mA cm^{-2})*	*CO_2 Pressure (bar)*	*Working or cell potential*	*Formate/Formic Acid concentration (mM)*	*FE formic acid / formate (%)*	*Time*	*[Ref.] – xxxx*
1	Divided stainless steel autoclave / Nafion 417®	Sn plate	0.1 M $KHCO_3$	163	30	-1.39 V vs Ag/AgCl	NA	92.3	3 h	[110] - 1995
2	Fixed-bed reactor / Nafion 417®	Sn granules	0.2 M K_2CO_3	0.4	1	-1.9 V vs SCE	NA	47	30 min	[117] - 2003
3	Fixed-bed reactor / Nafion 417®	Sn granules	0.2 M K_2CO_3	1.4	50	-1.9 V vs SCE	NA	91	30 min	[117] - 2003
4	Divided continuous trickle-bed / Nafion 117	Sn granule	0.45 M $KHCO_3$ + 2 M KCl	310	P_{in} = 6 P_{out} =1	Cell potential 3.9 V	1 M	63	100 min	[16] - 2007
5	Stailess-steel undivided cell	Sn Plate	0.1 M Na_2SO_4	11.6	1	-	30	27	6 h	[34] - 2015
6	Stailess-steel undivided cell	Sn Plate	0.1 M Na_2SO_4	11.6	5	-	46	41	6 h	[34] - 2015
7	Stailess-steel undivided cell	Sn Plate	0.1 M Na_2SO_4	11.6	10	-	50	43	6 h	[34] - 2015
8	Stailess-steel undivided cell	Sn Plate	0.1 M Na_2SO_4	90	30	-	460	55	6 h	[34] - 2015
10	Semi-continuous two compartment batch cell / BPMs	Sn plate	0.5M $KHCO_3$	30	50	Cell potential 3.5 V	200	80	20 min	[119] - 2019
11	Semi-continuous two compartment batch cell / BPMs	Sn plate	0.5M $KHCO_3$	100	50	Cell potential 4 V	440	65	20 min	[119] - 2019

[a]Electolyses were perfomed at ambient temperature.
*Evaluated by the authors according to the data contains in the related paper
NA: not available in the related paper

4.1.2 Synthesis of CO at silver based electrode

The effect of pressurized CO_2 on the performances of the CO_2 reduction to CO is even less studied than the production of formic acid via electrochemical paths.

First data about high pressure CO_2 electrochemical conversion to carbon monoxide at silver cathodes were reported by Hara et al. [110] in 1995, showing that it is possible to work at high CO_2 reduction rate (~ 160 mA cm^{-2}) for about 3 h with a quite high selectivity for CO (FE_{CO} ~ 75%) at 30 bar using an Ag plate electrode in 0.1 M $KHCO_3$ aqueous electrolyte.

To date, the effect of the pressure on the performances of the process for CO production was mainly studied using a GDE with promising results for a short time electrolysis. The advantages of the utilization of the pressure were shown by Dufek and colleagues [120,121], using an Ag-GDE in a pressurized system shown in *Figure 4.9*. They achieved an improvement in FE_{CO} up to 80% and in the reduction rate over to 220 mA cm^{-2} with a corresponding suppression of the hydrogen evolution reaction by working in K_2SO_4 aqueous electrolyte at elevate pressure of about 20 bar for 1 hr. More in general, as shown in *Figure 4.10*, the selectivity of the CO_2 reduction to CO increases with the CO_2 pressure. Although this work presented quite good results in term of FE_{CO} and *j*, there is no stability test of the process and the system suffer from the issues linked to the utilization of a GDE; furthermore, as shown in this system design (*Figure 4.9*), it is not clear how the CO_2 gas can flow on the back of the GDE maintain the crucial three-phase contact, while it seems reasonable that the CO_2 gas go through the GDE, limiting the presence of the liquid electrolyte inside the GDE.

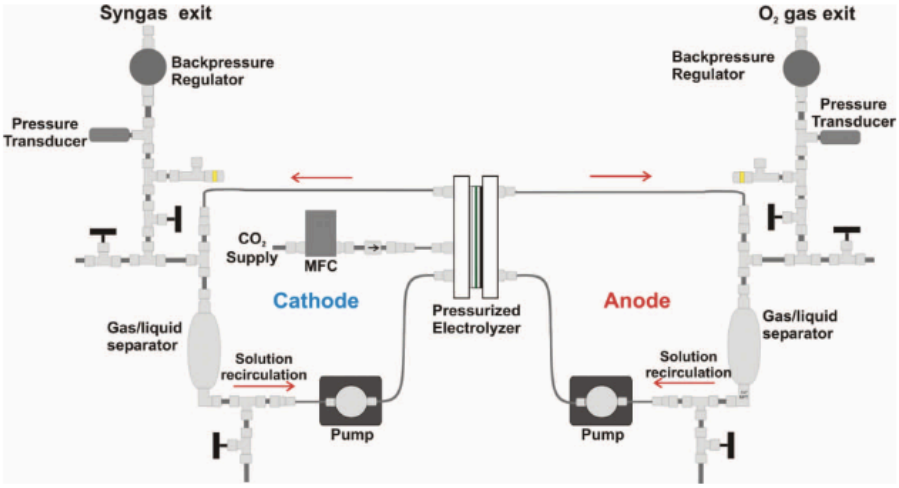

Figure 4.9 Schematic system for CO_2 reduction at high pressure used by Dufek et al. [120]. Reproduced from Journal of the Electrochemical Society, 159, E.J. Dufek, T.E. Lister, S.G. Stone, M.E. McIlwain, Operation of a Pressurized System for Continuous Reduction of CO_2, 514 – 517, Copyright (2012), with permission from IOP Publishing, Ltd.

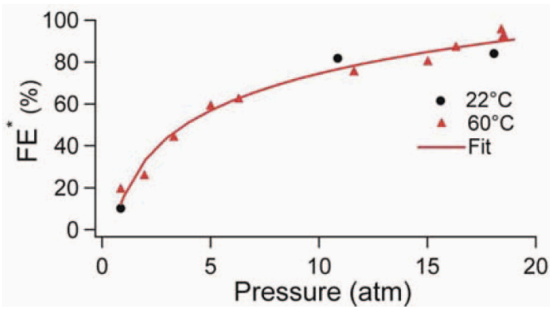

Figure 4.10 Effect of pressure on FE_{CO} at 225 mA cm^{-2} in 0.5 M K_2SO_4 [120]. Reproduced from Journal of the Electrochemical Society, 159, E.J. Dufek, T.E. Lister, S.G. Stone, M.E. McIlwain, Operation of a Pressurized System for Continuous Reduction of CO_2, 514 – 517, Copyright (2012), with permission from IOP Publishing, Ltd.

More recently, Gabardo et al. [122] have investigated the effect of the pressure under highly alkaline reaction environment (1-7 M KOH aqueous electrolyte) using a Ag-based GDE on the CO production. They have shown that an improvement of the performances of the process can be achieved due to the synergetic effect of pressurized CO_2 system (up to 7 bars), which inhibits the production of other CO_2 reduction products (thus increasing the selectivity) and very highly alkaline reaction environment, which decreases the

overpotentials (thus enhancing the energetic efficiency). The effect of the pressure on the CO_2 reduction process at 300 mA cm^{-2} and various KOH concentration is shown in *Figure 4.11*. Additionally, the same authors investigated the stability with the time using a modified Ag-GDE design, showing a quite good stability of the process for 10 h (FE_{CO} ~ 85-90% and j ~ 80-100 mA cm^{-2}) (*Figure 4.12*) under extremely alkaline and pressurized environments: 7 M KOH and 7 bars, respectively, which are operative conditions where the process has exhibited the lowest overpotential for CO. Furthermore, in spite of the good stability with the time, it is worth to mention that the utilization of very high alkaline electrolyte is less convenient in the applicative perspective, for the high cost of the electrolyte and the final purification of the aqueous exhaust solution.

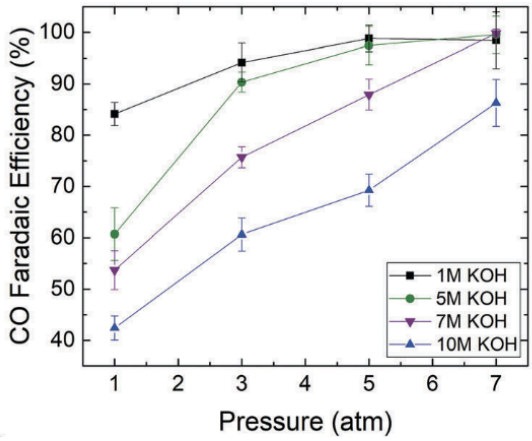

Figure 4.11 Effect of the pressure up to 7 atm on the FE_{CO} under various KOH concentration at 300 mA cm^{-2} [122]. Reproduced from Energy & Environmental Science, 11, C.M. Gabardo, A. Seifitokaldani, J.P. Edwards, C. Dinh, T. Burdyny, G. Kibria, C.P.O. Brien, E.H. Sargent, D. Sinton, Combined high alkalinity and pressurization enable efficient CO_2 electroreduction to CO, 2531 – 2539, Copyright (2018), with permission from Royal Society of Chemistry.

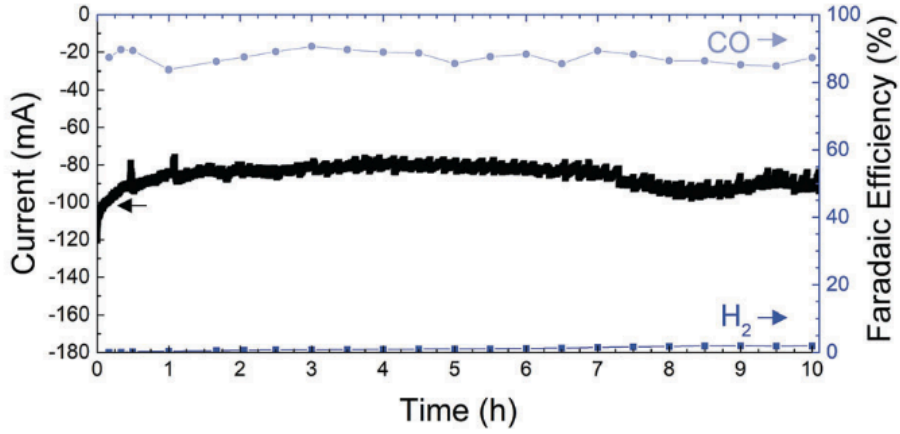

Figure 4.12 Effect of the time on the CO_2 reduction at 7 atm, in 7 M KOH aqueous electrolyte and cell potential of 2.8 V [122]. Reproduced from Energy & Environmental Science, 11, C.M. Gabardo, A. Seifitokaldani, J.P. Edwards, C. Dinh, T. Burdyny, G. Kibria, C.P.O. Brien, E.H. Sargent, D. Sinton, Combined high alkalinity and pressurization enable efficient CO_2 electroreduction to CO, 2531 – 2539, Copyright (2018), with permission from Royal Society of Chemistry.

4.2 Comparison between the synthesis of CO and HCOOH under pressurized conditions

Figure 4.13 reports the more relevant data reported in literature for the electrochemical conversion of CO_2 to both CO and formic acid under pressurized conditions in terms of j, FE and time passed. It is possible to observe that for the synthesis of CO, quite high j and FE were achieved working at relatively low pressures (e.g. 7 or 20 bar) with a good stability tested up to 10 hours. In particular, the figure shows that under pressurized conditions better figures of merit were achieved for CO synthesis with respect to formic acid one. Hence, it seems that in the case of formic acid more efforts should be done in order to improve the performances of the process. More in general, from an applicative point of view, taking in account the problems and costs of GDEs based electrodes, it would be interesting to focus more on the utilization of simpler and cheaper cathodes under pressurized conditions.

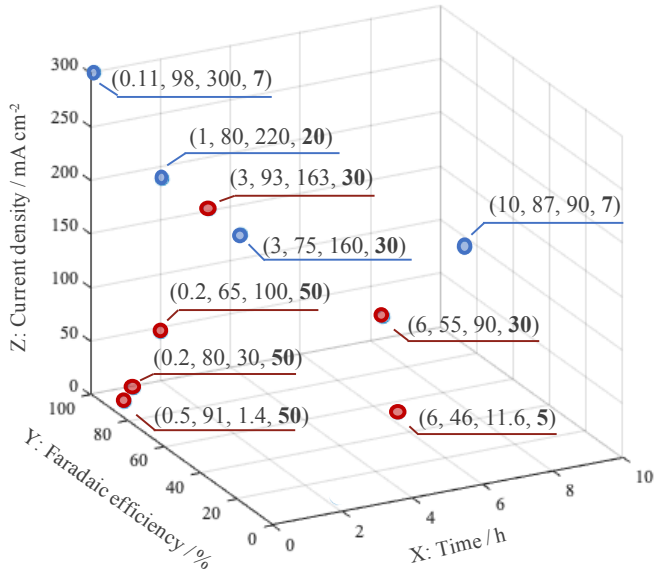

Figure 4.13 3D-scatter points representation of data achieved in literature in terms of current density, FE_{HCOOH} and duration of the test for all the electrolyses under pressurized conditions for the synthesis of HCOOH (red symbols) reported in *Table 4.1* and some key results for the CO production (blue symbol).

Chapter 5

Materials and Methods

5. Materials and Methods

5.1 Reagents and electrodes

Electrolytic solutions were composed by bi-distillate water as solvent and Na_2SO_4 (assay > 99%, Janssen Chimica), K_2SO_4 (assay > 99%, Janssen Chimica), KOH (assay > 86.7%, VWR Chemicals), $KHCO_3$ (assay > 99.7%, Aldrich), KCl (assay > 99.5%, Fluka), CsOH (assay ≥ 99.5%, Sigma Aldrich) or NaOH (assay ≥ 97%, Sigma Aldrich) as supporting electrolyte has been employed.
H_2SO_4 (assay > 98%, Sigma-Aldrich) was used to fix the initial pH of the solution.
To feed the systems, CO_2 (99.999% purity) supplied from Rivoira or Criomed and N_2 (99.999% purity) supplied by Air Liquide were employed.

Several electrodes (listed below) were employed and pretreated or prepared before each experiment as followed:

i) Sn cathode

Tin sheet electrode (metallic tin foil RPE, assay > 99%) was supplied by Carlo Erba. Since Sn electrode could be affected by degradation and/or deactivation under cathodic polarizations [48], after each test, the tin cathode was subjected to mechanically smoothing treatment, chemically pre-treated with a water solution of 11% HNO_3 (Romil Chemicals) for 2 min and, subsequently, cleaned with an ultrasound bath in distillate water for 5 min before each test using a LabSonic FalcSonicator.

ii) Ag cathode

Silver plate electrode was firstly polished with an alumina powder suspension (size 1 μm), sonicated in bi-distillate water for 10 min using a LabSonic FalcSonicator., and then rinsed with bi-distillate water, before each test.

iii) hs-Ag cathode

A high surface silver electrode, namely hs-Ag, was made by commercial nanoparticles supported on carbon fiber paper (PTFE treated to 5%). The hs-Ag electrodes were prepared via hand-painting techniques, previously reported in detail in [123]; the catalyst ink was prepared by mixing Ag catalyst (unsupported Ag nanoparticles, < 100 nm particle size, 99.5% trace metals basis, Sigma-Aldrich), deionized H_2O (200 μL), Nafion® perfluorinated resin solution (5 wt%, in lower aliphatic alcohols and water, ρ = 0.874 g/mL, Sigma Aldrich; 10:1 catalyst-to-Nafion ratio) and isopropyl alcohol (200 μL). Subsequently, the ink was sonicated for 20 minutes by a LabSonic FalcSonicator, hand-painted using a paintbrush to cover with catalyst a total geometrical area of 1.5 cm^2 and dried under an atmosphere of N_2. The actual catalyst loading was of 0.5 ± 0.07 mg cm^{-2}, determined by weighing the carbon fiber paper before and after deposition. New electrode was used for each experiment.

iv) Ag-GDE cathode

The gas diffusion electrodes were prepared by airbrushing the catalyst ink on Sigracet 35 BC (GDLs) (Fuel Cell Store) using an automated airbrushing setup [123]. The catalyst inks were prepared by mixing Ag nanoparticles (commercial Ag-NPs < 100 nm, purity: 99.5% trace metals basis, Sigma Aldrich) with 1600 μL of Millipore DI water (> 18 MΩ cm), Nafion solution (5 wt%, Fuel Cell Earth; 10:1 catalyst-to-Nafion ratio), and 1600 μL of isopropyl alcohol (IPA). The ink was sonicated (Vibra-Cell ultrasonic processor, Sonics & Materials) for 20 minutes and then airbrushed onto the gas diffusion layer with a geometric area of 5 x 2 cm^2, in order to obtain 4 electrodes by cutting it.

v) Ti/IrO_2-Ta_2O_5 anode

Ti/IrO_2-Ta_2O_5 sheet electrode, commercial DSA®, was supplied by ElectroCell AB. It was polished by ultrasound bath in bi-distillate water for 10 min using a LabSonic FalcSonicator.

vi) Compact graphite anode

Compact graphite was supplied by Carbon Lorraine. It was mechanically scrubbed with sandpaper (P-800) and sonicated in bi-distillate water until the water resulted in transparently.

vii) IrO_2-GDE anode

The gas diffusion electrodes were prepared by airbrushing the catalyst ink on Sigracet 35 BC (GDLs) (Fuel Cell Store) using an automated airbrushing setup [123]. The catalyst inks were prepared by mixing iridium oxide IrO_2 nanoparticles (commercial IrO_2-NPs, purity: 99.99% metals basis, Ir 84.5% min., Alfa-Aeser) with 1600 µL of Millipore DI water (> 18 MΩ cm), Nafion solution (IrO_2-NPs/Nafion = 0.28 g/mL$_{Nafion}$; 5 wt%, Fuel Cell Earth), and 1600 µL of isopropyl alcohol (IPA). The ink was sonicated (Vibra-Cell ultrasonic processor, Sonics & Materials) for 20 minutes and then airbrushed onto the gas diffusion layer with a geometric area of 5 x 2 cm^2, in order to obtain 4 electrodes by cutting it. The final catalyst loadings were 3 ± 0.3 mg$_{IrO_2}$ cm^{-2}.

Saturated calomel electrode (SCE) (supplied by Radiometer Analytical) was used as a reference electrode and all the working potentials were referred to it.

5.2 Electrochemical apparatus

Electrochemical conversion of CO_2 was performed using four different system:

i) system I: conventional undivided lab-glass cell;
ii) system II: stainless steel cell;
iii) system III: scale up system equipped with a filter press cell with a continuous recirculation of pressurized electrolyte;
iv) system IV: electrolyzer flow cell equipped with a Gas Diffusion Electrode (GDE).

To carry out the electrolyses, an Amel 2053 potentiostat/galvanostat at room temperature were used under amperostatic or potentiostatic mode. The current density was computed as the ratio between the current intensity and the wet surface area of cathode exposed to the anode Experiments were repeated at least twice, giving rise to reproducibility within 5% of the results.

5.2.1 System I: Conventional undivided lab-glass cell

The system I was a conventional undivided glass cell showed in *Figure 5.1*. The top of cell was characterized by five holes in which were located: *i)* a gas bubbler (inlet/outlet of CO_2 or N_2 gas), *ii)* a reference electrode, *iii)* and *iv)* cathode and anode electrode's collectors, and *v)* a glass cap. The gas bubbler outlet was connected to a glass gas sampler and, then, at a flow meter, in order to take a gas sample (by using a gastight syringe) and fix at a constant value the gas flow rate, i.e. 0.1 L min^{-1}, respectively. The volume of electrolyte solution was 50 mL. The stirring of the solution was performed with a magnetic stirrer.

Figure 5.1 System I - Conventional lab glass cell.

5.2.2 System II: Stainless steel cell

The system II consisted in an AISI 316 stainless steel cell showed in *Figure 5.2*. It was a batch undivided cell with a cylindrical geometry able to work at higher pressure than the atmospheric one. The high-pressure vessel was equipped with two insulated-copper collectors for the anode and cathode electrode, a pressure gauge and a dip tube connected to a pressure relief valve that was used to regulate the operative pressure. The system worked with a continuous supply of carbon dioxide without accumulation of gases. CO_2 was used to pressurize the reactor and fed to the system at 100 mL min^{-1}. A pressure reducer was used to control the operating pressure. Each connection was made in an AISI 316 stainless steel. The volume of the loaded electrolytic solution was 50 mL. The stirring of the solution was performed with a magnetic stirrer. The electrode gap was about 1 cm for both systems.

In the case of synthesis of formic acid, in order to try to increase the cathodic generation of formic acid and reducing its anodic consumption, a high ratio between cathode and anode surfaces was used.

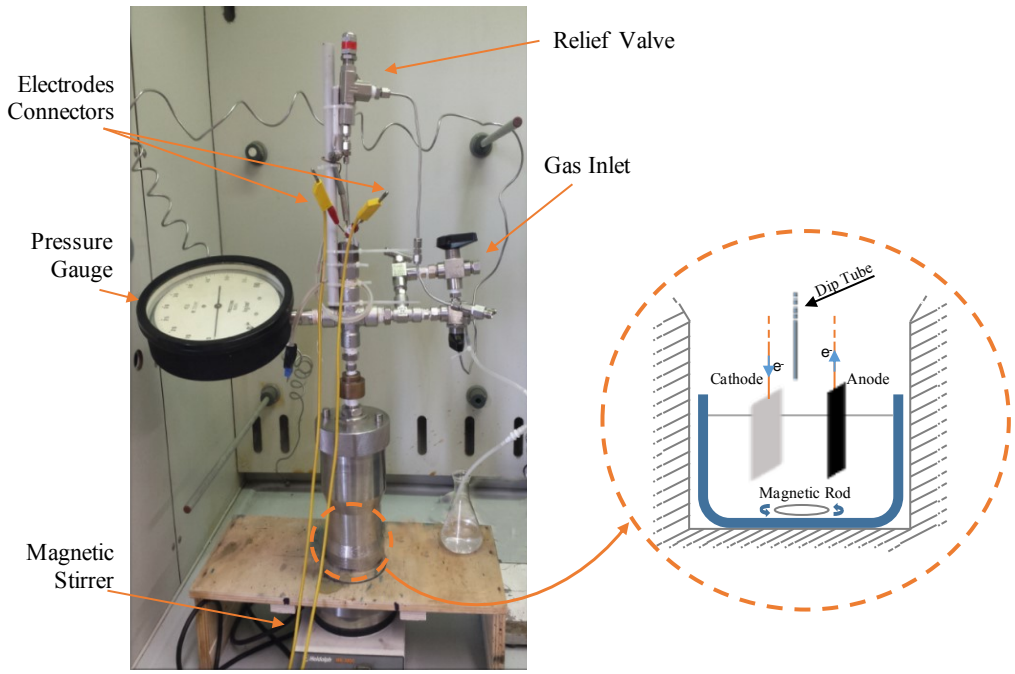

Figure 5.2 System II – Undivided stainless-steel cell able to work at high pressure.

5.2.3 System III: Scale up system equipped with a filter press cell

The system III was constituted of a continuous recirculation reaction system (*Figure 5.3*) equipped by: I) a pressurized undivided filter-press cell with parallel electrodes (in detail shown in ***Section 6.2.1*** – *Figure 6.6*); II) a centrifugal pump (*MicroPump GHA-V21* with a maximum power pumping of 200 mL min^{-1}); III) a stainless steel tank equipped with three connecting lines in the top: one for the CO_2 input, one for the products gas phase output and one connected with the bottom line for the circulation of the liquid phase; IV) a parallel line to the tank, equipped with a view-cell to check the liquid level in the system. The system was equipped with a pressure gauge and a pressure relief valve used to regulate the operative pressure; each connection is made in an AISI 316 stainless steel. CO_2 was fed to the system at a flow of 100 mL min^{-1} pressurizing the system. The system worked with a continuous supply of carbon dioxide without accumulation of gases. A continuous

circulation of distilled water washed the system after each experiment. The system volume is more of 1 L. The cell was equipped with a tin sheet cathode (metallic tin foil RPE, assay > 99%, supplied by Carlo Erba) and a Ti/IrO_2-Ta_2O_5 sheet anode (commercial DSA from ElectroCell AB); the electrodes gap was 0.5 cm. The working area of the electrodes was 9 cm^2. The current density was computed as the ratio between the current intensity and the wet surface area of the tin cathode exposed to the anode. The volume of the loaded electrolytic solution was 0.9 L for most of electrolyses and 0.5 L only for the experiment aimed to evaluate the time effect. Picture of the overall system is reported in ***Section 6.2.1*** – *Figure 6.6.*

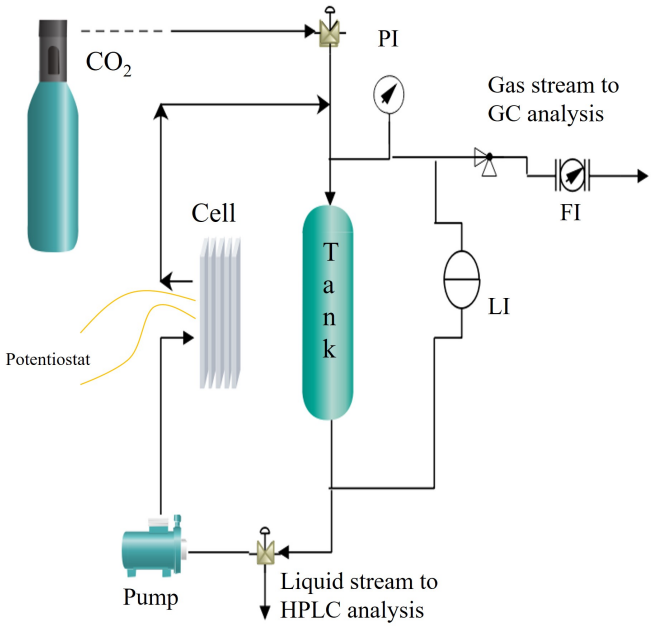

Figure 5.3 System III - Scale up system equipped with a filter press cell: overall arrangement of the pilot reactor. Reproduced from Electrochimica Acta, 277, F. Proietto, B. Schiavo, A. Galia, O. Scialdone, Electrochemical conversion of CO_2 to HCOOH at tin cathode in a pressurized undivided filter-press cell, 30 – 40, Copyright (2018), with permission from Elsevier.

5.2.4 System IV: GDE electrolyzer flow cell

The system IV was an electrolyzer flow cell fitted out with a GDEs, used at the University of Illinois at Urbana-Champaign. The overall set-up is showed in *Figure 5.4. Figure 5.5* reports a schematic design of the electrolizer flow cell; in particular, it was characterized by two external metallic current collectors and body of the cell (anode and cathode endplate) and one PEEK frame located in the middle of them, that is the electrolyte frame. Ag- or IrO_2-GDEs ($A_{cathode}$ =1 cm^2) was located between the electrode end plate and the electrolyte frame. Also, a gasket of soft solid silicone (HT6210 10 Durometer Silicone 0.015'') was placed as frame on the Ag-GDE to avoid gas leakages from the sides of the frames.

To set the electrolyte and CO_2 flow rate, respectively, a syringe pump (supplied by Pump 33, Harvard Apparatus) and a mass flow controller (supplied by Smart Trak 2, Sierra Instruments) were used. The effluent gas stream was sampled automatically by gas chromatography (Themo Finnegan Trace GC) with a thermal conductivity detector (TCD) at 200°C.The GC was equipped with a Carboxen-1000 column (temperature was kept constant at 150°C) (supplied by Supelco) and helium was the carries gas at flow rate of 20 mL min^{-1}. The only gas product was CO and H_2. For each test, both cathode and anode GDE was replaced with a new one.

Potentiostatic or galvanostatic electrochemical experiments were carried out by using a Metrohm Autolab PGSTAT302N.

To ensure that the anode side was never rate-limiting, we used a very high anode catalyst loading of 3 mg cm^{-2} unless otherwise noted.

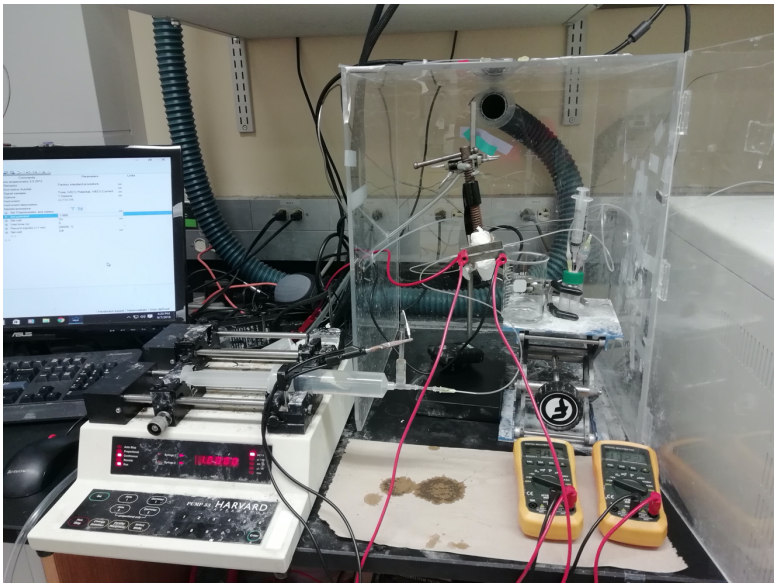

Figure 5.4 Overall arrangement of GDE electrolizer flow rate used at University of Illinois at Urbana Champaign

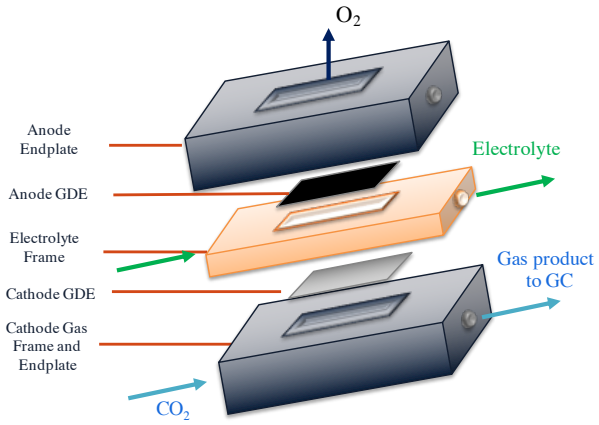

Figure 5.5 Schematic design of GDE electrolyzer flow cell.

5.3 Electrochemical characterizations

LSV and CV characterizations were performed by using: I) a conventional three-electrode cell (*System I*) with a Saturated Calomel Electrode reference and a Pt wire counter electrode; and II) an AISI316 stainless steel cell (*System II*) with cylindrical geometry. The latter was used to carry out the pseudo-polarization curves at CO_2 pressure higher than the atmospheric one by changing the overall cell potential. The characterizations were performed at several values of mixing rate (0 - 600 rpm), of CO_2 pressure (1- 30 bar) and at different pH values, i.e. 2, 3 and 4; H_2SO_4 (Sigma Aldrich) was used to set the pH. Stirring of the solution was made with a magnetic stirrer. Prior to all characterization, the solution was purged for 25 minutes by either N_2 (99.999% purity; supplied by Air Liquide) or CO_2 (99.999% purity; supplied by Rivoira). The geometric area of the working electrode, i.e. Sn, Ag or hs-Ag, was 0.1 cm^2. LSVs and CVs were acquired with a scan rate of 0.005 and 0.030 V s^{-1}, respectively, using an AutoLab PG- STAT12.

The partial current of CO_2 reduction, j_{CO_2},was computed under the assumption that the current of the H_2 evolution in a CO_2 atmosphere is the same as in an atmosphere of an inert gas, i.e., the current of hydrogen evolution and carbon dioxide reduction are additive.

The limiting current density is defined as follows:

$$j_{lim} = z * F * \frac{D}{\delta} * c^b_{CO_2}$$

where z is the number of electrons involved in the CO_2 reduction, F the faraday constant (96487 C mol^{-1}), D the diffusion coefficient, δ the thickness of the stagnant layer and $c^b_{CO_2}$ the bulk CO_2 concentration.

It was computed considering the solubility of CO_2 in water, $c^b_{CO_2}$, at 25°C [106], D_{CO_2}= 1.94 10^{-9} m^2 s^{-1} [124] while δ was previously estimated in our laboratory for each adopted mixing rate trough a well-known diffusion limiting current technique.

The thickness of the stagnant layer, δ, in the adopted condition was defined through a well-known diffusion limiting current technique using a very stable redox couple (i.e., Fe^{2+}/Fe^{3+}). The electrolytic solutions were constituted of aqueous solutions with the same concentrations of $K_4Fe(CN)_6$ thrihydrate 99% (Carlo Erba reagents) and $K_3Fe(CN)_6$ 99% (Merk) (20, 40 and 80 mM). The diffusion coefficient D values in water were assumed of: i) 6.631 10^{-10} m^2 s^{-1} for this couple [125,126]; ii) 1 10^{-9} m^2 s^{-1} for the formic acid; and iii) 1.94 10^{-9} m^2 s^{-1} for the CO_2 [124].

Hence, the thickness of the stagnant layer was evaluated using the following equation:

$$\delta = z\ F\ D * \ \partial c/\partial j_{lim}$$

where z is 1 for the Fe^{2+}/Fe^{3+} and $\partial c/\partial j_{lim}$ is the experimental slope obtained plotting the concentrations of the used redox couple, i.e. 20, 40 and 80 mM, vs. the j_{lim} recorded by using a AutoLab PG- STAT12 at 0.005 V s^{-1} scan rate.

Table 5.1 reports the δ at various rpm/electrolyte flow rate estimated for *System I - II* and *System III*.

Table 5.1 Estimated thickness of the stagnant layer, δ.

Entry	*Mixing rate or electrolyte flow rate*	*δ / m*
1	0 rpm	110 10^{-6}
2	500 rpm	55 10^{-6}
3	30 mL min^{-1}	144 10^{-6}
4	100 mL min^{-1}	96 10^{-6}
5	200 mL min^{-1}	57 10^{-6}

5.4 Analysis

5.4.1 Liquid analysis

Agilent HP 1100 HPLC fitted out with Rezex ROA-Organic Acid H^+ (8%) column (Phenomenex) at 55 °C and coupled with a UV detector working at 210 nm was used to evaluate the formic acid concentration. The used mobile phase is a 0.005 N H_2SO_4 water solution at pH 2.5 eluted at 0.6 mL min^{-1}. A pure standard of formic acid (purity: 99-100% supplied by Sigma-Aldrich) was adopted to calibrate the instrument for its quantitative determination. The formic acid production rate was expressed as the formic acid produced per unit of the working area and unit of time (mmol h^{-1} cm^{-2}).

The faradaic efficiency, *FE*, and the instantaneous faradaic efficiency, *IFE*, were defined, as follows:

$$FE = 2\,F\,V\,[HCOOH]_t / I\,t$$

$$IFE = 2\,F\,V\,([HCOOH]_{t+\Delta t} - [HCOOH]_t) / I\,\Delta t$$

where F is the faradic constant (96485), V the solution volume, $[HCOOH]_t$ the concentration of formic acid at the time t and I the current intensity.

5.4.2 Gas analysis

The gas composition was evaluated by gas chromatography using an Agilent 7890B GC fitted out with a Supelco Carboxen® 60/80 column and a thermal conductivity detector (TCD), working at 230°C. Helium (99.999%, Air Liquide) at 1 bar was used as carrier gas. The temperature of the column was programmed, that is: an isotherm at 35°C for 5 min followed by a 20°C min^{-1} ramp up to 225°C and by an isothermal step for 40 min. A gas-

tight syringe of 250 µL was used to take a gaseous sample from a pierceable septum located in the effluent gas stream.

The faradaic efficiency, *FE*, energetic efficiency, *EE*, and the energetic consumption (Wh/mol_{CO}) for gas products were defined, as follows:

$$FE_i = 2\,F\,n_i/I\,t$$

$$EE = E°_{cell}\,FE_i/\Delta V$$

$$Energetic\ Consumption = I * \Delta V/n_{CO}$$

where F is the faradaic constant (96485 C mol^{-1}), n_i mole of i product and I the current intensity, t the time, $E°_{cell}$ is the standard cell potential: -1.33 for the electroreduction for CO_2 to CO coupled to O_2 evolution, ΔV the applied cell potential.

The CO production rate, $r_{CO,}$ (mol h^{-1} m^{-2}) was calculated as follow:

$$r_{CO} = FE_{CO}\,j * 3600/2\,F$$

where the FE_{CO} is the current efficiency of CO, j the current density (A m^{-2}); 3600 s/h.

Chapter 6

Synthesis of formic acid: results and discussion

6 Synthesis of formic acid: results and discussion[6]

In this chapter, electrochemical conversion of CO_2 to formic acid was investigated using a simple and cheap foil Sn cathode and an undivided cell under pressurize conditions. In order to optimize the process, the effect of various operating parameters, including the pressure, the current density, the mixing rate, was evaluated by both polarization and electrolyses. The scale-up of the system was carried out as well as the development of a theoretical model that allowed to describe and predict the effect of operative parameters. Eventually, the stability of the system was studied for more than 40 hours.

6.1 Polarization and electrolysis experiments and discussion of reaction mechanism

In the first stage, a preliminary series of polarization and electrolyses was performed both a 1 bar and under pressure to achieve information on the reaction mechanism and to evaluate the effect of some operative parameters on the performances of the process, evaluated in terms of final formic acid concentration and faradaic efficiency.

6.1.1 Reaction mechanism: polarization and electrolysis experiments

The mechanism of the electrochemical reduction of CO_2 at different cathodes in aqueous media was largely investigated in literature in order to characterize the process. Among

[6] The following sections have partially reproduced from the content of articles of mine: ChemElectroChem, 6, F. Proietto, A. Galia, O. Scialdone, Electrochemical conversion of CO2 to HCOOH at Tin Cathode: Development of a Theoretical Model and Comparison with Experimental Results, 162–172, Copyright (2019), with permission from John Wiley and Sons. Electrochimica Acta, 277, F. Proietto, B. Schiavo, A. Galia, O. Scialdone, Electrochemical conversion of CO_2 to HCOOH at tin cathode in a pressurized undivided filter-press cell, 30–40, Copyright (2018), with permission from Elsevier.Electrochimica Acta, 199, O. Scialdone, A. Galia, G. Lo Nero, F. Proietto, S. Sabatino, B. Schiavo, Electrochemical reduction of carbon dioxide to formic acid at a tin cathode in divided and undivided cells: Effect of carbon dioxide pressure and other operating parameters, 332–341, Copyright (2016), with permission from Elsevier.

these studies, several authors [34,38,41,44] have proposed that the reaction mechanism for CO_2 reduction at tin cathode involves the following steps:

i)dissolution of gaseous carbon dioxide;

ii) mass transfer of dissolved CO_2 to the cathode surface (whose rate is given by k_m ($[CO_2]^b$-[$CO_2]^0$), where $[CO_2]^b$ and $[CO_2]^0$ are the concentrations of CO_2 in the bulk and at the electrode surface, respectively, and k_m is the mass transfer coefficient for CO_2);

iii) adsorption of CO_2

$$CO_{2_{(aq)}} = CO_{2_{(ads)}} \quad (6.1)$$

iv) cathodic reduction of adsorbed CO_2 to adsorbed $CO_2^{-\cdot}$

$$CO_{2_{(ads)}} + e^- = CO_{2_{(ads)}}^{-\cdot} \quad (6.2)$$

v) cathodic reduction of adsorbed $CO_2^{-\cdot}$ to HCOOH

$$CO_{2_{(ads)}}^{-\cdot} + H^+ = HCO_{2_{(ads)}} \quad (6.3)$$

$$HCO_{2_{(ads)}} + H^+ + e^- = HCOOH \quad (6.4)$$

Some authors have proposed that on some electrodes [118,127], the reduction of carbon dioxide can take place with a different mechanism based on the reaction between adsorbed H and adsorbed carbon dioxide:

$$H_{(ads)} + CO_{2_{(ads)}} = HCO_{2_{(ads)}} \quad (6.5)$$

$$HCO_{2_{(ads)}} + H^+ + e^- = HCOOH \quad (6.4)$$

In particular, according to Paik and co-authors [127], this mechanism is likely to be involved at Hg for weakly acidic pH. However, as shown in the following sections, in our case experimental data seem to be more easily described by the reaction mechanism shown in *Equations 6.1 – 6.4*. Hence, this mechanism, which involves the *Eq. 6.5*, will not be considered in the following.

In this context, the main competitive process to the CO_2 reduction in aqueous electrolyte is the H_2 evolution in acid media. The H_2 evolution is expected to take place by the following reactions:

i) cathodic reduction of protons to adsorbed H

$$H^+ + e^- = H_{(ads)} \qquad \text{(Volmer reaction)} \qquad (6.6)$$

ii) evolution of hydrogen by

$$H_{(ads)} + H^+ + e^- = H_2 \qquad \text{(Heyrovsky reaction)} \qquad (6.7a)$$

or

$$H_{(ads)} + H_{(ads)} = H_2 \qquad \text{(Tafel reaction)} \qquad (6.7b)$$

According to Azizi et al. [128] at tin in acidic conditions and low negative potentials, the Heyrovsky step (*Eq. 6.7a*) prevails on Tafel one (*Eq. 6.7b*), it is the r.d.s. (e.g. $r_{6.6} > r_{6.7a} > r_{6.7b}$) and the superficial coverage by adsorbed hydrogen is negligible. Conversely, at high negative potentials, the surface coverage of the electrode by adsorbed hydrogen reaches a higher value and the mechanism of the HER is a consecutive combination of Volmer and Heyrovsky steps with equal rates, the rate of Tafel reaction being negligible (e.g. $r_{6.6} \sim r_{6.7a} > r_{6.7b}$).

In order to understand the influence of the H_2 evolution on the process, a series of polarization experiments was recorded at different pH values in N_2 or CO_2 aqueous solution

of 0.1 M Na_2SO_4 (*Figure 6.1*). Na_2SO_4 was chosen as supporting electrolyte because, in undivided cell, according to previous studies [34] discussed in previous paragraph (see ***Section 2.3***), it gives rise to higher concentration and FE of formic acid.

As shown in *Figure 6.1a*, under N_2 atmosphere and pH 4, the hydrogen evolution starts at a potential of about -1.55 V (vs. SCE) and the dependence of the current density vs. the potential becomes more relevant at potentials slightly more negative than -2 V. When CO_2 is added to the system (at 1 bar), an increase of the current is observed for potentials close to -1.5 V (*Figure 6.1a*). The difference between the overall current and the current recorded in the absence of CO_2, called j_{CO_2}, increases up to about -1.8 V (*Figure 6.1d*); it assumes an almost constant value for a potential between -1.8 and about -2.05 V and decreases for more negative potentials. When CO_2 is removed from the system, the current density comes back again to the values recorded during the first polarization recorded under N_2 atmosphere.

A similar behavior was observed at pH 3 (*Figure 6.1b*) and pH 2 (*Figure 6.1c*), even if at pH 2 the hydrogen evolution starts at a potential of about -1.1 V (vs. SCE).

As shown in *Figure 6.1d*, at all pH the maximum value of j_{CO_2} is close to the limiting current density, j_{lim}, estimated for a process under the kinetic control of the mass transfer in the absence of mixing (j_{lim} ~ 10 mA cm^{-2} at 0 rpm).

Figure 6.1e reports the cyclic voltammogram achieved at pH 4 and 30 mV s^{-1}; the anodic peaks between −0.75 and −1 V and the cathodic peak at about −1.1 V (which can be attributed to the formation and the reduction of tin oxides, respectively) are partially suppressed under CO_2 atmosphere. Furthermore, the addition of CO_2 gives rise to a shoulder at potentials close to -2.0 V and also in this case, for very negative potentials, j_{CO_2} decreases with the potential (*Figure 6.1e, inset*).

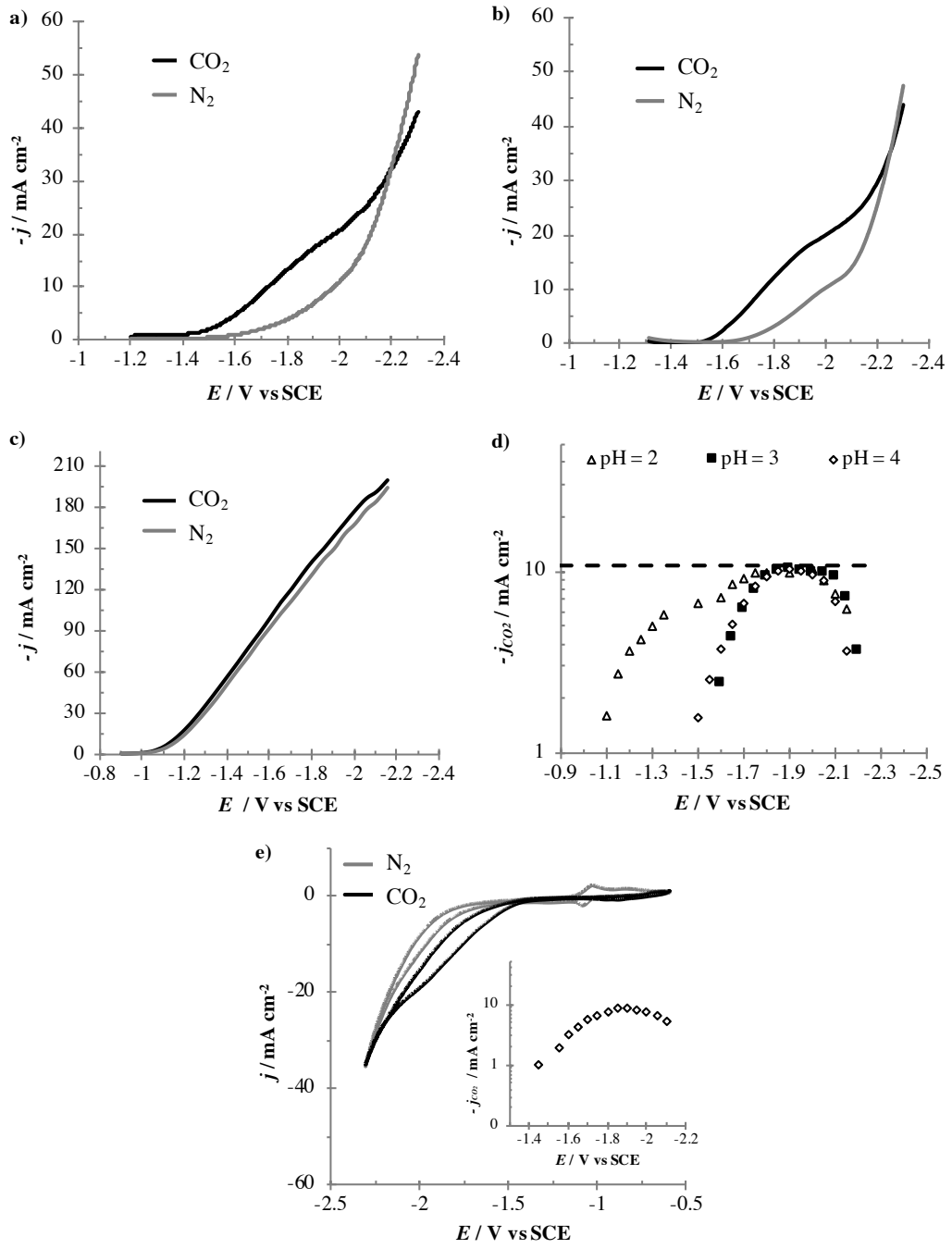

Figure 6.1 LSVs at 5 mV s^{-1} under 1 bar N_2 (grey line) and CO_2 (black line) -saturated water solution of 0.1 M Na_2SO_4 at (a) pH = 4, (b) pH = 3 and (c) pH = 2. (d) Comparison of the CO_2 partial current density at different pH values. (e) CV at 30 mV s^{-1} under N_2 (grey line) and CO_2 (black line) -saturated solution of 0.1 M Na_2SO_4 at pH = 4. System I. Volume of the solution (V): 0.05 L. $A_{cathode}$ = 0.1 cm^2. Working electrode: Sn. Counter electrode: Pt wire.

Figure 6.1. Reproduced from ChemElectroChem, 6, F. Proietto, A. Galia, O. Scialdone, Electrochemical conversion of CO_2 to HCOOH at Tin Cathode: Development of a Theoretical Model and Comparison with Experimental Results, 162 – 172, Copyright (2019), with permission from John Wiley and Sons.

According to the proposed reaction mechanism and to experimental results reported in *Figure 6.1*, four relevant regions can be considered in the polarization curves recorded at pH 3 and 4:

Region 1. For not sufficiently negative potentials, E > -1.5 V vs SCE, CO_2 reduction does not take place in a significant way (j < 1 mA cm^{-2}) for kinetic reasons. According to the literature [129] for these very low current densities, the r.d.s. would be the second electron transfer (*Eq. 6.4*).

*Region 2***.** For potential values between -1.5 and -1.75 V, the more negative is the potential the higher is j_{CO_2}. The slope of the Tafel curve has a value of ca. -352 mV. According to Vassiliev et al. [129], under these conditions, the process is limited by the first electron transfer (*Eq. 6.2*).

Region 3. For potentials between -1.75 V and -2.1 V, j_{CO_2} reaches a maximum value which is close to j_{lim}, since the process is under the kinetic control of the mass transfer of CO_2 to the cathode surface.

Region 4. For potentials more negative than -2.2 V, j_{CO_2} decreases with the potential. A similar behaviour was observed in literature [129], but not commented in detail. Under these conditions, the cathodic reduction of water (*Eq.s 6.6 and 6.7*) is expected to be very fast, thus limiting or suppressing the formation of HCOOH for various reasons: (i) the H coverage is expected to increase, thus limiting the rate of CO_2 adsorption (*see Eq. 6.1*); (ii) the concentration of protons at the tin surface is expected to decrease, thus reducing the rate of both *Eq.s 6.3 and 6.4*; (iii) the high hydrogen evolution can cause a partial covering of the electrode surface, thus decreasing the rate of the mass transfer of CO_2 to the cathode. In particular, by assuming a competition between the adsorption of CO_2 and H, this region is expected to be shifted to more negative potentials by both higher mixing rates or higher CO_2 pressures.

a) Effect of mixing

In order to better characterize the process and the reaction scheme proposed, a series of polarizations and electrolyses at tin cathode was performed at pH 4 and different mixing rates, *N*, in CO_2 saturated aqueous electrolyte of Na_2SO_4 (*Figure 6.2*). As shown in *Figure 6.2a*, for polarization, a curve with a maximum was obtained for j_{CO_2} at all rpm, i.e. 0, 300, 500 rpm. In detail, j_{CO_2} did not depend on rpm for E > -1.75 V (j_{CO_2}< 6 mA cm^{-2}), when the process is not limited by the mass transfer of CO_2 to the cathode (regions 1 and 2), while j_{CO_2} increased with the mixing rate for more negative values of E, when the process is kinetically influenced by the mass transfer (region 3), according to the picture depicted previously. In particular, it is relevant to mention that the maximum values of j_{CO_2} achieved at different rpm are closer (even if slightly lower) to the corresponding estimated values of j_{lim} (ca. 10 and 22 mA cm^{-2} at 0 and 500 rpm, respectively); thus, confirming our assumption that in region 3 the CO_2 reduction, at atmospheric pressure, is under kinetic control of the mass transport. Moreover, as expected, at all mixing rates, j_{CO_2} decreases at higher negative potential for all the reasons above listed (region 4).

In order to validate these results, the effect of the mixing rate on the CO_2 reduction at tin cathode was investigated at 11.6 mA cm^{-2}, a value slightly higher than j_{lim} estimated in the absence of mixing rate, performing short electrolyses of about 1 h. As shown in *Figure 6.2b*, the enhancement of mixing rate increases the formic acid production and the faradaic efficiency. In particular, the rate of production of formic acid after 1 h increases from about 0.08 to 0.11 millimoles h^{-1} cm^{-2} and FE from about 39 to 48% enhancing the *N* from 0 to 600 rpm, according to results of polarization curves.

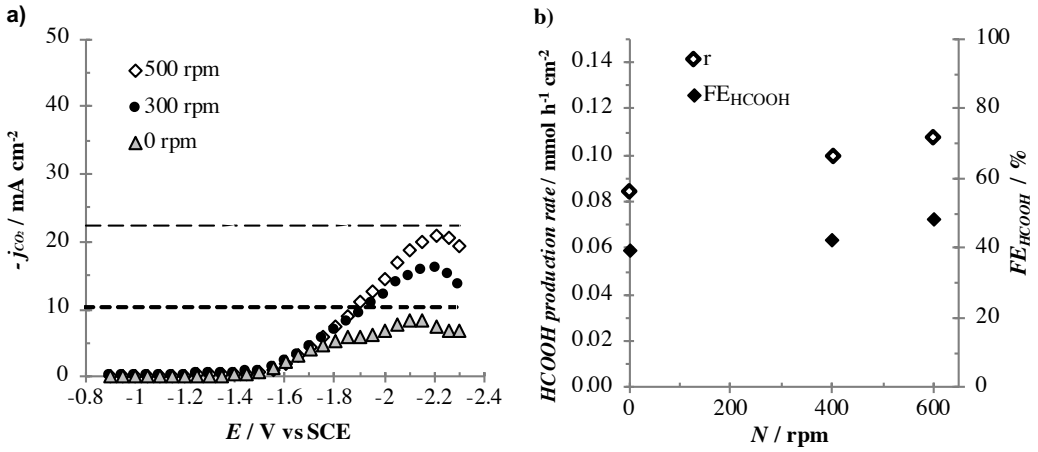

Figure 6.2 (a) Effect of the mixing rate on the CO_2 partial current density. The dotted lines are referred to the limit current density evaluated at 0 (**---**) and 500 (— — —) rpm. The relative polarizations were performed in a conventional-lab cell (System I). Volume of the solution (V): 0.05 L. $A_{cathode}$= 0.1 cm^2. Working electrode: Sn. Counter electrode: Pt wire. (b) Effect of the mixing rate on the formic acid production rate and on FE. Electrolysis performed in a conventional-lab glass cell (System I) equipped with Sn cathode (4.5 cm^2) under amperostatic condition (11.6 mA cm^{-2}) and atmospheric CO_2 pressure. Volume of the solution (V): 0.075 L. Time: 1h. Reproduced from ChemElectroChem, 6, F. Proietto, A. Galia, O. Scialdone, Electrochemical conversion of CO_2 to HCOOH at Tin Cathode: Development of a Theoretical Model and Comparison with Experimental Results, 162 – 172, Copyright (2019), with permission from John Wiley and Sons.

b) Effect of pressure

In a second stage, in order to characterize the steps involved in the process at high CO_2 pressure, current densities were recorded as a function of cell potential in the presence of N_2 and with different pressures of CO_2 in the range 1 – 30 bar using a stainless-steel batch cell (System II, previously described in ***Section 5.2.2***), evaluating the effect of the CO_2 concentration in water on the CO_2 reduction. As shown in *Figure 6.3a*, for each value of P_{CO_2}, a similar curve j_{CO_2} vs. ΔV, characterized by the presence of a maximum, is observed, thus showing the existence of four regions in polarization curves also for pressurized systems. In particular, for not too negative potentials (region 2), j_{CO_2} increases with the pressure even if the enhancement becomes very small for the highest P_{CO_2} or, in other words, as shown in *Figure 6.3b*, j_{CO_2} increases proportionally to [CO_2] for lower values of [CO_2] and tend to a plateau value for high values. Vassiliev et al. [129] have shown that the rate of CO_2 electroreduction at various electrodes including tin increases proportionally to a fractional power of P_{CO_2}. According to these authors, the fractional order of the reaction

indicates that the rate-determining steps of the reaction involve adsorbed molecules with a strongly repulsion between them.

Also in our case, experimental data indicate that the r.d.s. involve adsorbed molecules. In particular, as shown in *Figure 6.3c* at -2.55 V data are well fitted by a Langmuir-Hinshelwood type expression (*Eq. 6.8*):

$$r = k(E)\frac{b\,[CO_2]}{1+b\,[CO_2]} \qquad (6.8)$$

thus, reinforcing the hypothesis that the r.d.s. in the region 2 is the cathodic reduction of adsorbed CO_2 to adsorbed $CO_2^{-\cdot}$ (*Eq. 6.2*) and indicating that the adsorption of carbon dioxide can be assumed at the equilibria and described by the Langmuir model. In particular, according to the fitting reported in *Figure 6.3c* for region 2, the coverage of the surface by carbon dioxide, θ, can be estimated to change from about 0.08 to about 0.71 increasing P_{CO_2} from 1 to 30 bar. As shown in *Figure 6.3c*, at more negative potentials (ΔV = -3.25 V; region 3), the maximum j_{CO_2} (▲) was significantly lower than j_{lim} (•••), thus showing that the r.d.s. for a pressurized system is no more the mass transfer even at very negative potentials. However, when experimental data at -3.25 V were fitted using the Langmuir-Hinshelwood expression (— • —) (*Figure 6.3c*); the fitting cannot be considered excellent. Conversely, the data in region 3 were well fitted considering a process under the mixed kinetic control of the mass transfer of CO_2 to the cathode surface and of the reduction of adsorbed CO_2 (the last, described by the Langmuir- Hinshelwood expression) (---) (*Figure 6.3c*). In particular, in this case, the coverage of the surface by carbon dioxide, θ, can be estimated to change from about 0.04 to about 0.64 and the ratio $[CO_2]^b/[CO_2]^\circ$ from 2.4 to 1.5 changing P_{CO_2} from 1 to 30 bar. Hence, the pressurized CO_2 reduction process is under mixed kinetic control of mass transport and reduction of adsorbed CO_2; in particular, it is more limited by mass transfer for lower values of P_{CO_2} and by the reduction stages for higher values of P_{CO_2}.

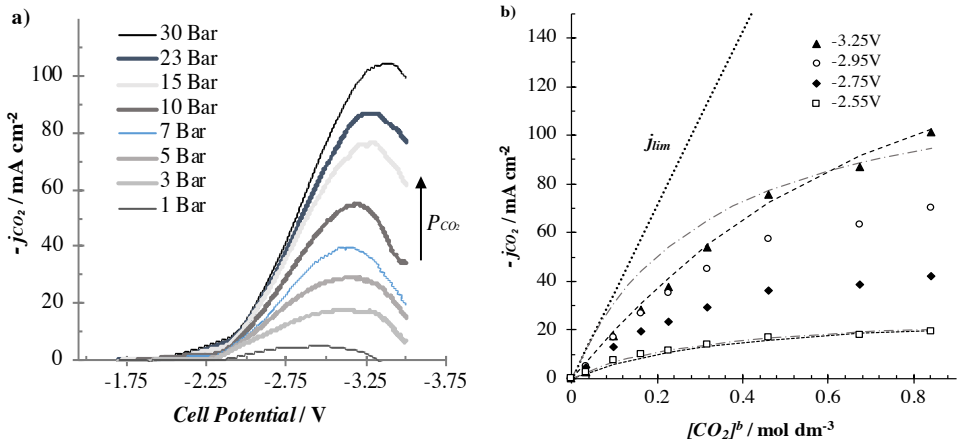

Figure 6.3 (a) CO_2 partial current density recorded by polarizations achieved at different CO_2 pressure. (b) CO_2 partial current density shown in *Figure 6.3a* plotted versus the bulk CO_2 concentration at different cell potentials: -2.55 V (□), -2.75 V (♦), -2.95 V (◯) and -3.25 V (▲). Data achieved at -2.55 V are compared with theoretical predictions based on the Langmuir-Hinshelwood expression (— • —) or on a mixed kinetic control of the mass transfer of CO_2 to the cathode surface and of the reduction of adsorbed CO_2 (where adsorption is described by the Langmuir expression) (- - -). Data achieved at -3.25 V (▲) are compared with the limiting current density (•••), the theoretical predictions based on Langmuir-Hinshelwood expression (— • —) and on a mixed kinetic control of the mass transfer of CO_2 to the cathode surface and of the reduction of adsorbed CO_2 (described by the Langmuir expression) (- - -). Pseudo-LSVs were performed in a stainless steel cell (System II) at 5mV s^{-1} in water solution of 0.1M Na_2SO_4 at pH = 4. Volume of the solution (V): 0.05 L. $A_{cathode}$ = 0.1 cm^2. Reproduced from ChemElectroChem, 6, F. Proietto, A. Galia, O. Scialdone, Electrochemical conversion of CO_2 to HCOOH at Tin Cathode: Development of a Theoretical Model and Comparison with Experimental Results, 162 – 172, Copyright (2019), with permission from John Wiley and Sons.

6.1.1.1 Electrolyses at various pressures

According to the considerations reported in the previous paragraph, the cathodic reduction of carbon dioxide can be drastically affected by the pressure. Hence, a large number of electrolyses were carried out at different pressures. Furthermore, the effect of other relevant operating parameters, such as the current density and the mixing rate on pressurized process was evaluated in detail.

6.1.1.1.1 Effect of the mixing rate

In order to evaluate the effect of the flow-dynamic for relatively high pressures, a series of electrolyses at tin cathode was performed at a relatively high pressure (23 bar) at 30 and 160 mA cm^{-2} at different rpm (0, 300 500 rpm) in CO_2 saturated aqueous electrolyte of

Na_2SO_4 (0.1 M). The electrolyses were performed using an undivided stainless-steel bath cell of about 0.05 L of solution for 1 h; according to literature [34], DSA anode was used as it favors the water oxidation with respect to formic acid one. According to theoretical considerations developed above, the mixing rate had not a significant effect of HCOOH production at the lower current density (region 2), when the process is not limited by the mass transfer of CO_2, as shown in *Figure 6.4*; indeed, at 30 mA cm^{-2}, even increasing the mixing rate from 0 to 600 rpm the HCOOH productions remain almost constant at about 0.28 mmol h^{-1} cm^{-2} and selectivity at about 46%. Conversely, according with the hypothesis that at high cell potentials (region 3) the process is under the mixed kinetic control of mass transfer of CO_2 and reduction of adsorbed CO_2, the flow-dynamics effect had an appreciable influence at very high values of current density (region 3 - 4); in particular, at 160 mA cm^{-2}, an enhancement of the mixing rate from 0, 300 to 500 rpm, step by step, give rise to an increase of the HCOOH production rate from 0.26, 0.40 to 0.46 mmol h^{-1} cm^{-2}, respectively, (*Figure 6.4*).

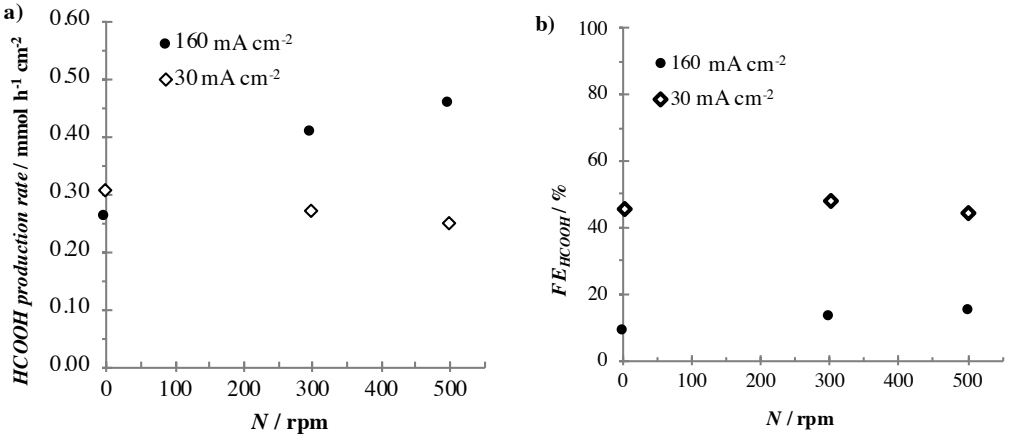

Figure 6.4 Combined effect of the mixing rate and current density on the (a) HCOOH production rate and (b) faradaic efficiency. Electrolyses were performed in a stainless-steel cell (System II) in water solution of 0.1M Na_2SO_4 at pH = 4. P_{CO_2} = 23 bar. Volume of the solution (V): 0.05 L. $A_{cathode}$ = 0.1 cm^2. Time: 1h. Reproduced from ChemElectroChem, 6, F. Proietto, A. Galia, O. Scialdone, Electrochemical conversion of CO2 to HCOOH at Tin Cathode: Development of a Theoretical Model and Comparison with Experimental Results, 162 – 172, Copyright (2019), with permission from John Wiley and Sons.

6.1.1.1.2 Effect of current density

The effect of current density was better evaluated carrying out a large number of electrolyses of 6 hours at various pressures (1- 30 bar) in a large range of current densities (11.6 – 90 mA cm^{-2}) without mixing in CO_2 saturated aqueous electrolyte of Na_2SO_4. *Figure 6.5* reports the final concentration of formic acid (*Figure 6.5a*) and the faradaic efficiency (*Figure 6.5b*) achieved at the end of the electrolyses as a function of the working pressure at different adopted current densities. According to the literature, for a fixed value of the current density, the generation of formic acid increased with the pressure reaching a plateau value for the highest values of P. As an example, at 30 mA cm^{-2}, an enhance of the pressure from 1 to 5 and 10 bar, step by step, gave rise to higher formic acid concentration from about 20 to 100 mM and up to a plateau value close to 150 mM, respectively (*Figure 6.5a*). Indeed, a further increase of the pressure up to 15 bars does not result in an appreciable variation of the performances of the process (*Figure 6.5*). Quite interestingly, these results are in good agreement with polarizations and with the reaction mechanism discussed in the previous section. Indeed, the rate of the process is determined, at least for pressurized systems, by the reduction of adsorbed CO_2, (whose rate is given by *Eq. 6.8*), which is affected by both the coverage of CO_2 and the working potential. Hence, for low CO_2 pressure (when the coverage of the surface is low), the increase of CO_2 at the cathode surface gives rise to an increase of the surface coverage, thus accelerating the reduction step. However, for high CO_2 pressure, the coverage of the surface becomes high and a further increase of carbon dioxide cannot affect significantly the reduction step.

However, according to this hypothesis, an increase of the generation of formic acid could be achieved by a coupled increase of both pressure (thus accelerating the mass transfer and adsorption stages) and of the current density (and of related working potential, thus accelerating the reduction of adsorbed CO_2). Indeed, an enhancement of the pressure and current density up to 30 bar and 90 mA cm^{-2} allows to reach concentrations of formic acid as high as 0.46 M coupled with FE_{HCOOH} of 55% (*Figure 6.5*).

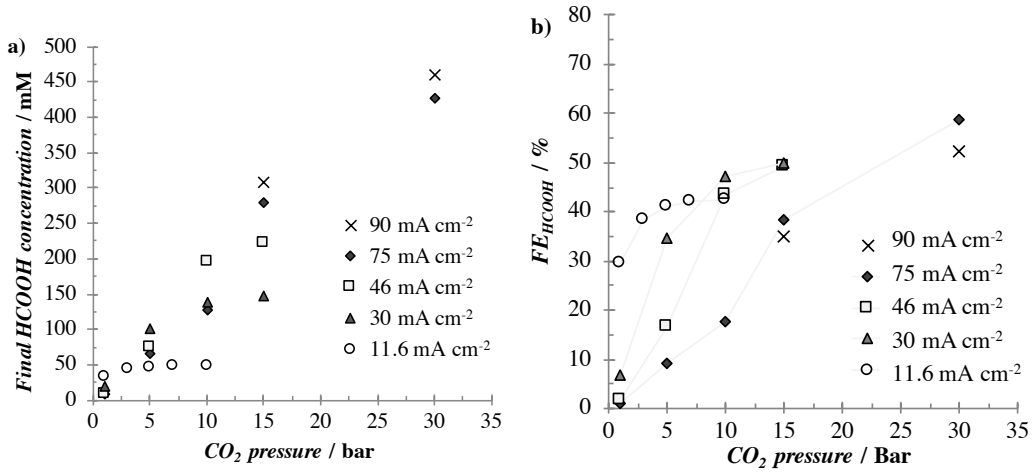

Figure 6.5 Effect of the current density on the (a) formic acid concentration and (b) faradaic efficiency. Electrolyses were performed in undivided stainless-steel cell (System II) without mixing rate and equipped with Sn cathode (4.5 cm^2) under amperostatic condition (11.6 – 90 mA cm^{-2}), range CO_2 pressure (1 - 30 bar). Volume of the solution (V): 0.05 L. Time: 6h. Reproduced from Electrochimica Acta, 199, O. Scialdone, A. Galia, G. Lo Nero, F. Proietto, S. Sabatino, B. Schiavo, Electrochemical reduction of carbon dioxide to formic acid at a tin cathode in divided and undivided cells: Effect of carbon dioxide pressure and other operating parameters, 332 – 341, Copyright (2016), with permission from Elsevier.

6.2 CO_2 electrochemical conversion in pressurized undivided filter-press cell

In spite of these good and promising results achieved at high pressure using a batch autoclave cell (System II), some steps have to be done to better evaluate the process from an applicative point of view: in particular, the scale-up in a filter-press cell under pressure has to be done and the stability of the system has to be evaluated for longer times. Indeed, up to now the carbon dioxide reduction in filter-press cells was evaluated only at room pressure and most of experiments reported in the literature concern quite low amounts of time (from few minutes to few hours) and of the charge passed [25,41,42]. Hence, in the following sections, the electrochemical reduction of CO_2 was evaluated in a simple undivided filter-press cell with 0.9 L of electrolytic solution at cheap tin cathodes under pressure (1 - 30 bar). The effect of various operating parameters, such as the current density, the flow rate and the pressure, was investigated in detail, allowing to find very

promising operating conditions for the production of formic acid. Furthermore, the performances of the process were evaluated for many hours for an amount of charge passed up to about 70 kC.

6.2.1 Development of the system

The system was scaled-up using a filter-press cell with a continuous recirculation of the pressurized solution. The picture of the system is reported in *Figure 6.6*. The overall detail of the system was described in ***Section 5.2.3***. Briefly, the experimental system was constituted of a continuous recirculation reaction system equipped by I) a pressurized undivided filter-press cell with parallel electrodes (shown in detail in *Figure 6.6b*); II) a centrifugal pump; III) a stainless steel tank equipped with three connecting lines in the top: one for the CO_2 input, one for the products gas phase output and one connected with the bottom line for the circulation of the liquid phase; IV) a parallel line to the tank, equipped with a view-cell to check the liquid level in the system. The system was equipped with a pressure gauge and a pressure relief valve used to regulate the operative pressure. It is worth to note that the system volume is more of 1 L, significantly higher than the volume of the cell currently reported in literature, and the cell was equipped with a cheaper and simple Sn sheet cathode.

6.2.2 Electrochemical conversion of CO_2

Electrochemical conversion of CO_2 to formic acid at a tin cathode was attempted in an undivided pressurized filter-press cell with a continuous recirculation of the solution (0.5 or 0.9 L). The effect of several operating parameters, including pressure, current density, flow rate and time, on the performances of the process, in terms of formic acid concentration and faradic efficiency, was investigated.

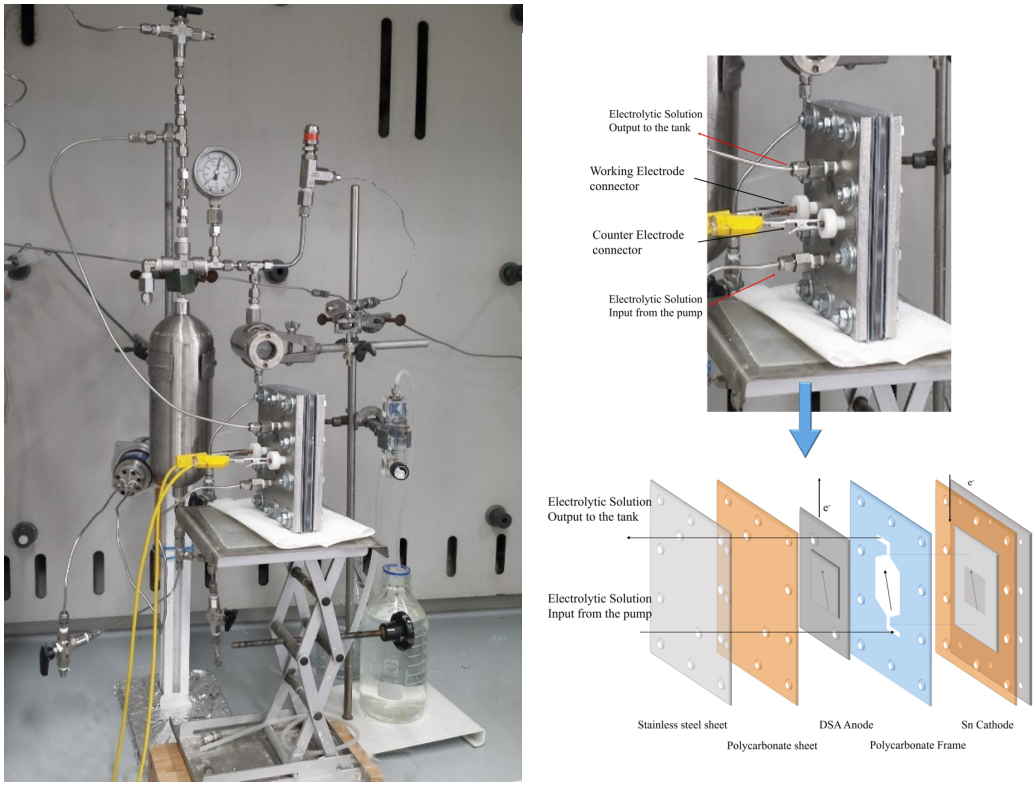

Figure 6.6 Electrochemical scaled-up system equipped with a filter-press cell (characterized by a similar industrial geometry cell) with a continuous recirculation of the pressurized solution. Reproduced from Electrochimica Acta, 277, F. Proietto, B. Schiavo, A. Galia, O. Scialdone, Electrochemical conversion of CO_2 to HCOOH at tin cathode in a pressurized undivided filter-press cell, 30 – 40, Copyright (2018), with permission from Elsevier.

6.2.2.1 First experiments at room pressure

In order to evaluate the possibility to generate HCOOH using an undivided pressurized filter-press cell with a continuous recirculation of the solution, first electrolyses were performed under galvanostatic mode at 7.8 mA cm^{-2} for 4 h using 0.9 L of 0.1 M Na_2SO_4 aqueous solution (pH 4) at 200 mL min^{-1} of electrolyte flow rate. The current density was chosen in order to be significantly lower than the limiting current density, which was estimated to be close to 22 mA cm^{-2} (see ***Section 5.3***). The carbon dioxide was fed at ambient pressure into the system in a continuous mode. As shown in *Figure 6.7*, upon increasing the time, the concentration of formic acid increases up to 2 mM after 4 h with a

rate of production of formic acid of about 0.081 mmol h^{-1} cm^{-2}. In order to achieve other data on the process, the potential products of the process were analytically determined and quantified. Formic acid was detected as the only main product in liquid phase from CO_2 reduction ($CO_2 + 2H^+ + 2e^- \rightarrow HCOOH$). In the gas phase, trace of CO, with a very low faradaic efficiency even less than 4%, ($CO_2 + 2H^+ + 2e^- \rightarrow CO$), hydrogen, produced by the water reduction (*Eq.s 6.6 and 6.7*), and oxygen, which originates from water anodic oxidation ($2H_2O = O_2 + 4H^+ + 4e^-$), were detected. Indeed, the sum of the faradic efficiencies in formic acid, carbon monoxide and hydrogen was about 99%. Hence, under adopted operating conditions the reduction of CO_2 leads almost only to formic acid, the anodic oxidation of HCOOH can be neglected (probably for the relative low concentrations of formic acid achieved coupled with the utilization of a DSA anode) and the main parasitic process is the hydrogen evolution.

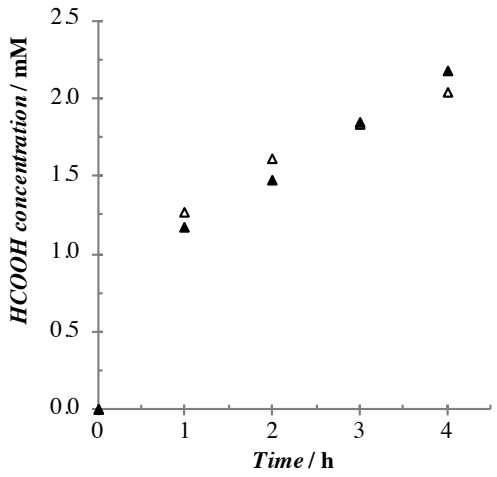

Figure 6.7 Formic acid generation at Sn cathode (9 cm^2) for 4 h using an undivided pressurized filter-press cell with a continuous recirculation of the solution at 200 mL min^{-1} (System III). Electrolyses were performed at 7.8 mA cm^{-2} in 0.1 M Na_2SO_4 aqueous electrolyte (pH 4). Reported data refers to two different electrolyses carried out under the same operating conditions, in order to evaluate the reproducibility of data. CO_2 pressure = 1 bar. Volume of the solution (V): 0.9 L.

According to polarization, CV experiments and previously results achieved in the small cell (see ***Section 6.1.1.1***), the current density dramatically is expected to affect both the rate of production and the FE of formic acid; hence, in order to better characterize the process at atmospheric pressure of CO_2, electrolysis was repeated by changing the *j* from 7.8 to 80 mA cm^{-2} at pH 4 for 2 h. In all cases, the main product of CO_2 reduction was formic acid. As shown in *Figure 6.8*, the curve HCOOH production rate vs. *j* (*Figure 6.8a*) gave a maximum for 20 mA cm^{-2}, which is very close to the j_{lim} = 22 mA cm^{-2} for adopted operating conditions, while FE decreases with *j* in all the range of adopted current density (*Figure 6.8b*). The increase of the *j* gave rise to a negative shift of the working potential, thus resulting first in an enhancement till a maximum and then in a reduction of the HCOOH production. According to polarization experiments, at higher current densities and atmospheric pressure the process is expected to be limited by mass transfer of CO_2 to the cathode surface and the production of HCOOH should remain constant. However, the decrease of the HCOOH production shows that other phenomena are involved at very negative potentials. Probably, under these conditions, the carbon dioxide reduction is hindered by one or more of the following factors all related to the hydrogen evolution which is strongly accelerated at these potentials: i) a high coverage of the electrode surface by hydrogen atoms [128], thus limiting the active sites available for CO_2; ii) the high production of H_2 gas bubbles that can partially cover and reduce the active area; iii) the acceleration of reactions *6.6* and *6.7* that can cause an increase of the local pH, thus limiting the reactions *6.3* and *6.4*.

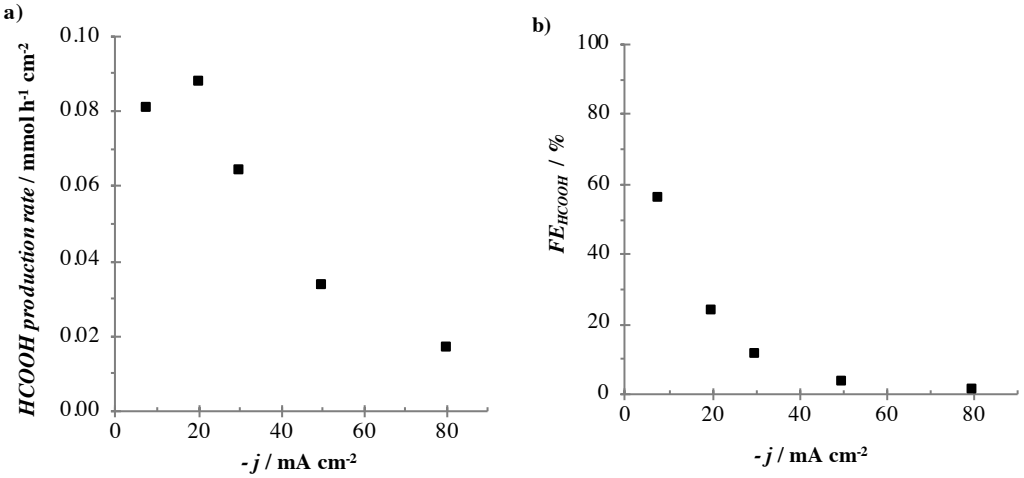

Figure 6.8 Effect of the current density on the (a) formic acid production rate and (b) faradaic efficiency. Electrolyses performed in a pressurized filter-press cell (System III) equipped with Sn cathode (9 cm^2) under amperostatic condition, fixed CO_2 pressure (1 bar) and a constant flow-rate value (200 mL min^{-1}). Volume of the solution (V): 0.9 L. Time: 2h. Reproduced from ChemElectroChem, 6, F. Proietto, A. Galia, O. Scialdone, Electrochemical conversion of CO2 to HCOOH at Tin Cathode: Development of a Theoretical Model and Comparison with Experimental Results, 162 – 172, Copyright (2019), with permission from John Wiley and Sons.

6.2.2.2 Electrolyses at high pressure

According to the polarization experiments, the j_{CO_2} increases by enhancing the amount of the CO_2 dissolved in water (*Figure 6.3a*); hence in order to improve the performances of the CO_2 electroreduction process, a series of experiments was planned in a wide range of CO_2 pressure from 1 to 30 bar at 20 mA cm^{-2} and 200 mL min^{-1}. At this current density, j_{lim} is higher than j for all adopted pressure with the exception of 1 bar. As shown in *Figure 6.9*, an improvement of the performances of the electrochemical process was achieved increasing the CO_2 pressure. An increasement from 1 to 5 bar allowed to enhance the final formic acid concentration from about 2 to 5.8 mM (*Figure 6.9a*) and the faradaic efficiency from about 15 to 40% (*Figure 6.9b*). It is worth to mention that at 1 bar the process is limited by the rate of the mass transfer of the CO_2 to the cathode surface. Hence, the enhancement of the formic acid concentration, achieved increasing the pressure from 1 to 5 bar, is likely to be due mainly to the acceleration of the mass transfer of carbon dioxide to the cathode surface. Indeed, at all other adopted carbon dioxide pressures (5 - 30 bar),

the concentration of CO_2 in the bulk is sufficiently high to speed up its mass transfer to the cathode so that the process takes place under the kinetic control of the CO_2 cathodic reduction. As an example, at 5 bar the limiting current density is slightly higher than 100 mA cm^{-2}, which is drastically higher than the adopted current density (20 mA cm^{-2}).

The rise of the pressure of CO_2 from 5 to 10, and 15 bars, step by step, determines a further enhancement of the formic acid generation (*Figure 6.9a*) and of the faradaic efficiency (*Figure 6.9b*) as a result of greater concentration of dissolved CO_2 in solution, which favors, as a consequence, not only the dissolution and the mass transfer stages but also the adsorption stage (*Eq. 6.1*). For example, the enhancement of the CO_2 pressure from 5 to 15 bars, enhanced the final concentration of HCOOH from about 5.8 to 9.6 mM and the faradaic efficiency from 39 to 64%. However, the effect of the pressure became less relevant for high CO_2 pressure; indeed, an additional increase of the pressure above 15 bars did not result in a significant improvement of the process performances (*Figure 6.9*). According to the polarization experiments and the discussed reaction mechanism, it is reasonable to assume that upon enhancing the pressure the fractional surface coverage by adsorbed CO_2 approaches the unity, saturating the active site of the electrode; hence, a further increase of the pressure does not help the cathodic CO_2 reduction (no limited by mass transfer) and the process is under kinetic control of the reduction of the adsorbed CO_2 (*Eq. 6.2*).

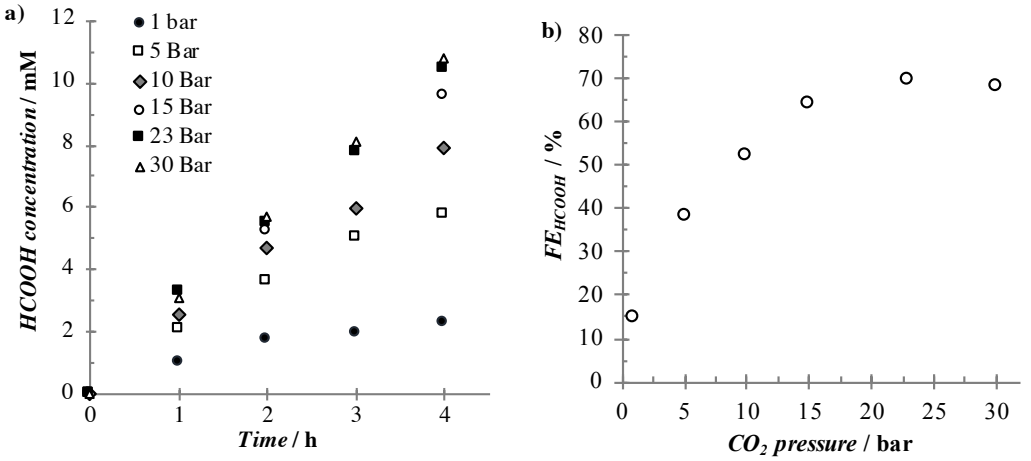

Figure 6.9 Effect of the CO_2 pressure on the (a) formic acid generation and (b) final faradaic efficiency. Electrolysis performed in a pressurized filter-press cell equipped (System III) with Sn cathode (9 cm^2) under amperostatic condition (20 mA cm^{-2}), a wide range of CO_2 pressure (1 - 30 bar) and a constant flow-rate value (200 mL min^{-1}) for 4 h. Volume of the solution (V): 0.9 L. Reproduced from Electrochimica Acta, 277, F. Proietto, B. Schiavo, A. Galia, O. Scialdone, Electrochemical conversion of CO_2 to HCOOH at tin cathode in a pressurized undivided filter-press cell, 30 – 40, Copyright (2018), with permission from Elsevier.

According to these results and to polarizations and reaction mechanism (discussed in ***Section 6.1.1***), the rate of the process is affected by both the pressure of CO_2 and the applied working potential (*Eq. 6.8*; $r = k(E)\, b\, [CO_2]/(1+b[CO_2])$. Hence, in order to improve the performances of the CO_2 reduction performed in a pressurized filter-press cell, a large series of experiments was carried out in a wide range of current density (7.8 – 80 mA cm^{-2}) and at different CO_2 pressure (1 – 30 bar) in a 0.9 L of CO_2 saturated aqueous electrolyte of 0.1 M Na_2SO_4.

First, the effect of current density was studied at 5 bar in galvanostatic mode for 4 h in the range 7.8 - 50 $mAcm^{-2}$ at 200 mL min^{-1}. All the adopted current densities were significantly lower than j_{lim} and were chosen to avoid the high potentials of region 4 (see ***Section 6.1.1***). As shown in *Figure 6.10a*, which reports the final formic acid vs. the current density, the rise of the current density resulted in a maximum value for the final value of the HCOOH concentration close to 6 mM and in a strong decrease of the faradaic efficiency from about 50 to 13% increasing j from 7.8 to 50 mA cm^{-2} (*Figure 6.10b*). In particular, in order to

understand the data, it is useful to remember that also in pseudo-polarization experiments (*Figure 6.3*), the trend j_{CO_2} vs. cell potential gave a plot with a maximum value.

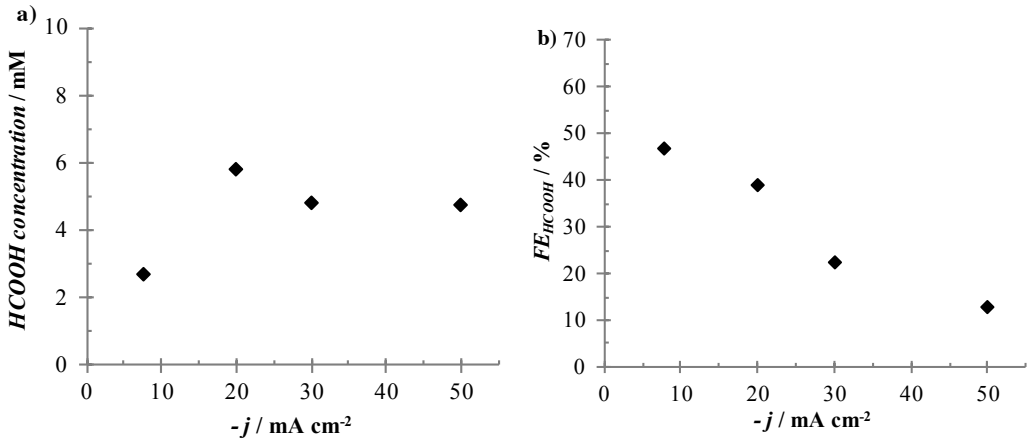

Figure 6.10 Effect of the current density on the (a) final formic acid concentration and (b) faradaic efficiency. Electrolysis performed in a pressurized filter-press cell equipped (System III) with Sn cathode (9 cm^2) under amperostatic condition (range: 7.8 - 50 mA cm^{-2}), fixed CO_2 pressure (5 bar) and a constant flow-rate value (200 mL min^{-1}). Volume of the solution (V): 0.9 L. Reproduced from Electrochimica Acta, 277, F. Proietto, B. Schiavo, A. Galia, O. Scialdone, Electrochemical conversion of CO_2 to HCOOH at tin cathode in a pressurized undivided filter-press cell, 30 – 40, Copyright (2018), with permission from Elsevier.

When these experiments were repeated at various carbon dioxide pressures, similar trends were achieved, but the maximum value of both HCOOH concentration and the final faradaic efficiency increased with the CO_2 pressure, as shown in *Figure 6.11a and 6.11b*, which report the final HCOOH concentration and the final FE, respectively, vs. the adopted current density for various values of carbon dioxide pressure. As an example, at 1, 5 and 10 bar a maximum value close to 2, 6 and 13 mM, respectively, was achieved for the formic acid concentration. In particular, the plateau value was achieved for higher values of *j* when the pressure was enhanced. Furthermore, for the highest pressures (23 and 30 bar), the plateau value was not achieved (*Figure 6.11a*), at least for adopted current densities.

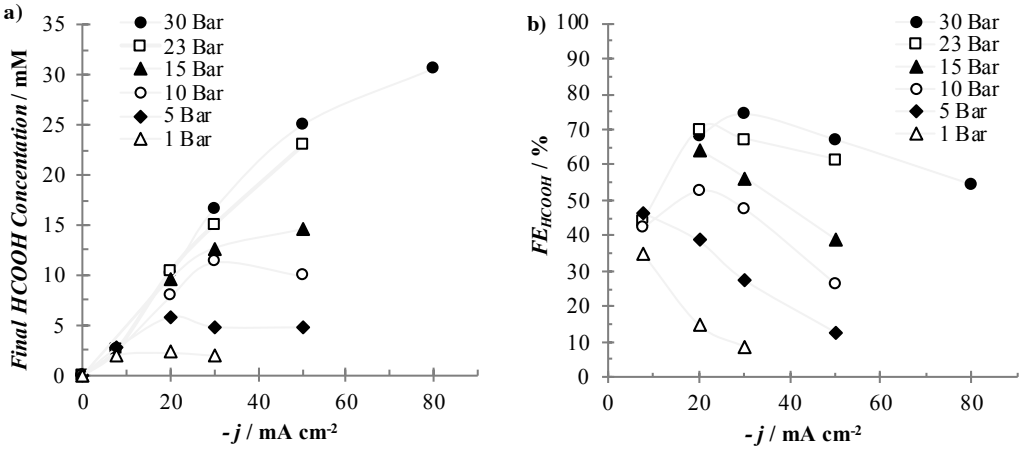

Figure 6.11 Plot of the (a) final formic acid concentration and (b) relative faradaic efficiency vs current density at different pressure. Curve are just guides for the eyes. Experiments performed in pressurized filter press cell (System III) with Sn cathode (9 cm^2) for 4 h under amperostatic condition (range: 7.8 – 80 $mAcm^{-2}$) and a constant flow-rate value (200 mL min^{-1}). Volume of solution (V): 0.9 L. Reproduced from Electrochimica Acta, 277, F. Proietto, B. Schiavo, A. Galia, O. Scialdone, Electrochemical conversion of CO_2 to HCOOH at tin cathode in a pressurized undivided filter-press cell, 30 – 40, Copyright (2018), with permission from Elsevier.

On overall, *Figure 6.11 and 6.12* show that a coupled enhancement of both the current density and pressure can allow to enhance significantly both the HCOOH generation and the faradaic efficiency. In particular, it can be observed that, at each studied current density (7.8, 20, 30, 50 mA cm^{-2}), the plot of HCOOH concentration vs CO_2 pressure gave almost plateau value for high pressure, whose value increased with the adopted current density (*Figure 6.12a*). As an example, at 7.8 mA cm^{-2} the plateau value of formic acid concentration was slightly lower than 3 mM, which increased to about 25 mM at 50 mA cm^{-2}.

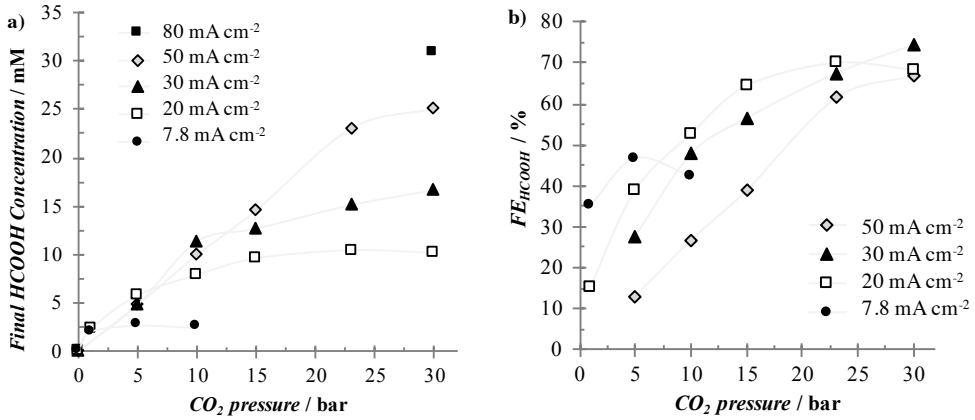

Figure 6.12 Plot of the final formic acid concentration (a) and relative faradaic efficiency (b) vs CO_2 pressure at different current density. Curve are just guides for the eyes. Experiments performed in pressurized filter press cell (System III) with Sn cathode (9 cm^2) for 4 h under amperostatic condition (range: 7.8 – 80 $mAcm^{-2}$) and a constant flow-rate value (200 mL min^{-1}). Volume of solution (V): 0.9 L. Reproduced from Electrochimica Acta, 277, F. Proietto, B. Schiavo, A. Galia, O. Scialdone, Electrochemical conversion of CO_2 to HCOOH at tin cathode in a pressurized undivided filter-press cell, 30 – 40, Copyright (2018), with permission from Elsevier.

Quite interestingly, the trends reported in *Figure 6.12,* achieved with the large systems (System III), are quite similar to that presented in *Figure 6.5* and related to the small batch system (System II) that were discussed and rationalized in the previous section using the reaction mechanism proposed in ***Section 6.1.1***. This is probably due to the fact that under adopted operating conditions the reactor kind is not expected to affect the kinetic of the process. On overall, the coupling of data achieved in the small system and in the large one allows to confirm that cathodic reduction of CO_2 at tin under pressurized conditions can be well rationalized according to the reaction mechanism proposed in ***Section 6.1.1***. In particular, according to the polarization and the reaction mechanism discussed previously (see ***Section 6.1.1***), under pressurized conditions, the rate of the process is linked to reduction rate of adsorbed CO_2, which is affected by both the applied potential (or *j*) and the CO_2 coverage of the surface. At fixed current density, the rate (*Eq. 6.8*) depends to the CO_2 concentration at lower pressure ($r = k(E)\ b\ [CO_2]$) and to the potential ($r = k(E)$) at higher pressure; indeed, at constant *j*, the final concentration of formic acid increases with the CO_2 pressure up to a plateau value (where the superficial coverage by adsorbed CO_2 is

expected to be close to 1) which increase with j (since the HCOOH generation rate should become independent from the [CO_2] and increase with the potential) (*Figure 6.12a*).
According to these hypotheses, the instantaneous faradic efficiency IFE should not depend on the [CO_2] (see next ***Section 6.3.1.1***, *Eq. 6.12b*). Indeed, for the highest adopted CO_2 pressures, at all adopted current densities with the exception of the lowest one, the IFE approached similar values close to 70% (*Figure 6.12b*).

6.2.3 Comparison between pressurized filter-press cell and cylindrical stainless-steel cell

In order to evaluate the passage from a simple batch cylindrical system of about 0.05 L (System II) to the system characterized by continuous recirculation of the electrolytic solution, a filter-press cell and drastically higher volume (0.9 L) (System III) (scaling factor of about 1/18), the results achieved at different pressures in the two systems were compared in *Figure 6.13*.
As shown in *Figure 6.13*, faradaic efficiency of the process has the same trend for both systems; in particular, slightly better performances were achieved, for all the values of investigated operating parameters (pressure and current density), using the scaled-up system equipped with a pressurized filter press cell allowing to obtain quite high faradaic efficiency close to 75%. For instance, in *Table 6.1* the number of the formic acid moles obtained by the two system at 20 mA cm^{-2} were reported. It is relevant to note that the number of the moles was very similar for the two systems (*Table 6.1*).

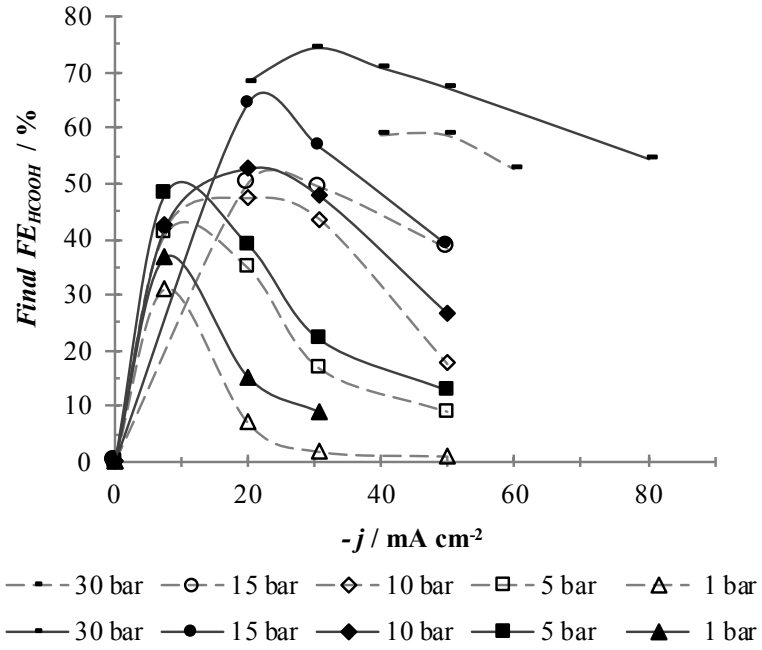

Figure 6.13 Comparison between cylindrical stainless steel cell (System II) and pressurized filter-press cell (System III). The open symbol refers to the cylindrical batch cell of about 0.05 L, the closed one to the filter-press cell system of about 0.9 L. Electrolysis were performed in aqueous solution of Na_2SO_4 (0.1 M) under amperostatic condition.
Reproduced from Electrochimica Acta, 277, F. Proietto, B. Schiavo, A. Galia, O. Scialdone, Electrochemical conversion of CO_2 to HCOOH at tin cathode in a pressurized undivided filter-press cell, 30 – 40, Copyright (2018), with permission from Elsevier.

Table 6.1 Final formic acid moles of the two compared systems at different pressure.

Entry	*CO_2 pressure (bar)*	*Final formic acid moles (10^3 mol)*	
		Pressurized cylindrical cell[a]	*Pressurized filter-press cell*[b]
1	1	1.01	2.04
2	5	5.07	5.21
3	10	6.90	7.11
4	15	7.31	8.65

[a] Electrolysis performed in a cylindrical stainless steel cell (System II) with an aqueous solution of Na_2SO_4 (0.1 M) of about 0.05 L using Sn and compact graphite as cathode and anode, respectively. Experiments carried out for 6 h under amperostatic condition of 20 mA cm^{-2}.

[b] Electrolysis performed in a pressurized filter-press cell (System III) with a continuous recirculation of the solution (0.1 M Na_2SO_4) of about 0.9 L using Sn and DSA as cathode and anode, respectively. Experiments carried out for 4 h under amperostatic condition of 20 mA cm^{-2}.

6.2.4 Effect of the electrolyte flow rate and time on the CO_2 reduction

Since many authors have previously shown that the electrochemical reduction of carbon dioxide can be influenced by the mass transport phenomena [31,34,130], a focused study was devoted to evaluate the effect of the electrolytic flow rate on the formic acid generation and its corresponding FE. A series of electrolyses was performed in a wide range of flow rate/area cathode ratio, Q/A_{cath}, (3.3 - 22.2 mL min^{-1} cm^{-2}) at 23 bar and 50 mA cm^{-2} in CO_2 saturated aqueous solution of Na_2SO_4. As shown in *Figure 6.14*, the flow rate had a very small effect on the FE. In particular, a slight increase of the FE was achieved upon increasing Q/A_{cath} from 3.3 to 16.7 mL min^{-1} cm^{-2}, while a further increase of Q/A_{cath} to 22.2 mL min^{-1} cm^{-2} resulted in a small decrease of the FE.

In order to rationalize these results, it is necessary to take in consideration that, according to polarizations and reaction mechanism discussed previously, under the adopted operative conditions (region 2 in polarization curves), the rate is affected by the cathodic reduction of the adsorbed CO_2 (i.e. the first electron transfer, $CO_{2_{(ads)}} + e^- = CO_{2_{(ads)}}^{-\cdot}$; *Eq. 6.2*, see ***Section 6.1.1***), and the cathodic process is slightly influenced by mass transport phenomena. However, it is possible to suppose that higher flow rates enhance the mass transport of the HCOOH to the anode, favoring its anodic oxidation; indeed, the experimental results shown that for the highest Q/A_{cath} the FE decrease probably due to the detrimental effect of the anodic destruction of HCOOH.

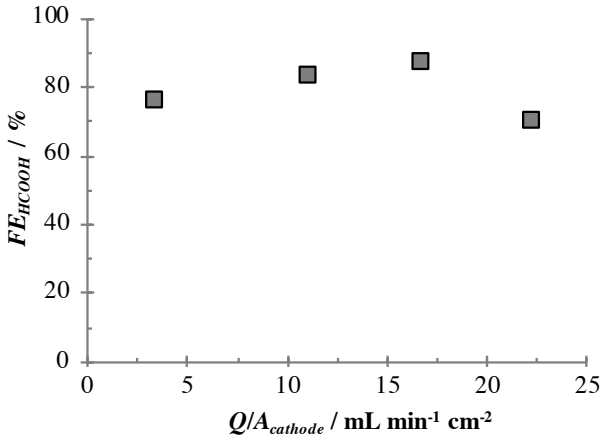

Figure 6.14 Effect of the flow rate/area cathode ratio on the faradaic efficiency of formic acid. Electrolysis performed in a pressurized filter-press cell (System III) with a continuous recirculation of the solution (0.1M Na_2SO_4) equipped with Sn cathode (9 cm^2) under amperostatic condition (50 mA cm^2), fixed CO_2 pressure value (23 bar). Volume of the solution (V): 0.9 L. Reproduced from Electrochimica Acta, 277, F. Proietto, B. Schiavo, A. Galia, O. Scialdone, Electrochemical conversion of CO_2 to HCOOH at tin cathode in a pressurized undivided filter-press cell, 30 – 40, Copyright (2018), with permission from Elsevier.

From the applicative standpoint, it is worth to evaluate the long-term performances of the electrochemical conversion of CO_2 to HCOOH to check the stability of the system and, moreover, to increase the concentration of HCOOH in solution. The purity of the commercial formic acid is typically about 85%wt; so the higher is the HCOOH concentration of the obtained solution, the lower are the costs for its concentration process (distillation process) [15,33]. Firstly, to assess the long-term stability of the process, electrochemical reduction of CO_2 was performed in a pressurized filter-press cell type with 0.5 L of electrolyte. Electrolysis was carried out for more than 40 h at CO_2 pressure of 23 bar, current density of 50 mA cm^{-2} and flow rate of 200 mL min^{-1} (22.2 mL min^{-1} cm^{-2}). As shown in *Figure 6.15*, the concentration of formic acid increase with a quite linear trend during the time up to 200 mM and 56% of HCOOH concentration and faradaic efficiency, respectively, after about 20 h (i.e. charge passed through to the system of about 33'000 C). However, the apparent formic acid production rate decreases until to obtain a plateau value of formic acid concentration at about 290 mM (with a FE of 42%) after 41 h (i.e. 66'500 C) of electrolysis (*Figure 6.15*), due to the anodic oxidation of the accumulated formic acid

in solution. Indeed, working in undivided cell, the higher is the concentration of the formic acid, the higher is the oxidation rate of formic acid, which can be considered negligible at the beginning of the electrolysis and became notably with the charge passed due to the accumulation of HCOOH in solution; indeed, as shown in *Figure 6.16* a strong decrease of IFE with the time was observed (probably, due to the anodic oxidation of the accumulated formic acid in solution); after 40 h the IFE is very close to 0.

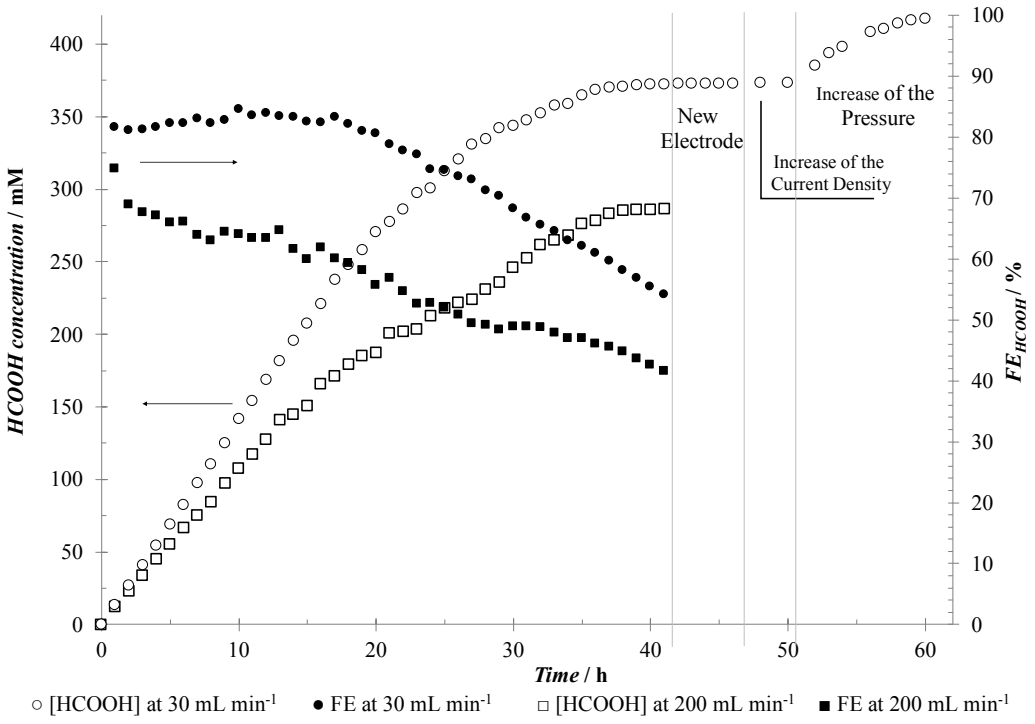

Figure 6.15 Effect of the time on the stability of the reduction of CO_2 to formic acid. Plot of formic acid concentration obtained at (□) 200 and (○) 30 mL min^{-1} and relative faradaic efficiency at (■) 200 and (●) 30 mL min^{-1} vs time. Electrolysis performed in a pressurized filter-press cell (System III) equipped with Sn cathode (9 cm^2) under amperostatic condition (50 - 80 mA cm^{-2}), fixed CO_2 pressures (23 and 30 bar) and constant flow-rate values of about (■) 200 and (●) 30 mL min^{-1}. Volume of the solution (V): 0.5 L. Reproduced from Electrochimica Acta, 277, F. Proietto, B. Schiavo, A. Galia, O. Scialdone, Electrochemical conversion of CO_2 to HCOOH at tin cathode in a pressurized undivided filter-press cell, 30 – 40, Copyright (2018), with permission from Elsevier.

In order to increase the performance of the process, in line to the study described previously, the long-term stability was studied at lower $Q/A_{cathode}$ ratio, i.e. 3.3 mL min^{-1} cm^{-2}. A similar profile of formic acid generation and FE vs time, under the adopter operative conditions, was achieved (*Figure 6.15*). It is relevant to note that at the beginning of the electrolyses the apparent production rate of formic acid is almost similar for both flow rates, 30 and 200 mL min^{-1}, while it is lower at the higher flow rate (200 mL min^{-1}) for high time passed (*Figure 6.15*); indeed, after about 37 h, the value of formic acid reached a plateau of about 375 mM with a corresponding FE of 55%. Here, for the first 20 h of electrolysis the profile of FE vs time is almost constant at about 82.5%; after 20 h, the FE decreased almost linearly (*Figure 6.15*) up to the recorded IFE was close to 0 (*Figure 6.16*).

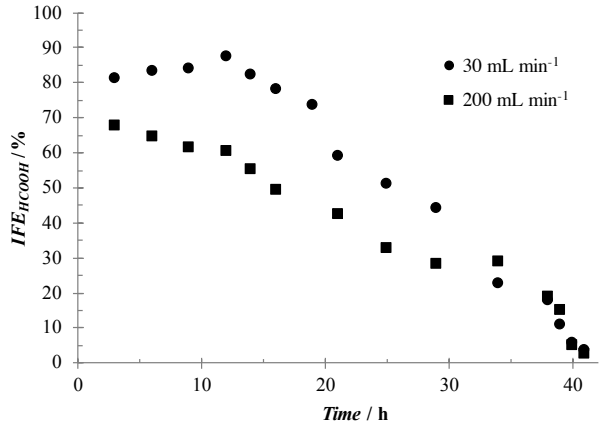

Figure 6.16 Effect of the time on the instantaneous faradaic efficiency. Electrolysis performed in a pressurized filter-press cell (System III) equipped with Sn cathode (9 cm^2) under amperostatic condition (50 mA cm^{-2}), fixed CO_2 pressure (23 bar) and constant flow-rate values of about (■) 200 and (●) 30 mL min^{-1}. Volume of the solution (V): 0.5 L. Reproduced from Electrochimica Acta, 277, F. Proietto, B. Schiavo, A. Galia, O. Scialdone, Electrochemical conversion of CO_2 to HCOOH at tin cathode in a pressurized undivided filter-press cell, 30 – 40, Copyright (2018), with permission from Elsevier.

The decrease of the flow rate gave rise to an improvement of the performances of the CO_2 electrochemical reduction in terms of both formic acid concentration and FE. According to the polarization and the discussed reaction mechanism, under these adopter operative

conditions, the cathodic process is under kinetic control of the reduction of the adsorbed CO_2 to its corresponding radical anion (*Eq. 6.2*, see ***Section 6.1.1***) and is almost not limited by mass transport phenomena. Hence, it is possible to conclude that the oxidation on the anode surface of formic acid, under adopted operative conditions, is more influenced than the CO_2 reduction by the more effective mass transport. Indeed, the long time passed allowed to obtain high concentrations of HCOOH that enhance its anodic oxidation.

The decrease of IFE to zero is due to the fact that, for sufficiently high values of formic acid concentration, the generation rate of HCOOH is equal to its anodic oxidation. The increase of the flow rate, reducing the thickness of the diffusion layer, results in higher mass transfer coefficients of formic acid, thus speeding up its anodic oxidation. In order to confirm this interpretation and to evaluate why the IFE was close to zero (due to the plateau value of the HCOOH concentration), one of the experiments was prolonged changing different operative conditions. Hence, the electrolysis was continued changing the current density, the CO_2 pressure and the Sn electrode. As shown in *Figure 6.15*, no changes on the formic acid generation were achieved by changing the electrode with a new one, thus showing that the decrease of IFE is not due to the deactivation of the cathode. An increase of the current density from 50 to 80 mA cm^{-2} did not change the concentration of HCOOH. This result shows that under these operative conditions, the rate for HCOOH generation does not depends on *j* (and E) or *j* affects in a similar way the rates of both generation and degradation of HCOOH, respectively, at cathode and anode surface.

According to the polarization and the proposed reaction mechanism, the cathodic process is influenced by the rate of the reduction of adsorbed CO_2 (*Eq. 6.8*; $r = k(E)\ b\ [CO_2]°/(1 + b\ [CO_2]°)$) and it is expected to depend mainly on CO_2 pressure. According to this hypothesis, the pressure was increased up to 30 bar (increasing the amount of CO_2 dissolved in solution) and an enhancement of the formic acid concentration up to new plateau value at about 418 mM (19.2 g L^{-1}) was observed. Therefore, it is possible to conclude that after 41 h (passed charge: 67'000 C) the process was not limited by the deactivation of the Sn electrode or the insufficient electrons supply.

6.3 Mathematical model and comparison with experimental results

The theoretical model is a crucial point to well understand the process and a step closer to the appealing scale-up of the process. In the following, according to the reaction mechanism presented in ***Section 6.1.1*** and the relative rate determining steps, a simple theoretical model is developed based on the cathodic conversion of pressurized CO_2 to HCOOH and on its anodic oxidation, in order to describe the process and to evaluate the effect of operative parameters, including current density and pressure, time passed, kind of reactor and flow-dynamic. Furthermore, the experimental results are compared with the theoretical data. The theoretical model is in good agreement with experimental results collected and well describes the effect of several operative parameters.

6.3.1 Theoretical model

The theoretical model is based on various simplified assumptions for both the cathodic reduction of carbon dioxide and the anodic oxidation of formic acid to limit the number of fitting parameters. In particular, the rate of HCOOH generation will be estimated as the difference between r_{CO_2} (the rate of cathodic CO_2 conversion to HCOOH) and r_{HCOOH} (the rate of HCOOH oxidation at the anode).

6.3.1.1 Cathodic reduction of carbon dioxide

According to experiments reported in previous sections and on the reaction mechanism presented in ***Section 6.1.1***, the reduction of CO_2 at tin cathode strongly depends on the adopted potential (or current density) and CO_2 pressure. As shown in the previous paragraph (see ***Section 6.1.1***), for too low (region 1) and too high (region 4) current densities, the production of formic acid is expected to be small; hence, the attention is focused on experiments performed in regions 2 and 3, where the highest rates for CO_2 production can be achieved, thus leading to the highest productivity.

In order to develop the theoretical model, the following assumptions are considered. Firstly, the cathodic reduction of carbon dioxide leads to formic acid by the reaction mechanism reported in ***Section 6.1.1*** (*Eq.s 6.1 – 6.4*) and the only competitive process is the cathodic reduction of water; this latter hypothesis is reasonable since at adopted operating condition only a very minor amount of CO_2 is converted to CO (< 5%) and no other products were detected.

According to the proposed reaction mechanism and the results previously discussed, the rate of CO_2 reduction, r_{CO_2}, takes place under the mixed kinetic control of mass transfer of CO_2 to the cathode ($r_{CO_2} = k_m \left([CO_2]^b - [CO_2]^0\right)$ and reduction of adsorbed CO_2 (*Eq. 6.2*; $CO_{2_{(ads)}} + e^- = CO_{2_{(ads)}}^{-\cdot}, r_{6.2} = k_{6.2}(E)\,\theta$):

$$r_{CO_2} = k_m \left([CO_2]^b - [CO_2]^0\right) = k_{6.2}(E)\,\theta \qquad (6.9)$$

where $k_{6.2}(E)$ is the heterogeneous rate constant for the CO_2 adsorbed reduction and the superficial coverage of CO_2, θ, according to the polarization, can be described by Langmuir expression:

$$\theta = \frac{b\,[CO_2]^0}{1 + b\,[CO_2]^0} \qquad (6.10)$$

in which $b = k_{ads}(E)/k_{dea}(E)$ is assumed to be constant with the potential.

On the bases of these assumptions, the total current density is expected to be simply given by the sum of the current densities due to the cathodic reduction of CO_2 to formic acid (j_{CO_2}) and of water (j_{H_2O}), respectively:

$$j = j_{CO_2} + j_{H_2O} = 2Fk_{6.2}(E)\,\theta + 2Fk'(E) = 2Fk_{6.2}(E)\,\frac{b\,[CO_2]^0}{1 + b\,[CO_2]^0} + 2Fk'(E) \qquad (6.11)$$

where *2* is the number of electrons to reduce carbon dioxide and water, respectively, to formic acid and hydrogen, *F* is the Faraday constant (96487 C mol^{-1}) and $k'(E)$ is the

product of the heterogeneous rate constant for the reduction of the water and water concentration.

Hence, in this framework, it is worth to introduce the concept of the instantaneous faradaic efficiency (*IFE$_{cat}$*) that can be estimated as a ratio between j_{CO_2} and $j_{CO_2} + j_{H_2O}$ resulted in the following equation:

$$IFE_{cat} = \frac{j_{CO_2}}{j_{CO_2}+j_{H_2O}} = \frac{k_{6.2}(E)\frac{b[CO_2]^0}{1+b[CO_2]^0}}{k_{6.2}(E)\frac{b[CO_2]^0}{1+b[CO_2]^0}+k'(E)} = \frac{\frac{b[CO_2]^0}{1+b[CO_2]^0}}{\frac{b[CO_2]^0}{1+b[CO_2]^0}+\frac{k'(E)}{k_{6.2}(E)}} \qquad (6.12)$$

in which, for the sake of simplicity, the ratio between $k'(E)$ and $k_{6.2}(E)$is considered to assume a constant value. The *Eq. 6.12* could be approximated to *Eq. 6.12a* and *6.12b* for low and high values of P_{CO_2}, respectively.

$$IFE_{cat} = \frac{b[CO_2]^0}{b[CO_2]^0+k'(E)/k_{6.2}(E)} \qquad Low\ P_{CO_2} \qquad (6.12a)$$

$$IFE_{cat} = \frac{1}{1+k'(E)/k_{6.2}(E)} \qquad High\ P_{CO_2} \qquad (6.12b)$$

and $[CO_2]^0$ can be easily estimated by equating the rate of mass transfer of carbon dioxide and the rate of cathodic reduction of adsorbed CO_2 (*Eq. 6.9*).

Hence, the experimental results will be fitted by theoretical prediction based on *Eq. 6.9 and 6.12* using $\beta = k'(E)/k_{6.2}(E)$ and b as fitting parameters, while $k_m = D/\delta$ (D is the diffusion coefficient and δ the stagnant layer thickness) was estimated by diffusion limiting current technique (as described in ***Section 5.3***).

6.3.1.2 Anodic oxidation of formic acid

Since experiments were performed in an undivided cell, the anodic oxidation of formic acid has to be considered. In particular, in order to describe this process, a simple theoretical model reported in literature [131] was used and briefly reported in the following. According

to the literature [131], the following assumptions are made for the sake of simplicity to describe the anodic oxidation of HCOOH:

i) the oxidation of the organic is assumed to take place only by anodic reactions (e.g., no homogeneous oxidation processes are considered to take place);
ii) the only competitive process to the oxidation of HCOOH is assumed to be the oxidation of water to oxygen;
iii) the chemi-adsorption of HCOOH and its oxidation products is negligible or it does not affect significantly the water and HCOOH oxidation rates.

Furthermore, for the sake of simplicity, the ratio between $k_{an}'(E)$ (i.e., the product of the heterogeneous rate constant for the oxidation of the water and water concentration) and $k_{HCOOH}(E)$ (the heterogeneous rate constant for the oxidation of HCOOH) is considered to assume a constant value.

According to the above-mentioned assumptions, the anodic oxidation of formic acid r_{HCOOH} is assumed to take place under the mixed kinetic control of mass transfer of HCOOH to the anode and the anodic oxidation of HCOOH:

$$r_{HCOOH} = k_{m,HCOOH}([HCOOH]^b - [HCOOH]^0) = k_{HCOOH}(E)[HCOOH]^0 \qquad (6.13)$$

where $k_{m,HCOOH}$ is the mass transfer coefficient for HCOOH and $[HCOOH]^b$ e $[HCOOH]^0$ are the concentrations of HCOOH in the bulk and at the anode surface, respectively.

On the bases of these assumptions, the total current density is expected to be simply given by the sum of the current densities due to the anodic oxidation of formic acid to CO_2 (j_{HCOOH}) and of water ($j_{H_2O,an}$), respectively:

$$j = j_{HCOOH} + j_{H_2O,an} = 2Fk_{HCOOH}(E)[HCOOH]^0 + 2Fk_{an}'(E) \qquad (6.14)$$

Hence, the instantaneous faradaic efficiency (IFE_{anod}) can be estimated by the following equation:

$$IFE_{anod} = \frac{k_{HCOOH}(E)[\mathrm{HCOOH}]^{\circ}}{k_{HCOOH}(E)[\mathrm{HCOOH}]^{\circ}+k_{an}{}'(E)} = \frac{1}{1+\frac{k_{an}{}'(E)}{k_{HCOOH}(E)[\mathrm{HCOOH}]^{\circ}}} \qquad (6.15)$$

and [HCOOH]° can be easily estimated by equating the rate of mass transfer of HCOOH and the anodic oxidation of HCOOH (*Eq. 6.13*). Hence, since $k_{m,HCOOH}$ can be estimated by diffusion limiting current technique, the only unknown parameter is $\gamma = k_{an}'(E)/k_{HCOOH}(E)$, which was estimated as fitting parameter comparing the experimental results and theoretical predictions.

6.3.1.3 Evolution of formic acid concentration

Hence, according to the above-mentioned assumptions, the theoretical concentration of formic acid was estimated as:

$$[HCOOH]_{t+\Delta t} = [HCOOH]_t + \frac{(n_{HCOOH,cat} - n_{HCOOH,anod})_{\Delta t}}{V} \qquad (6.16)$$

where: $[HCOOH]_{t+\Delta t}$ and $[HCOOH]_t$ are respectively the concentration of HCOOH at the time $t + \Delta t$ and t, $n_{HCOOH,cat}$ moles of formic acid produced at the cathode surface in the time interval Δt, $n_{HCOOH,anod}$ moles of formic acid decomposed at the anode surface in the time interval Δt and V the volume of the solution.
In detail, the $n_{HCOOH,cat}$ can be evaluated from the definition of the cathodic instantaneous faradaic efficiency (*Eq. 6.17*):

$$n_{HCOOH,cat} = \frac{IFE_{cat}\,(Q_{t+\Delta t} - Q_t)}{2\,F} \qquad (6.17)$$

in which IFE_{cat} (*Eq. 6.12*), can be reformulated as follows (*Eq. 6.18*):

$$IFE_{cat} = \frac{j_{CO_2}}{j_{CO_2}+j_{H_2O}} = 2\,F\,\frac{k_{6.2}(E)\,\theta}{j} = \frac{2\,F\,k_{6.2}(E)}{j}\,\frac{b\,[CO_2]^0}{1+b\,[CO_2]^0} \qquad (6.18)$$

where $[CO_2]^0$ is easily estimated by equating the rate of mass transfer of carbon dioxide and the rate of cathodic reduction of adsorbed CO_2 (*Eq 6.9*) taking in consideration that $[CO_2]^0 = \alpha\,[CO_2]^b$:

$$k_m\left([CO_2]^b - [CO_2]^0\right) = k_{6.2}(E)\,\frac{b\,[CO_2]^0}{1+ b\,[CO_2]^0} \qquad (6.19)$$

Hence, we have two equations and 4 variables (namely, IFE_{cat}, $[CO_2]^0$, $\boldsymbol{b}$ and $\beta = \frac{k'(E)}{k_{6.2}(E)}$). Hence, in order to obtain IFE_{cat} from these two equations, we have decided to obtain b and β as fitting parameters, in order to have a system of two equations and two unknown variables. In particular, we assume that β does not change with the potential. Hence, it can obtain under specific conditions and used changing the operating parameters. Interestingly, $k_{6.2}(E)$ can be explicated from the *Eq. 6.11*; indeed, multiplying and dividing the second member for $k_{6.2}(E)$, the total current density (see eq. 6.11) is given by:

$$j = 2Fk_{6.2}(E)\,\frac{b\,[CO_2]^0}{1+ b\,[CO_2]^0} + 2Fk'(E)\frac{k_{6.2}(E)}{k_{6.2}(E)} = 2Fk_{6.2}(E)\left(\frac{b\,[CO_2]^0}{1+ b\,[CO_2]^0} + \frac{k'(E)}{k_{6.2}(E)}\right) \qquad (6.20)$$

and $k_{6.2}(E)$ is given by the following expression:

$$k_{6.2}(E) = \frac{j}{2\,F\left(\frac{b[CO_2]^0}{1+ b\,[CO_2]^0} + \beta\right)} \qquad (6.21)$$

Similar considerations can be done for $n_{HCOOH,anod}$

$$n_{HCOOH,anod} = \frac{IFE_{anod}\,(Q_{t+\Delta t} - Q_t)}{2\,F} \qquad (6.22)$$

Indeed, IFE_{anod} is given by *Eq. 6.15*, reported below for the sake of clarity:

$$IFE_{anod} = \frac{1}{1+\frac{\gamma}{[\mathrm{HCOOH}]^\circ}} \qquad (6.15)$$

and [HCOOH]° is given by *Eq. 6.13*

$$r_{HCOOH} = k_{m,HCOOH}([HCOOH]^b - [HCOOH]^0) = k_{HCOOH}(E)[HCOOH]^0 \quad (6.13)$$

Hence, we have two equations and 3 variables (namely, IFE_{anod}, $[HCOOH]^0$, and $\gamma = \frac{k_{an}'(E)}{k_{HCOOH}(E)}$). Hence, in order to obtain IFE_{anod} from these two equations, we have decided to obtain γ as fitting parameter.

6.3.2 Comparison with experimental data

In the following, the experimental data discussed in previous sections were compared with the theoretical values estimated on the bases of the model above described.

6.3.2.1 Effect of pressure

The effect of pressure on the CO_2 reduction into formic acid at 20 mA cm^{-2} and various pressures (1 - 30 bars) for 4 h was discussed in ***Section 6.2.2.2***. Briefly, it was found that, under the adopted operative conditions, the enhance of the pressure (up to 15 bars) improves the generation of formic acid, even if the effect of the pressure became less relevant at high CO_2 pressure; indeed, similar productions of HCOOH were observed for 23 and 30 bar (*Figure 6.9*).

These experimental results were fitted with the mathematical model presented in ***Section 6.3.1***. As shown in *Figure 6.17*, the model fits quite well the experimental trends. It was found a good agreement between the experimental data and the theoretical one by using $\beta = k'(E)/k_{6.2}(E)$ = 0.18, $\gamma = k_{an}'(E)/k_{HCOOH}(E)$ = 0.3 M, b = 1 as values of fitting parameters. According to the experimental data, the theoretical formic acid concentration estimated with the mathematical model increases with the time for each values of pressure. Furthermore, according to the theoretical model, the effect of the pressure becomes less

relevant at the highest adopted values of P_{CO_2}, since a higher superficial coverage occurs, in fully agreement with the polarization and the reaction mechanism discussed in ***Section 6.1.1***.

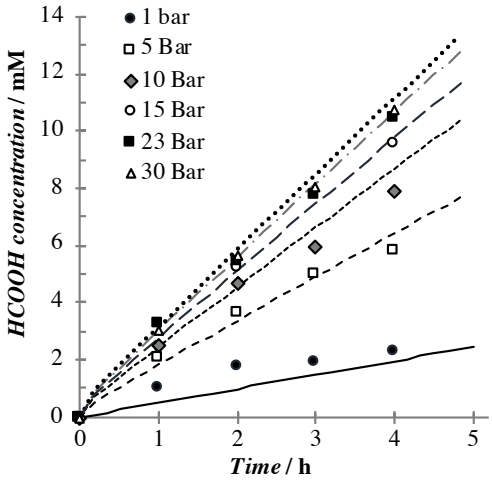

Figure 6.17 Plot of the formic acid concentration vs time at 20 mA cm^{-2}. Comparison of the experimental [HCOOH] with the theoretical [HCOOH] at several value of pressure: 1 (—); 5(- -); 10 (---); 15 (— — —); 23 (— • —); 30 (•••) bar. Theoretical [HCOOH] was evaluated under the assumptions described in the *Section 6.3.2* with the following fitting parameters: $\beta = k'(E)/k_{6.2}(E) = 0.18$; $\gamma = k_{an}'(E)/k_{HCOOH}(E) = 0.3$ M; $b = 1$. System III. Reproduced from ChemElectroChem, 6, F. Proietto, A. Galia, O. Scialdone, Electrochemical conversion of CO2 to HCOOH at Tin Cathode: Development of a Theoretical Model and Comparison with Experimental Results, 162 – 172, Copyright (2019), with permission from John Wiley and Sons.

6.3.2.2 Effect of current density

In order to validate the theoretical model, the formic acid concentration (selected from some electrolysis presented in previous ***Section 6.2***) was reported as a function of the time at different values of current density at 10 bar (7.8, 20 and 30 mA cm^{-2}) and 23 bar (7.8, 20, 30 and 50 mA cm^{-2}). Not very high current densities were selected in order to avoid region 4 (in which the HER is expected to occurs in an excessive way). As shown in *Figure 6.18*, experimental results shown that, at both pressures, the higher was j the higher was the production of formic acid.

Also in this case, the experimental results were compared with the model, here used entirely in predictive mode since the parameters values, β, γ and b estimated in ***Section 6.3.2.1***, were used. As shown in *Figure 6.18*, the model well captured the effect of j at both adopted pressures.

According to the assumptions developed in the model, a similar coverage θ was obtained for the same value of the pressure changing the current density; furthermore, under adopted conditions, the process was slightly limited by mass transfer; hence quite similar values of faradaic efficiencies were achieved at all adopted current densities (55 and 68% at 10 and 23 bar, respectively) that were well predicted by the model.

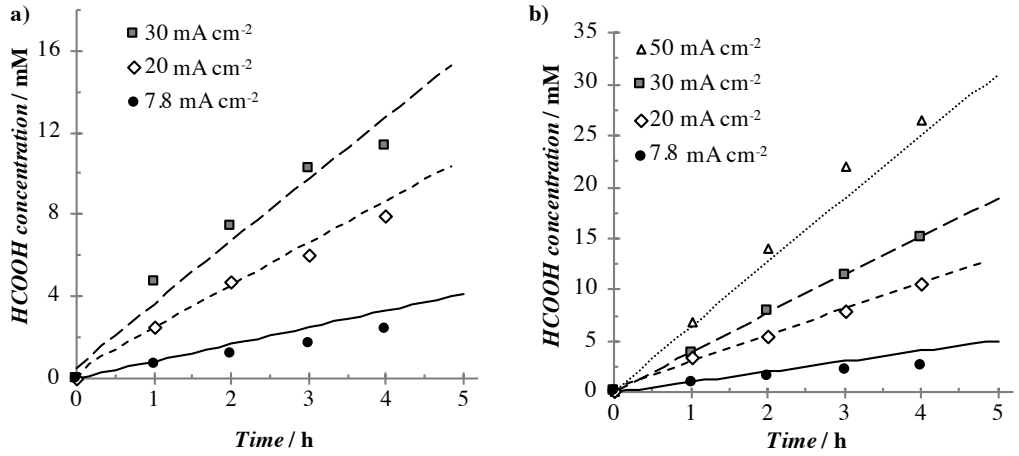

Figure 6.18 Plot of formic acid concentration vs. time at 10 (a) and 23 (b) bar. Comparison of the experimental [HCOOH] with the theoretical [HCOOH] at several value of current density: 7.8 (—); 20 (- - -); 30 (— —); 50 (•••) mA cm^{-2}. Theoretical [HCOOH] was evaluated under the assumptions described in the *Section 6.3.2* with the following fitting parameters: $k'(E)/k_{6.2}(E)$ = 0.18; $kan'(E)/k_{HCOOH}(E)$ = 0.3 M; b = 1. System III. Reproduced from ChemElectroChem, 6, F. Proietto, A. Galia, O. Scialdone, Electrochemical conversion of CO2 to HCOOH at Tin Cathode: Development of a Theoretical Model and Comparison with Experimental Results, 162 – 172, Copyright (2019), with permission from John Wiley and Sons.

As shown in *Figure 6.17 and 6.18*, the plot HCOOH concentration vs. time is almost linear. This is due to the fact that under adopted operating conditions the anodic oxidation of formic acid is quite limited due to the rather low values of formic acid concentration. As

an example, at 23 bar and 30 mA cm^{-2}, the IFE for the anodic oxidation of HCOOH after 4 h was estimated to be about 4% in face of an IFE for the HCOOH generation at the cathode close to 70%.

Figure 6.19 reports the results of a larger set of experiments obtained changing both pressure (from 1 to 23 bar) and current density (from 7.78 to 50 mA cm^{-2}) selected from the data reported in previous sections in order to work in regions 2 and 3. In order to put in the same graph all the data, the final concentration of each experiment after 4 hours was reported. It can be clearly observed that for a constant current density the final concentration of HCOOH increases with P_{CO_2} up to a plateau value, which increases with j. The data can be rationalized considering that: i) the kinetic is strongly influenced by the rate of the reduction of adsorbed CO_2 which increases with the potential (and the current density) and with the superficial coverage of CO_2, θ; and, ii) the dependence of θ by $[CO_2]$ can be described by a Langmuir-type equation and θ is expected to increase with $[CO_2]$ up to a plateau value.

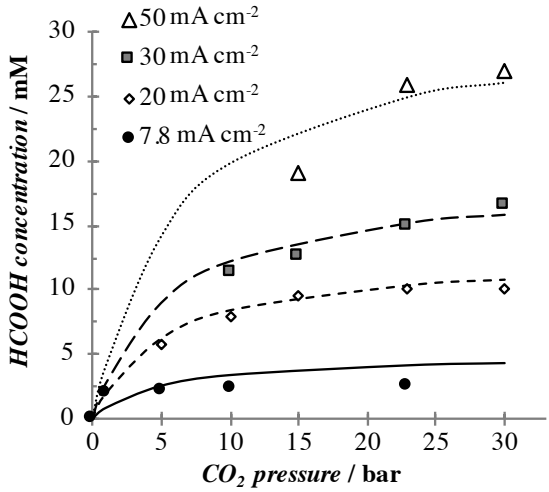

Figure 6.19 Plot of formic acid concentration achieved after 4 h vs. CO_2 pressure at several values of current density (range 7.8 - 50 mA cm^{-2}). Comparison of the experimental [HCOOH] with the theoretical [HCOOH] at several value of current density: 7.8 (—); 20 (---); 30 (— — —); 50 (•••) mA cm^{-2}. Theoretical [HCOOH] was evaluated under the assumptions described in the *Section 6.3.2* with the following fitting parameters: $\beta = k'(E)/k_{6.2}(E) = 0.18$; $\gamma = k_{an}'(E)/k_{HCOOH}(E) = 0.3$ M; $b = 1$. System III. Reproduced from ChemElectroChem, 6, F. Proietto, A. Galia, O. Scialdone, Electrochemical conversion of CO2 to HCOOH at Tin Cathode: Development of a Theoretical Model and Comparison with Experimental Results, 162 – 172, Copyright (2019), with permission from John Wiley and Sons.

6.3.2.3 Effect of time

In order to evaluate better the contribution of the anodic oxidation of HCOOH, the results of a long electrolysis (presented in detail in ***Section 6.2.3)***, were compared with the previsions of the theoretical model. *Figure 6.20* reports the formic acid generation obtained by CO_2 reduction at 50 mA cm^{-2}, 23 bar and 200 mL min^{-1} for more than 40 hours. It is clear that the model well describes the evolution of the concentration of formic acid vs. time and the overall FE observed for long electrolyses for undivided cells (*Figure 6.20*). In particular, FE decreases from an initial value close to 70% to a final one close to 42%. According to the proposed theoretical model, the trend of FE is due to the fact that the formation of HCOOH occurs with a constant FE_{cath} of about 70% while the anodic oxidation of HCOOH occurs with an increasing FE_{anod} (from 0 to about 44%) due to the enhancement of the concentration of formic acid in the solution with the time passed.
It is relevant to note that, also under these adopted conditions, the model well predict the performances of the process used in fully predictive mode.

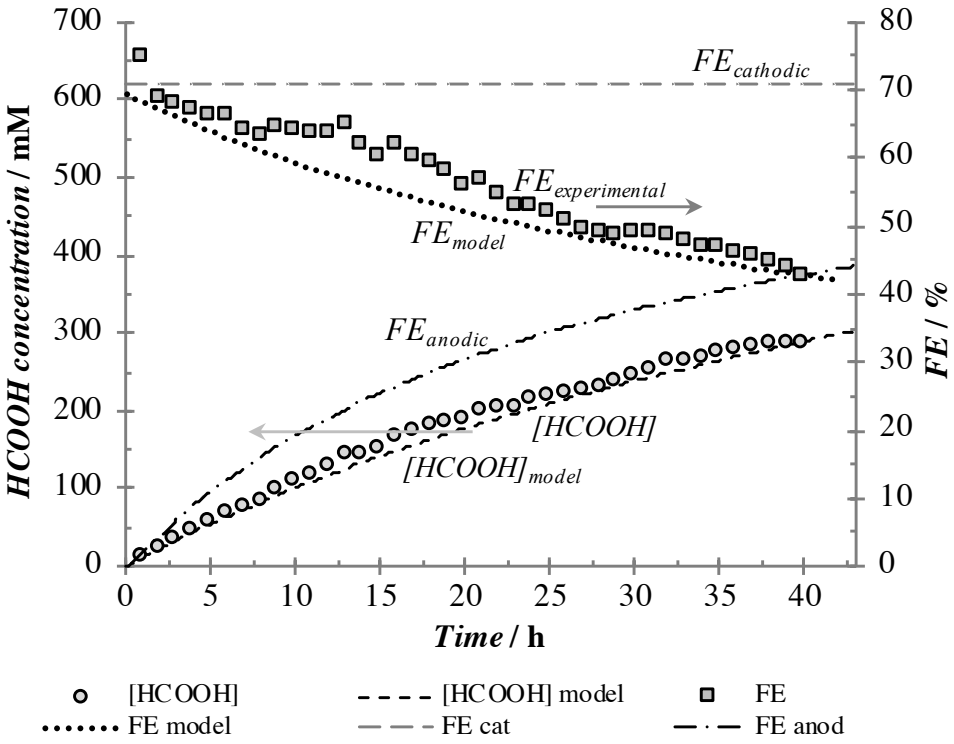

Figure 6.20 Comparison of the experimental generation of HCOOH and of the relative FE with the theoretical model. Electrolyses were performed at 200 mL min^{-1} (previous presented in *Section 6.2.3*). Theoretical [HCOOH] was evaluated under the assumptions described in the *Section 6.3.2* with the following fitting parameters: $\beta = k'(E)/k_{6.2}(E) = 0.18$; $\gamma = k_{an}'(E)/k_{HCOOH}(E) = 0.3$ M; $b = 1$. System III. Reproduced from ChemElectroChem, 6, F. Proietto, A. Galia, O. Scialdone, Electrochemical conversion of CO_2 to HCOOH at Tin Cathode: Development of a Theoretical Model and Comparison with Experimental Results, 162 – 172, Copyright (2019), with permission from John Wiley and Sons.

6.3.2.4 Effect of reactor type and fluid-dynamics regime

In order to evaluate the robustness of the proposed model, the theoretical predictions based on fitting parameters, evaluated in ***Section 6.3.2.1,*** for a filter-press cell with continuous recirculation of the pressurized solution with an area of tin cathode, A, of 9 cm^2 and a volume, V, of 0.9 L were compared with results achieved in a very different reactor after 6 h: a batch cell with a volume of 0.05 L, an area of the tin electrode of 4.5 cm^2 and no mixing (data reported in ***Section 6.1.1.1***). As shown in *Figure 6.21a*, in spite of the drastic change of reactor, ratio A/V and flow-dynamic regime, a quite good agreement between the

theoretical model (here used in a fully predictive mode) and the experimental results is achieved. Also in this case experimental data relative to regions 2 and 3 were selected. In particular, in this case very high HCOOH concentrations were achieved using both high pressures and j, because of the high ratio A/V. *Figure 6.21b* reports a comparison between the experimental FE achieved after 6 h at 30 mA cm^{-2} and different pressures and the FE predicted by the model. A quite good agreement is observed also in this case; in particular, the theoretical FE increases with the pressure and it is significantly lower than the cathodic FE, related to the formation of HCOOH, since a significant anodic FE, relative to the anodic oxidation of HCOOH, occurs, due to the high HCOOH concentration speeding up the process.

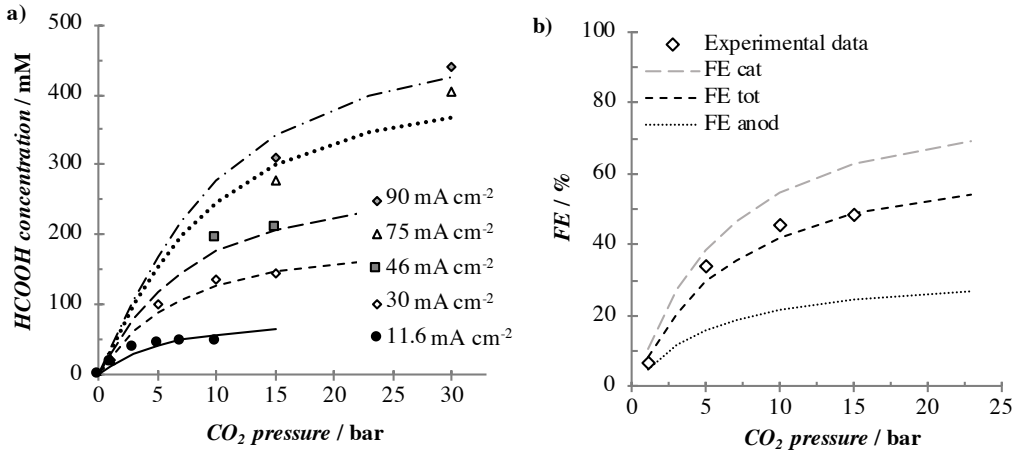

Figure 6.21 (a) Plot of formic acid concentration vs. CO_2 pressure at several values of current density (range 11.6 - 90 mA cm^{-2}). Comparison of the experimental [HCOOH] achieved after 6 h with the theoretical [HCOOH] at several value of current density: 11.6 (—); 30 (---); 46 (— — —); 75 (•••); 90 (— • —) mA cm^{-2}. (b) Plot of experimental FE and theoretical FE prediction vs CO_2 pressure at 30 mA cm^{-2}. Theoretical [HCOOH] was evaluated under the assumptions described in the *Section 6.3.2* with the following fitting parameters: $\beta = k'(E)/k_{6.2}(E) = 0.18$; $\gamma = k_{an}'(E)/k_{HCOOH}(E) = 0.3$ M; $b = 1$. System II. Reproduced from ChemElectroChem, 6, F. Proietto, A. Galia, O. Scialdone, Electrochemical conversion of CO_2 to HCOOH at Tin Cathode: Development of a Theoretical Model and Comparison with Experimental Results, 162 – 172, Copyright (2019), with permission from John Wiley and Sons.

Chapter 7

Conversion to carbon monoxide: results and discussion

7 Conversion to carbon monoxide: results and discussion

Carbon monoxide is one of the main appealing C-derivate products of CO_2 reduction. To date, promising results on the CO_2 electrochemical conversion to CO were achieved by the utilization of Ag-GDE by different research groups (see ***Chapter 3*** *and* ***4***); however, due to the problems and costs of GDEs, it would be interesting to evaluate, as a possible alternative, the utilization of simpler cathodes under pressurized conditions. Hence, the electrochemical conversion of CO_2 to CO was studied at simple silver electrodes with the aim to evaluate the effect of the pressure (1 – 30 bar) and the nature of the supporting electrolyte (K_2SO_4, KCl, $KHCO_3$ and KOH) under pressurized conditions on the performances of the process using an aqueous solution and an undivided and simple cell in order to avoid the penalties given by the presence of the separator. As previously mentioned, the utilization of electrodes with high active surface for CO_2 reduction could be an interesting alternative to improve the performances of the process; hence, the synergetic utilization of a cathode with high surface and pressurized CO_2 was studied, comparing the results with that achieved with a silver plate cathode. Eventually, it was studied the stability of the CO production at relatively high pressure (15 bars) using different electrolytes for 10 hours. Furthermore, the process was also studied using Ag-GDEs focusing on the effect of various operating parameters and on the stability of performances with time.

7.1 CO_2 electrochemical conversion to CO at silver based electrode

Several reaction mechanisms about the CO generation via electrochemical pathway have been proposed by many authors. In particular, according to Hori [42] and Ma [103], the reduction of carbon dioxide at silver cathode proceeds trough the formation of adsorbed CO_2^-, as shown in the following reaction steps (*Eq.s 7.1 – 7.4*), where * indicates a free active site)

$$CO_2 + * + e^- \rightarrow CO^-_{2(ads)} \quad (7.1)$$

$$CO^-_{2(ads)} + H^+ \rightarrow COOH_{ads} \quad (7.2)$$

$$COOH_{ads} + e^- + H^+ \rightarrow CO_{ads} + H_2O \quad (7.3)$$

$$CO_{ads} \rightarrow CO + * \quad (7.4)$$

Conversely, Rosen and co-authors [132] considered that CO_2 and CO_2^- present no stable interactions with Ag, thus making unlikely that these species can be adsorbed at Ag cathodes. Hence, they proposed the direct formation of $COOH_{ads}$ in the presence of HCO_3^-:

$$CO_2 + HCO_3^- + e^- + * \rightarrow COOH_{ads} + CO_3^{2-} \quad (7.5)$$

To achieve information on the process, firstly, a series of polarizations and pseudo-polarizations was performed both at 1 bar and under pressure, followed by electrolyses carried out at different CO_2 pressures, current densities and mixing rates.

7.1.1 Experiments using K_2SO_4 as supporting electrolyte

A first series of experiments was performed at a silver plate cathode using K_2SO_4 as supporting electrolyte, since this salt according to the literature [85,133,134] can give quite good results in terms of CO production and it presents a quite high conductivity. *Figure 7.1a* reports some polarizations recorded under nitrogen or carbon dioxide atmosphere (1 bar) at a silver plate electrode at 0 and 500 rpm. As shown in *Figure 7.1a*, under nitrogen atmosphere, current density starts to increase significantly at a working potential close to -1.65 V vs. SCE as a result of hydrogen evolution reaction. When N_2 is replaced with CO_2 at 0 rpm, the current density starts to increase significantly at a working potential close to -1.45 V vs. SCE, thus showing that there is a range of potential of about 0.2 V where CO_2

reduction can potentially take place with a very limited hydrogen evolution. For working potentials more negative than -1.7 V vs SCE (when hydrogen evolution takes place in a relevant way), the addition of CO_2 gives rise to a decrease of the overall current density. The nominal partial current density of CO_2, j_{CO_2}, simply obtained by the difference between the current density recorded with nitrogen and that obtained with CO_2 is reported in *Figure 7.1b* as a function of the working potential. It is seen that j_{CO_2} presents positive values for potentials up to -1.77 V (with a maximum at -1.67 V) and negative values for more negative potentials. Hence, it can be inferred that the addition of CO_2 reduces the hydrogen evolution in spite of the fact that it leads to a decrease of the pH of the solution, similarly to the polarizations obtained at tin cathodes.

According to the reaction mechanism (*Eq.s 7.1 – 7.4*), the decrease of the current in the presence of CO_2 may be related to the fact that the reduction derivatives of carbon dioxide are adsorbed on the silver surface (CO_{ads}, $CO^-_{2(ads)}$ and/or $COOH_{ads}$), thus reducing the active sites for hydrogen evolution reaction.

When the polarization was repeated at 500 rpm, an increase of both current density (*Figure 7.1a*) and j_{CO_2} (*Figure. 7.1b*) were obtained for potentials more negative than -1.6 V, this is probably due to the fact that a higher mixing rate enhances the mass transfer of CO_2 and protons to the cathode, thus favoring the CO production.

To evaluate the effect of CO_2 concentration in water on the CO_2 reduction, current densities were recorded as a function of cell potential ΔV in the presence of N_2 or with different pressures of CO_2 in the range 10 - 30 bar. As shown in *Figure 7.1c and 7.1d*, both the total and the CO_2 nominal partial current density increase upon enhancing the CO_2 pressure, thus showing that the rate of carbon dioxide reduction strongly depends on the concentration of CO_2 in solution. Hence, the r.d.s. is likely to be the mass transfer of CO_2 from the bulk to the electrode surface or its reduction (*Eq. 7.1 or 7.5*). However, the limiting current density for a process under mass transfer control can be estimated to be more than 400 mA cm^{-2} at 20 bars. Hence, it can be inferred that the r.d.s. is not the mass transfer at relatively high pressures of carbon dioxide.

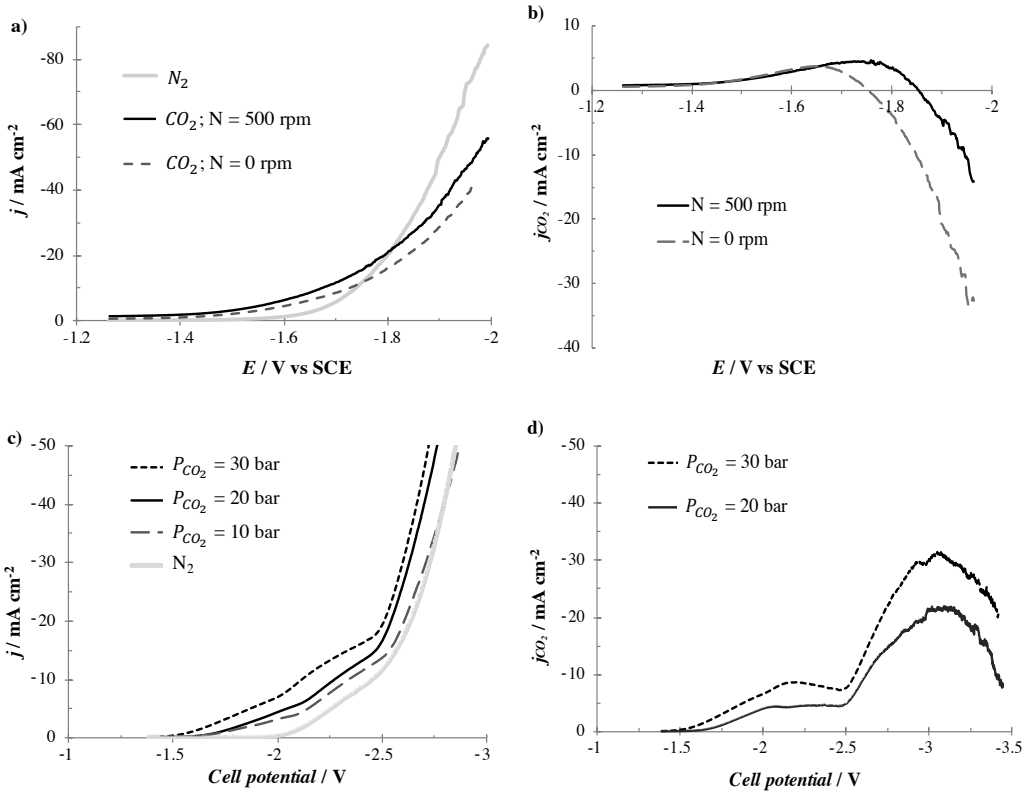

Figure 7.1 (a) LSVs at 5 mV s^{-1} under N_2 and CO_2 saturated water solution of 0.2 M K_2SO_4 at different mixing rate (0 and 500 rpm); the relative polarizations were performed using System I. (b) Plot of CO_2 partial current density vs working potential at 0 and 500 rpm; (c) pseudo-polarization curves performed at 5 mV s^{-1} under N_2 and CO_2 saturated water solution of 0.2 M K_2SO_4 at different CO_2 pressure (1 - 30 bar); the relative polarizations were performed using System II. (d) Plot of CO_2 partial current density vs cell potential at 20 and 30 bars. Working electrode: plate-Ag (0.1 cm^2). V= 0.05 L.

7.1.1.1 Electrolyses at high pressure

A series of galvanostatic electrolyses was performed at a silver plate cathode at 12 mA cm^{-2}, 500 rpm and different CO_2 pressures (from 1 to 30 bar) using an undivided stainless-steel cell (see ***Section 5.2.2****:* System II) in order to evaluate the effect of CO_2 concentration on the production of CO and other by-products. As shown in *Figure 7.2a*, at 1 bar CO was produced with a very low FE (< 5%), which corresponds to a current density devoted to CO production lower than 0.6 mA cm^{-2}. Indeed, various authors have previously reported that at Ag foil cathodes, quite low faradic efficiencies and current densities related to CO

production are obtained at 1 bar [91,92]. The presence of other products of CO_2 reduction, including formic acid, was checked with no results, while a high amount of hydrogen was generated. However, when the pressure was increased, a strong enhancement of the CO production was observed. Indeed, the FE_{CO} increased to 16, 26 and 67% enhancing the CO_2 pressure at 10, 15 and 30 bar, respectively, thus confirming that the enhancement of the CO_2 concentration in the bulk is a very effective way to favor the CO generation. Furthermore, at 15 and 30 bars, the presence of small amounts of formic acid in the liquid phase was observed (FE_{HCOOH} ~ 13%)

The effect of current density was evaluated at both 1 and 30 bars, carrying out a series of electrolyses at 7, 12 and 30 mA cm^{-2} and 500 rpm. As shown in *Figure 7.2b*, at 1 bar a very low FE_{CO} was achieved at all adopted current densities. Conversely, at 30 bar a strong effect of the current density was observed; indeed, the enhancement of the current density from 7 to 12 mA cm^{-2} resulted in a drastic increase of both the CO production (from 0.2 to 1.5 mol h^{-1} m^{-2}) and FE_{CO} (from 15 to 67%). Conversely, a further enhancement of the current density from 12 to 30 mA cm^{-2} resulted in a slightly increase of CO production but in a drastic decrease of FE_{CO}. The effect of the current density can be due to the fact that for current densities between 7 and 12 mA cm^{-2} (ΔV ~ 2 – 2.2 V), an increase of the potential leads to an enhancement of j_{CO_2} (*Figure 7.1c and 7.1d*) in a region where the hydrogen evolution is quite limited, while the increase of the current density to 30 mA cm^{-2} involves quite high ΔV (~ 2.6 V) that favor the hydrogen evolution and that, according to some authors, can limit the CO production since at very negative potentials CO could be more strongly adsorbed to the surface due to a back-donation of an electron to the CO molecule [115].

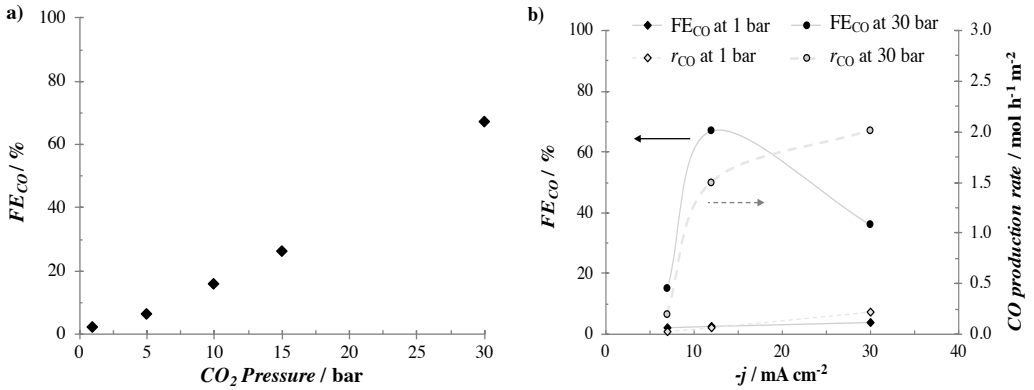

Figure 7.2 (a) Effect of the pressure of CO_2 on the current efficiency of CO at 12 mA cm^{-2}. (b) Effect of current density on the current efficiency of CO and the CO production rate at 1 and 30 bars. Electrolysis were performed in CO_2 saturated water solution of 0.2 M K_2SO_4 under amperostatic condition (7 - 30 mA cm^{-2}). System II. Working electrode: Ag plate (3 cm^2). Counter electrode: Compact Graphite. N = 500 rpm. V= 0.05 L.

To evaluate the effect of mixing on the performances of the process, a series of electrolyses was carried out at 30 bar and 12 mA cm^{-2} at different mixing rates (namely 0, 150, 300, 500 and 700 rpm). In this case, experiments were prolonged up to 3 hours. It was shown that FE_{CO} reaches a maximum for an intermediate value of 300 rpm (*Figure 7.3*). Indeed, for higher values of rpm, FE_{CO} decreases as a result of a higher generation of hydrogen. Conversely, for the lower values of the mixing rate, lower faradaic efficiencies for hydrogen are achieved and it was observed a little amount of methane with a current efficiency of about 4%. These results show that under particular operative conditions the reduction of CO_2 at silver can give rise to the formation of methane. The formation of methane at silver plate cathode was previously reported by He [135] and Kuhl [136] both in a divided cell using $KHCO_3$ as supporting electrolyte in the catholyte with current efficiencies lower than 4%. Other studies have shown that at high pressure the mixing rate can affect the process; indeed, working without mixing rate gave at copper based cathodes higher FE in light hydrocarbons [112]. In order to understand the effect of mixing rate on the selectivity of the process, it is relevant to observe that under adopted operating conditions (high pressures of CO_2 and moderate current densities), the reduction of carbon dioxide is not expected to be affected by the mass transfer of CO_2 from the bulk to the cathode surface. Conversely, the mixing rate could affect the mass transfer of CO from the

cathode to the bulk. Hence, at low stirring rate, the cathode should present a higher concentration of CO, thus favoring follow-up reduction paths, including the conversion of CO to methane. High stirring rate, furthermore, should enhance the mass transfer of protons from the bulk to the cathode surface, thus decreasing the local pH, and favoring the hydrogen evolution.

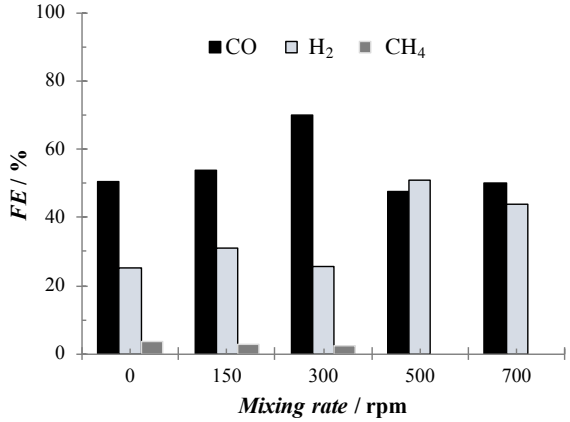

Figure 7.3 Effect of the mixing rate on the faradaic efficiency of CO, H_2 and CH_4. Electrolysis were performed in CO_2 saturated water solution of 0.2 M K_2SO_4 under amperostatic condition (12 mA cm^{-2}) at 30 bars. System II. Working electrode: Ag plate (3 cm^2). Counter electrode: Compact Graphite. V = 0.05 L.

7.1.2 Effect of the supporting electrolyte at different CO_2 pressure

In order to evaluate the effect of the nature of the supporting electrolyte on the reduction of CO_2 to CO at silver cathode, some electrolyses were performed at different CO_2 pressures replacing K_2SO_4 with KOH and KCl, that, according to the literature, allow to achieve good productivity of CO.

Table 7.1 reports the results achieved after 2 hours at 1 and 15 bars with the different adopted supporting electrolytes using a silver plate cathode under amperostatic conditions (12 mA cm^{-2}). As shown in *Table 7.1, entries 1 and 2,* at 1 bar, for K_2SO_4 and KCl, at a compact graphite anode very low faradaic efficiencies in CO were recorded (< 3%). In the presence of KOH, a slightly higher production of CO was observed (FE_{CO} about 4%, see

Table 7.1, entry 3). Furthermore, in the case of KOH a slight production of formic acid was obtained (FE_{HCOOH} about 7%). It was observed that the nature of the supporting electrolyte affects also the working potential (and consequently the cell potential), which presents the less negative values in the presence of KOH. At the end of the electrolyses, the presence in solution of small compact graphite particles, generated by the deterioration of the anode, was observed.

Hence, the electrolyses with KOH and KCl were repeated using DSA as anode. In both cases, higher FE_{CO} were obtained (*Table 7.1, entries 4 and 5*). It is not clear why the replacement of compact graphite with DSA gave an increase of the production of CO. A possible explanation is that small particles of graphite released by the cathode could deposit on the cathode affecting its performances. Hence, in the following experiments were performed using DSA as anode. When electrolyses were repeated at 15 bars (*Table 7.1, entries 6-8*), the productions of CO increased for all the adopted supporting electrolytes, thus confirming the beneficial effect of CO_2 pressure on the cathodic reduction of carbon dioxide.

Table 7.1 Effect of supporting electrolyte on the CO_2 reduction to CO at different CO_2 pressures.[a]

Entry	*Supporting electrolyte*[b]	*Counter electrode*	*CO_2 pressure (bar)*	*Cell potential (V)*	*E (V vs SCE)*	*pH final*	*FE_{CO} (%)*	*r_{CO} (mol h^{-1} m^{-2})*	*Energetic consumption (kWh/mol_{CO})*	*EE_{CO} (%)*
1	K_2SO_4	Graphite	1	-4.00	-2	5.5	< 3	0.07	7.2	1.0
2	KCl	Graphite	1	-3.30	-1.8	5.5	< 3	0.06	7.1	1.6
3	KOH	Graphite	1	-3.45	- 1.65	7.2	4	0.09	4.7	1.5
4	KOH	DSA	1	-3.30	-1.75	7	9.8	0.22	1.8	3.9
5	KCl	DSA	1	-3.30	-1.7	5.5	7	0.16	2.6	2.8
6	K_2SO_4	DSA	15	-3.08	NA[c]	5–5.5	44	1.00	0.35	20.5
7	KCl	DSA	15	-3.05	NA[c]	5.5	39	0.87	0.42	17.3
8	KOH	DSA	15	-2.85	NA[c]	7.3	65	1.46	0.24	30.3
9	$KHCO_3$	DSA	15	-3.00	NA[c]	7.6	51	1.15	0.31	22.6

[a] Electrolyses were performed under amperostatic conditions (-12 $mAcm^{-2}$). System I was used for electrolyses at ambient pressure, System II was used for electrolyses at 20 bars. Working electrode: plate-Ag. N= 500 rpm. V= 0.05 L.
[b] Concentration: 0.2 M K_2SO_4; 0.5 M KCl, $KHCO_3$ or KOH.
[c] NA: Not Available.

Furthermore, a strong effect of the nature of the supporting electrolyte on the performances of the process was observed. In particular, with K_2SO_4 and KCl, at 15 bars (*Table 7.1, entries 6 and 7*) quite similar FE_{CO} were obtained (44 and 39%), while at KOH (*Table 7.1, entry 8*), a higher production of CO was obtained with a FE of about 65%. Furthermore, with KOH a lower cell potential was recorded. In particular, the energetic consumption decreased drastically using KOH (0.24 kWh/mol_{CO}) instead of the other two supporting electrolytes (about 0.4 kWh/mol_{CO}), because of both the higher FE_{CO} and the lower cell potential recorded with this salt. Furthermore, in the presence of KOH the formation of formic acid was also observed (FE_{HCOOH} about 8%).

In our system, where carbon dioxide is continuously fed to the system, H_2CO_3 is expected to react with KOH to give $KHCO_3$, thus giving rise to the formation of a buffer solution. Hence, in order to better evaluate this aspect, some electrolyses were repeated at 15 bars with $KHCO_3$ as supporting electrolyte (*Table 7.1, entry 9*), that gave a production of CO with a current efficiency close to 50%, lower than that achieved with KOH. The effect of the nature of the supporting electrolyte on the cathodic reduction of CO_2 at silver based

cathodes was evaluated by several authors [49,93,94], as discussed more in detail in ***Section 3.3.1***. In particular, Verma and co-authors [49] have studied that effect of the nature of the supporting electrolyte on the reduction of CO_2 on Ag based GDEs using KOH, KCl and $KHCO_3$. These authors showed that the presence of KOH allows to reduce the onset potential for CO and to increase the FE_{CO} with respect to both KCl and $KHCO_3$ in line with our results. It is possible that the different results achieved with KOH and $KHCO_3$ could be due to a different composition of the solution in the proximity of the electrode surface where CO_2 is depleted by its reduction to CO.

The effect of the nature of the supporting electrolyte on the cathodic reduction of CO_2 at silver based cathodes was evaluated by several authors [91,93,137–139],

Since KOH gave the best results in terms of FE_{CO}, the reduction of CO_2 at silver in the presence of this supporting electrolyte was further investigated by polarization studies. *Figure 8.4a* reports the polarizations achieved using KOH or K_2SO_4 under nitrogen and carbon dioxide atmosphere (1 bar). Similar forms of the polarizations were achieved at the two electrolytes. However, at KOH higher current densities were recorded under both nitrogen and CO_2 atmosphere (*Figure 7.4a and 7.4b*). In particular, for KOH the replacement of N_2 with CO_2 gives rise to an increase of the current density for working potentials up to -1.7 V vs. SCE, when the hydrogen evolution is limited: hence, there is a range of potential (from -1.3 to -1.7 V) where hydrogen evolution is very limited and CO_2 reduction can take place. Conversely, for working potential more negative than -1.7 V (when hydrogen evolution takes place in a relevant way), the addition of CO_2 gives rise to a decrease of the overall current density. This is probably due, as previously observed for experiments performed with K_2SO_4, to the fact that the derivatives of carbon dioxide reduction are adsorbed at silver, thus reducing the active sites for water reduction, or to the depletion of protons at the cathode surface driven by CO formation. As shown in *Figure 7.4c*, when the pressure of CO_2 is enhanced from 1 to 20 bar, a significant increase of the current density is observed, thus showing that the rate of carbon dioxide reduction depends on the concentration of CO_2 also using KOH. However, when the pressure is increased from 20 to 30 bar, no a significant change of the current densities was observed, thus showing that at these relatively high pressures, the process is no more limited by the concentration of CO_2 in the bulk. It was also shown that higher current densities are

recorded for KOH with respect to K_2SO_4 for each value of the pressure and of the cell potential (*Figure 7.1c and 7.4c*), according to the above-mentioned results and considerations.

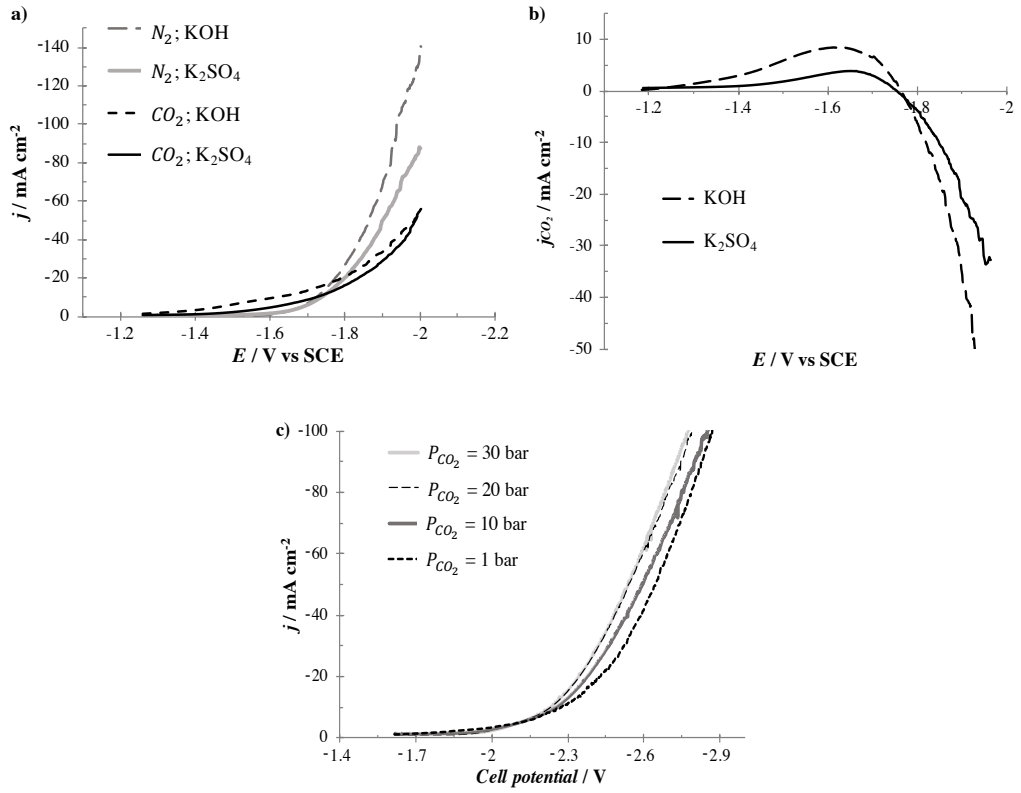

Figure 7.4 (a) LSVs at 5 mV s^{-1} under N_2 and CO_2 saturated water solution of 0.2 M K_2SO_4 or 0.5 M KOH; the relative polarizations were performed using system I. (b) Plot of CO_2 partial current density vs working potential using K_2SO_4 or KOH as supporting electrolyte; (c) pseudo-polarization curves performed at 5 mV s^{-1} under CO_2 saturated water solution of 0.5 M KOH at different CO_2 pressure (1 - 30 bar). The relative polarizations were performed using system II. Working electrode: plate-Ag (0.1 cm^2). V= 0.05 L.

7.1.3 Effect of the nature of cathode

The silver plate cathode (named plate-Ag) is characterized by a quite low surface. Hence, in order to increase the performances of the process some polarizations, pseudo-

polarizations and electrolyses were repeated with KOH as supporting electrolyte in the presence of a high surface Ag based electrode (hs-Ag).

7.1.3.1 Polarizations and pseudo-polarization measurements

Figure 7.5a reports some polarization curves recorded with two cathodes: the simple plate of silver, plate-Ag, and the hs-Ag which is characterized by a high active surface due to the utilization of commercial nanoparticle of Ag (particle size < 100 nm) supported on carbon fiber paper (described in detail in ***Section 5.1***). Under nitrogen atmosphere, high current densities are recorded for hs-Ag, probably for the higher surface due to the occurrence of pore structure. However, at the more negative working potentials, the polarizations achieved at the two electrodes become more similar. This behavior could be due to the fact that for very negative working potential, the massive hydrogen evolution could fill the pores, limiting the active surface available for water reduction. Under carbon dioxide atmosphere, the CO_2 reduction starts at similar potentials at the two electrodes, but a strong increase of the current density is recorded for hs-Ag with respect to plate-Ag, thus showing that the higher surface of hs-Ag can be exploited for CO_2 reduction. *Figure 8.5b* reports the value of j_{CO_2} achieved at the two cathodes in the absence and in the presence of mixing. It is shown that at both electrodes, j_{CO_2} presents a slight increase in the presence of the mixing, thus showing that at 1 bar the process is partially limited by the mass transfer of CO_2 to the cathode surface for both electrodes. *Figure 7.5c* reports the pseudo-polarizations achieved at the two cathodes at various CO_2 pressures. It is shown that (i) hs-Ag gives higher current densities with respect to plate-Ag at all adopted pressures and (ii) a smaller effect of pressure is observed for hs-Ag, thus showing that at this electrode the rate determining step, at least at pressure higher than 10 bar, depends in a limited way on the CO_2 concentration in the bulk.

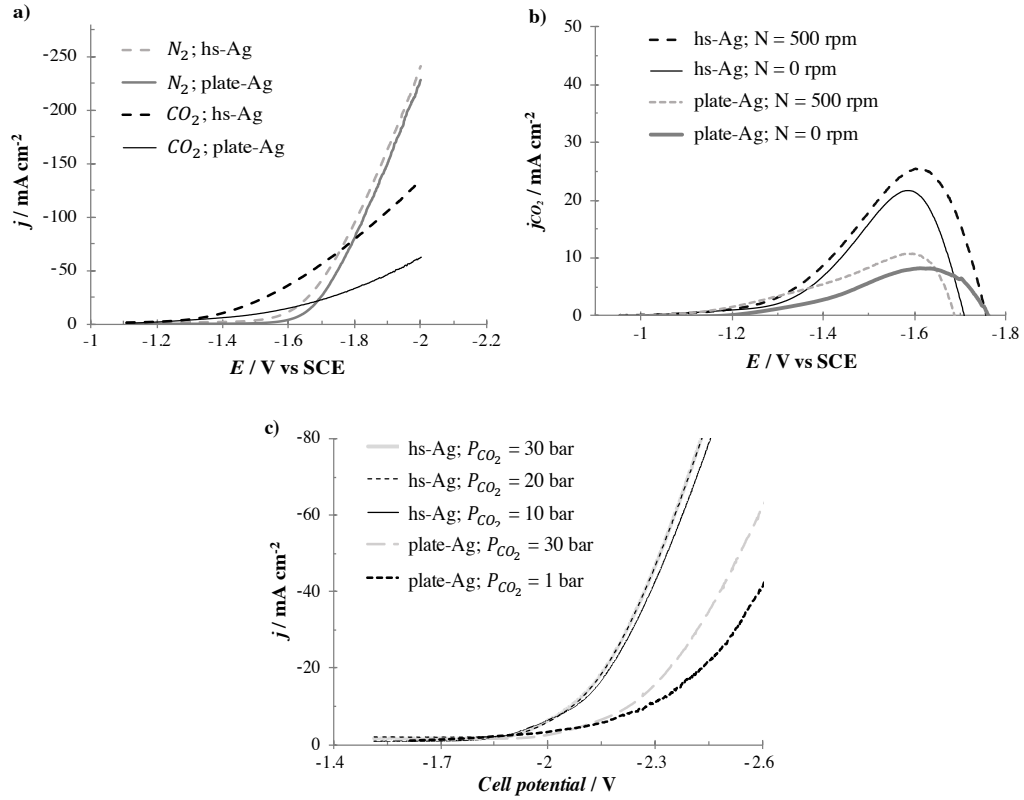

Figure 7.5 (a) LSVs at 5 mV s^{-1} under N_2 and CO_2 saturated water solution of 0.5 M KOH at two different electrodes: plate silver (plate-Ag) and a high surface silver electrode (hs-Ag) at 500 rpm; the relative polarizations were performed using system I. (b) Effect of the mixing rate on the CO_2 partial current density recorded at both plate-Ag and hs-Ag (N = 0 - 500 rpm). (c) Pseudo- polarization curves performed at 5 mV s^{-1} under CO_2 saturated water solution of 0.5 M KOH at different CO_2 pressure (1 - 30 bar) and at two different electrodes: plate-Ag and hs-Ag cathode. $A_{cathode}$= 0.1 cm^2. V= 0.05 L. The relative pseudo-polarizations were performed using system II.

7.1.3.2 Electrolyses

In order to study the effect of the nature of the cathode, electrolyses were performed using CO_2 saturated aqueous electrolyte of KOH at 1 bar and 12 mA cm^{-2}. As shown in *Table 7.2*, the replacement of the plate-Ag cathode with the hs-Ag one allowed to achieve a strong increase of CO production; indeed, the FE_{CO} were about 10 and 31% at the plate-Ag and hs-Ag cathodes (*entries 1 and 3*). In particular, at hs-Ag cathode the same value of current density was achieved with a lower value of the working potential, according with the

pseudo-polarization curves reported in *Figure 7.5*, thus allowing to reduce the impact of water reduction. When the electrolyses were repeated with KCl, an increase of FE_{CO} was still achieved at the hs-Ag cathode (*Table 7.2, entries 6 and 7*). However, at both cathodes the utilization of KCl gives rise to lower FE_{CO} with respect to that obtained with KOH (*Table 7.2, entries 1 and 3*) according to the considerations reported in the previous section.
In order to evaluate the effect of current density on the production of CO at the hs-Ag cathode, a series of amperostatic electrolyses was carried out at 1 bar and 12, 36 and 50 mA cm^{-2}. As shown in *Table 7.2*, at all adopted current densities, the replacement of plate-Ag (*entries 1 and 2*) with hs-Ag (*entries 3 and 4*) gave rise to an enhancement of about three times of the FE_{CO} and allowed to achieve a significant decrease of working and cell potentials. This is due to the fact that at low concentrations of carbon dioxide, the high surface of hs-Ag allows to speed up the process.
Focusing on hs-Ag cathode, the enhancement of the current density from 12 to 36 mA cm^{-2} (*Table 7.2, entries 3 and 4*) resulted in a strong increase of the CO production (from 0.69 to 1.61 mol h^{-1} m^{-2}) as a result of the higher amount of charge passed, even if with a decrease of the FE_{CO} from 31 to 24%, probably due to an increase of the hydrogen evolution due to the more negative working potential involved. When the current density was further increased to 50 mA cm^{-2} (*Table 7.2, entry 5*), the production of CO decreased, with a dramatic reduction of FE_{CO} to 9%, due to the occurrence of a quite negative working potential (-2.35 V vs SCE) that can favor the HER and decrease the CO desorption, as above discussed [115].

Table 7.2 Effect of cathode and supporting electrolyte on the performances of the CO_2 reduction to CO.[a]

Entry	*Cathode*	*Supporting electrolyte (0.5 M)*	*Current density (mA cm^{-2})*	*CO_2 pressure (bar)*	*Cell potential (V)*	*E (V vs SCE)*	*pH final*	*FE_{CO} (%)*	*r_{CO} (mol h^{-1} m^{-2})*	*Energetic consumption (kWh/mol$_{CO}$)*	*EE_{CO} (%)*
1	plate-Ag	KOH	- 12	1	-3.30	-1.75	7.0	9.8	0.22	1.83	3.9
2	plate-Ag	KOH	- 36	1	-4.90	-2.15	7.0	8.1	0.54	3.30	2.2
3	hs-Ag	KOH	- 12	1	-2.86	-1.60	7.3	31	0.69	0.50	14.7
4	hs-Ag	KOH	- 36	1	-4.00	-2.00	7.1	24	1.61	0.90	8.2
5	hs-Ag	KOH	- 50	1	-5.20	-2.35	7.3	9	0.84	3.10	2.3
6	plate-Ag	KCl	- 12	1	-3.30	-1.70	5.5	7	0.16	2.55	2.8
7	hs-Ag	KCl	- 12	1	-2.75	-1.55	5.7	14	0.31	1.05	6.8
8	plate-Ag	KOH	- 36	20	-4.10	NA	7.2	50	3.36	0.44	16.2
9	hs-Ag	KOH	- 36	20	-3.50	NA	7.3	57.8	3.90	0.32	22

[a]Electrolyses were performed using a DSA as counter electrode under amperostatic conditions. System I was used for electrolyses at ambient pressure, System II was used for electrolyses at 20 bars. N = 500 rpm. V= 0.05L

In order to evaluate the effect of the pressure on the process at the high surface cathode, a series of electrolyses was performed at different pressures (1, 10, 20 and 30 bar) and current densities (12, 36 and 50 mA cm^{-2}) at hs-Ag cathode. At 12 mA cm^{-2}, an increase of the pressure from 1 to 20 bars did not affect the performances of the process (*Table 7.3, entry 1 and 2*), according to the pseudo-polarization curves; indeed, a value of FE_{CO} of about 30% was achieved at both 1 and 20 bars, probably due to the fact that, under adopted operative conditions, the r.d.s. does not involve the mass transport of CO_2 or its cathodic reduction. Conversely, at 36 and 50 mA cm^{-2}, a strong effect of the pressure was observed; indeed, as an example, an increase of the pressure from 1 to 10 and 20 bar at 36 mA cm^{-2} resulted in a simultaneously reduction of the cell potential of about 115 and 550 mV, respectively, and in an enhancement of FE_{CO} from 24 up to 40 and 58% (*Table 7.3, entries 3-5*), probably due to the fact that at high current densities and working potentials the process becomes kinetically limited by the concentration of CO_2. Indeed, as shown in *Figure 7.5c*, at these values of current density and cell potentials, the current increases enhancing the pressure from 10 to 20 bars. However, a further increase of the pressure from 20 to 30 bars resulted in a slightly decrease of the FE_{CO} (from 58 to 50%) (*Table 7.3, entries*

5 and 6) and in a very small change of the total CO_2 reduction efficiency (computed taking in account both the CO and the formic acid formation), which was close to 59% at both 20 and 30 bars, according to the pseudo-polarizations reported in *Figure 7.5c*, because the concentration of carbon dioxide in the bulk at these high pressures becomes sufficient to sustain the mass transport and the cathodic reduction of CO_2 and the process is likely to be limited by a following step, similarly to what observed at low current densities.

The performances of hs-Ag and plate-Ag at high pressures were compared in *Table 7.2*. The increase of the pressure from 1 to 20 bar (*Table 7.2*, *entries 2, 4, 8 and 9*) allowed to increase drastically both the CO production and the corresponding FE_{CO} at both electrodes (from 8 to 50% at plate-Ag and from 24 to 58% at hs-Ag). However, at high pressures, the benefits of using hs-Ag is less important (FE_{CO} 50 % at plate-Ag and 58% at hs-Ag), because the high solubility of CO_2 achieved at high pressures makes less relevant the surface of the cathode.

Table 7.3 Effect of the pressure at hs-Ag cathode on the performances of the CO_2 reduction to CO.[a]

Entry	*CO_2 pressure (bar)*	*Current density (mA cm^{-2})*	*Cell potential (V)*	*pH final*	*FE_{CO} (%)*	*r_{CO} (mol h^{-1} m^{-2})*	*Energetic consumption (kWh/mol_{CO})*	*EE_{CO} (%)*
1	1	- 12	-2.86	7.3	31.0	0.69	0.50	14.4
2	20	- 12	-2.75	7.4	28.5	0.64	0.52	13.5
3	1	- 36	-4.00	7.1	24.0	1.61	0.90	8.0
4	10	- 36	-3.87	7.0	40.3	2.71	0.52	13.8
5	20	- 36	-3.45	7.4	57.8	3.90	0.32	22.3
6	30	- 36	-3.30	7.4	49.5	3.32	0.36	20.0
7	1	- 50	-5.20	7.3	9.0	0.84	3.10	2.3
8	20	- 50	-3.80	7.4	49.0	4.57	0.41	17.1

[a]Electrolysis were performed in water solution of 0.5M KOH electrode KOH under amperostatic conditions. System I was used for electrolyses at ambient pressure, System II was used for electrolyses at 20 bars. Working electrode: hs-Ag. Counter electrode: DSA®. N = 500 rpm. V= 0.05 L.

7.1.4 Evaluation of the stability at high pressure

To evaluate the stability of the performances of the process, two long amperostatic electrolyses were performed at simple plate-Ag with both KOH and K_2SO_4 electrolytes at 15 bar and 12 mA cm^{-2} (*Figure 7.6*). It was shown that the process takes place under very stable conditions in terms of production of CO, FE_{CO} and cell potential using KOH as supporting electrolyte; indeed, a FE_{CO} close to 70% was recorded for 10 hours for a very stable value of the cell potential. Conversely, for K_2SO_4, the FE_{CO} presented a small decrease from 53 to 45% after 2 hours, a period of stability for about 6 hours and a decrease for the last three hours to reach a value close to 20% after 10 hours and a correspondent increase of the cell potential up to 3.2 V, potentials values in which, according to the pseudo-polarization reported in *Figure 7.1d*, CO_2 and water reduction coexist and compete, thus limiting the CO_2 reduction.

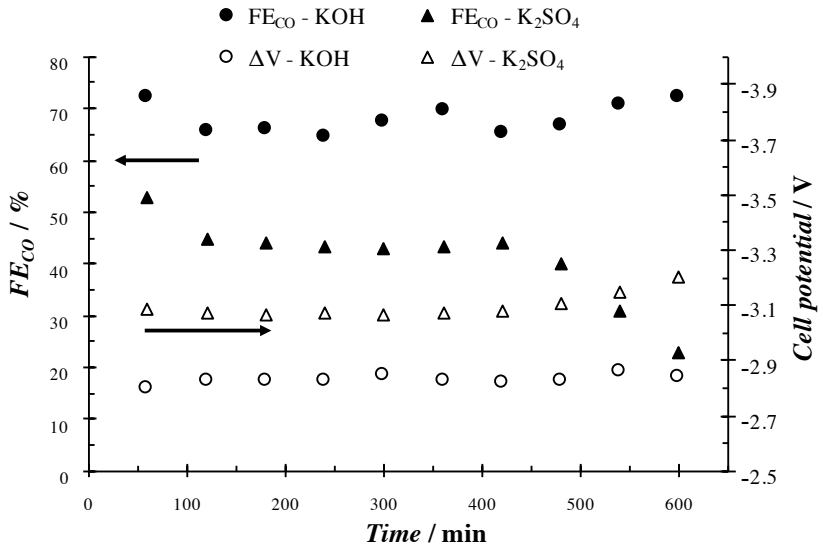

Figure 7.6 Effect of the time on the current efficiency of CO under pressurized condition (P_{CO_2}= 15 bar). Electrolysis was performed in water solution of 0.5 M KOH or 0.2 M K_2SO_4 at -12 mA cm^{-2}. System II. Working electrode: Ag plate (3 cm^2). Counter electrode: DSA®. N = 500 rpm. V = 0.05 L.

7.2 Electrochemical conversion of CO_2 at silver based GDE

According to the literature, the utilization of the GDE allows to achieve very high current densities. Hence, during a research stage at the *Chemical and Biomolecular Engineering Department, University of Illinois at Urbana-Champaign*, Illinois, *USA*, under the supervision of Dr. Paul J. A. Kenis, the effect of different operative parameters, including nature of the supporting electrolyte, catalyst cathode loading, electrolyte flow rate and concentration, on the performances of the CO_2 reduction to CO was investigated using an electrolyzer flow cell equipped with an Ag based gas diffusion electrode.

7.2.1 Effect of supporting electrolyte

As discussed in previous sections, the nature of the supporting electrolyte plays an important role in the electrochemical reduction of CO_2; in particular, some authors have shown that the utilization of alkaline solutions favors the CO production. In this context, a first series of electrolyses was performed at Ag-GDE using a electrolyzer flow cell (described in detail in ***Section 5.2.4***) using 3 M CsOH, KOH or NaOH as supporting electrolyte in order to compare the effect of the alkali metal cation. Electrolyses were performed at 17 mL min^{-1} of CO_2 flow rate, 1 mL min^{-1} of electrolyte flow rate, 2 mg_{Ag} cm^{-2} of catalyst cathode loading under potentiostatic condition (cell potential range: 1.6 – 3 V) for a very short time (~200 s to achieve the steady-state condition, i.e. constant current, and other 270 sec to collect three data point). *Figure 7.7* reports the partial current density of CO, j_{CO} (given by the products of the total current density, j, times the FE_{CO}), vs. the cell potential.

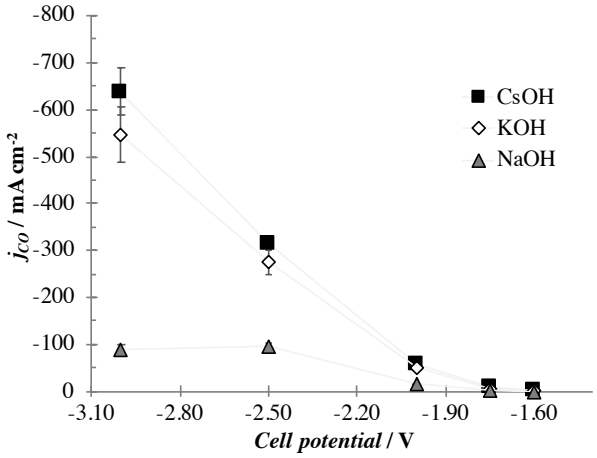

Figure 7.7 Effect of cations on the partial current density of CO. Electrolyses were performed at Ag-GDE (2 mg_{Ag} cm^{-2}) in aqueous electrolyte of CsOH, KOH, NaOH (3 M) using a flow electrolyzer cell. Cell potential range: -1.6 ÷ -3 V. Anode: IrO_2 (3 mg cm^{-2}). CO_2 flow rate: 17 mL min^{-1}. Electrolyte flow rate: 1 ml min^{-1}. System IV. Error bars refer to the difference in three injections.

Similar trends for all the investigated supporting electrolytes can be observed; in particular, an increase of the cell potential (i.e. cathode potential) gave rise to an enhancement of the CO_2 reduction rate. In particular, at low potentials there is not a relevant difference on the CO_2 reduction rate; however, at relatively high potentials, the effect of the nature of the supporting electrolyte on the performances of the process became more significant. More in detail, the utilization of CsOH and KOH are characterized by higher current densities and slightly lower onset potential with respect the NaOH (*Figure 7.7*), according to the literature (see ***Chapter 3***); this is due to the higher size of the cations, $Cs^+ > K^+ > Na^+$, thus, confirming that larger cations and alkaline solutions lead to high CO_2 reduction rate and lower overpotential to drive the reaction. Indeed, the highest current densities under the adopted operative conditions were achieved using CsOH based electrolyte; in particular the highest current density of about 637 mA cm^{-2} was recorded at -0.97 V vs RHE (cell potential: -3 V). In spite this promising result of the CsOH based electrolyte, it is necessary to mention that the utilization of this salt increase drastically the economics of the overall process due to its high commercial cost with respect to the utilization of the KOH.

Furthermore, it is worth to mention that NaOH was characterized by low faradaic efficiencies (FE_{CO} < 40%), at least at high cell potential, thus determining lower j_{CO} and a

scarce reproducibility of the results due the precipitation of salt on the GDE, limiting the active catalytic surface area and blocking the porous layers, and observed by visual inspection of the cell.

7.2.2 Effect of operative parameters on the CO production using CsOH and KOH

According to the data presented in the previous section, in the following one, the attention is focused on the CsOH and KOH as supporting electrolyte. In order to improve the performances of the CO_2 reduction to CO, a focused study was performed by changing some key parameters of the electrolyzer flow cell using Ag-GDE, i.e. electrolyte concentration, catalyst cathode loading and electrolyte flow rate.

7.2.2.1 Effect of electrolyte concentration

A series of experiments was performed at various electrolyte concentration of CsOH and KOH between 0.5 and 3 M in order to evaluate the effect of electrolyte concentration on the CO production. Electrolyses were carried out at Ag-GDE using a flow electrolizer cell at 3 V cell potential, 1 and 17 mL min^{-1} of electrolyte and CO_2 flow rate, respectively. *Figure 7.8* reports the current densities as a function of the electrolyte concentration for both CsOH and KOH based electrolyte. The CO_2 reduction rate increased by enhancing the electrolyte concentration in the investigated range of concentrations; indeed, a remarkably effects on the current densities can be observed by moving from 0.1 to 2 M for both the supporting electrolytes (ca. from about 35 mA cm^{-2} at 0.5 M for both KOH and CsOH to 440 and 540 mA cm^{-2} at 2 M for KOH and CsOH, respectively). Conversely, a further increase of the concentrations up to 3 M resulted in a slightly higher current densities for both CsOH and KOH based alkaline electrolytes. All the experiments here reported are characterized by very high selectivity towards CO close to 98-100% for all the investigated conditions. According to the literature, it is possible to suppose that high concentrations of

cations (higher amount of larger cation closer to the electrode surface) favors the stabilization of CO_2^- on the cathode surface.

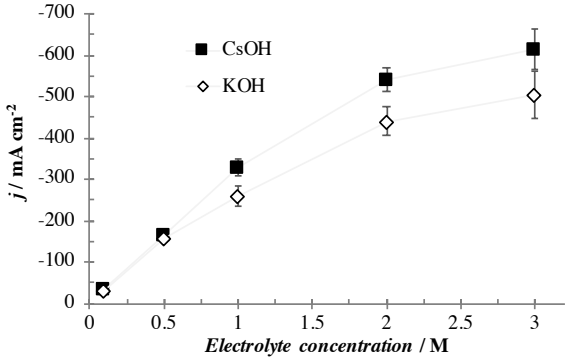

Figure 7.8 Effect of electrolyte concentration on the current density: 0.5 – 3 M CsOH and KOH. Electrolyses were performed at Ag-GDE (2 mg_{Ag} cm^{-2}) in aqueous electrolyte of CsOH and KOH using a flow electrolyzer cell. Cell potential: 3 V. Anode: IrO_2 (3 mg cm^{-2}). CO_2 flow rate: 17 mL min^{-1}. Electrolyte flow rate: 1 ml min^{-1}. System IV. Error bars refer to the difference in three injections.

7.2.2.2 Effect of cathode catalyst loading

In order to investigate the effect of the catalyst cathode loading on the CO production via electrochemical conversion of CO_2, a series of electrolyses was carried out in a wide range of catalyst loading between 0.5 to 3 mg_{Ag} cm^{-2} for both 3 M CsOH and KOH at 1 and 17 mL min^{-1} of, respectively, electrolyte and CO_2 flow rate. As shown in *Figure 7.9*, at relatively high cell potential, an increase of the catalyst loading from 0.3 to 1 mg_{Ag} cm^{-2} resulted in an enhancement of the CO_2 reduction rate for both CsOH and KOH; Indeed, at 3V, an enhancement of the current density from 565 to 610 mA cm^{-2} for CsOH by increasing the loading from 0.3 to 0.5 mg_{Ag} cm^{-2} and from 350 to 430 mA cm^{-2} for KOH was obtained by increasing the loading from 0.5 to 1 mg_{Ag} cm^{-2}. However, a further increase of the loading over 1 mg_{Ag} cm^{-2} did not affect the performances of the process reaching a plateau value (*Figure 7.9*) for both electrolytes. Under adopted operative conditions the selectivity is high and close to 98% and a really low amount of H_2 was detected, thus, showing that the process is affected by the number of active sites in which the reaction

takes place; indeed, for catalyst loadings below 1 mg_{Ag} cm^{-2} the CO_2 reduction rate seems to be limited by the low number of active sites, which increases at higher loading of catalyst. Above 1 mg_{Ag} cm^{-2} the reduction rate could be limited by mass transport limitation, as shown in the successive sections by experiments performed changing the flow rate.

These results show the possibility to work at low catalyst loading, reducing the investment costs, without losing the selectivity of the process.

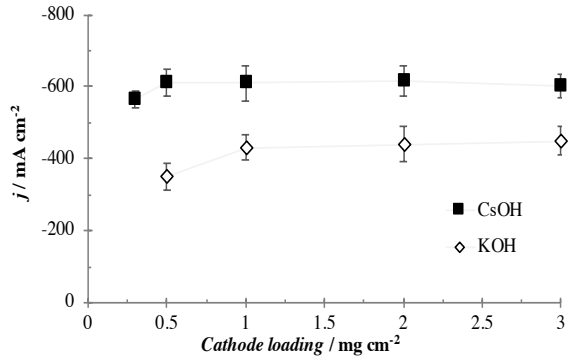

Figure 7.9 Effect of catalyst cathode loading 0.5 - 2 mg_{Ag} cm^{-2} on current density. Electrolyses were performed at Ag-GDE in aqueous electrolyte of CsOH and KOH (3 M) using a flow electrolyzer cell. Cell potential: 3 V. Anode: IrO_2 (3 mg cm^{-2}). CO_2 flow rate: 17 mL min^{-1}. Electrolyte flow rate: 1 ml min^{-1}. System IV. Error bars refer to the difference in three injections.

7.2.2.3 Effect of electrolyte flow rate

According to this hypothesis that the process may be limited by mass transfer stages, a series of experiments was planned with the aim to evaluate the effect of the electrolyte flow rate on the performances of the process; hence, electrolyses were carried out in a wide range of flow rate (0.1 – 5 mL min^{-1}) using 3M CsOH and KOH at 2 mg_{Ag} cm^{-2} and 17 sccm of CO_2 flow rate at cell potential of 3V. As shown in *Figure 8.10*, the electrolyte flow rate has a strong influence on the CO_2 reduction rate; in particular, under the adopted operative conditions, an increase of the electrolyte flow rate from 0.1 to 1 mL min^{-1} gave rise to higher current densities for both the investigated electrolyte (from 195 to 440 mA

cm^{-2} for KOH and from 318 to 637 mA cm^{-2} for CsOH). Furthermore, a further increase of the flow rate up to 5 mL min^{-1} increases the reduction rate of CO_2 up to about 886 mA cm^{-2} coupled with FE_{CO} of 98% using CsOH based electrolyte at 3 V cell potential, becoming the highest partial current density of CO reported in the literature at ambient condition.
Also in this case, the faradaic efficiencies for CO did not change significantly by varying the electrolyte flow rate and were closer of almost 100%.
The relevant effect of the flow rate indicates that the process is affected by a mass transfer stage due also to the very high current density employed. In particular, the process can be limited due to both the mass transfer of CO_2 to the cathode in spite of the triphasic contact achieved in the pores of GDE and/or, more likely, to the mass transport of the CO from the cathode to the bulk. In this framework, it seems reasonable to assume that a faster mass transport of CO, giving rise to a lower concentration of CO at the surface, can favor also the desorption of CO stage.
Higher flow rates than 5 mL min^{-1} were not investigated due to the high flooding rate in the flow cell.

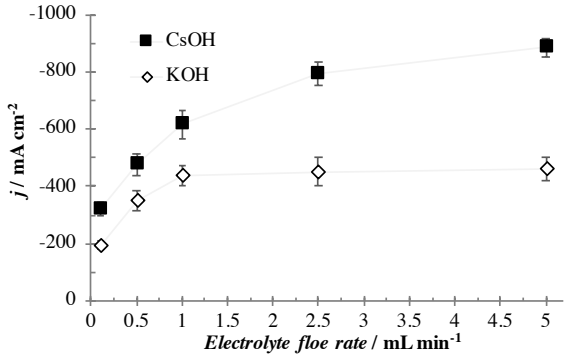

Figure 7.10 Effect of electrolyte flow rate 0.1 – 5 mL min^{-1} on the current density. Electrolyses were performed at Ag-GDE (2 mg_{Ag} cm^{-2}) in aqueous electrolyte of CsOH and KOH (3 M) using a flow electrolyzer cell. Cell potential: 3 V. Anode: IrO_2 (3 mg cm^{-2}). CO_2 flow rate: 17 mL min^{-1}. System IV. Error bars refer to the difference in three injections.

7.2.2.4 Effect of the temperature

Most of the studies on the CO_2 reduction to added value-products are reported at room temperature. However, in the framework of the electrochemical conversion of CO_2, an increase of the temperature would favor the kinetic of the process, speeding up the reduction rate, and, simultaneously, decreases the CO_2 solubility in water solution, increasing the mass transport limitation. Furthermore, high temperature, associated with the elevate pressure, could be an interesting way to integrate the CO_2 reduction process with a follow-up CO utilization for organic synthesis (i.e. Fischer-Trops process). Moreover, commercial electrolyzers generally operate at 75 - 120°C (due to the heat generated from the reactions during operation). Thus, suggesting the importance to investigate the effect of temperature on the performances of the CO_2 electrochemical conversion and the products distribution. For an example, the temperature effect (18, 35, and 70 °C) in a filter-press flow cell equipped with Ag-GDE and 0.5 M K_2SO_4 catholyte was investigated by Lister and co-worker [140]; they have shown that the highest FE for CO was achieved at 35°C, even if an increase of the temperature up to 70 °C allow to reduce the cell potential, enhancing the overall cell efficiency *Figure 7.11*.

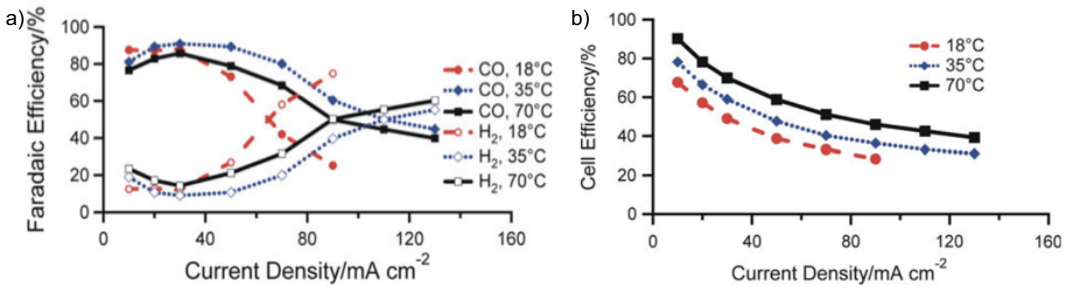

Figure 7.11 Effect of temperature and current density on the (a) faradaic efficiency of CO and H_2 and (b) cell efficiency [140]. Reproduced from ECS Transaction, 58, T.E. Lister, E.J. Dufek, S.G. Stone, Electrochemical Systems for Production of Syngas and Co-Products, 125-137, Copyright (2013), with permission from Electrochemical Society.

According to these considerations, a series of electrolyses was performed in a wide range of temperature (20 – 80°C) in an Ag-GDE (1 mg_{Ag} cm^{-2}) flow electrolyzer cell using 1 M

KOH based electrolyte at 0.5 mL min^{-1}, under potentiostatic mode (1.6 – 3 V cell potential), in order to investigate the effect of the temperature on the CO production, products distribution and on the overall process. As shown in *Figure 7.12a*, the total current density increases by enhancing the temperature at all the adopted cell potential; in particular, at 3 V the CO_2 reduction rate raises from 200 up to 300 mA cm^{-2} increasing the temperature from 20 to 60 °C. Conversely, the selectivity towards CO presented a maximum at 40°C (*Figure 7.12b*); hence, the enhancing of the temperature up to 40°C favors the kinetic of the reaction, speeding up the CO production, conversely a further increase of the temperature up to 80°C seems accelerate more the HER with respect the CO_2 reduction and increase the mass transport limitation (due to the low CO_2 solubility).

Figure 7.13 reports the distribution of the products process as a function of the of the cell potential at 20, 40 and 80°C; it is clear that an increase of the temperature decreased the selectivity of the process towards CO (EF_{CO} close to 100% at 20 - 40°C and 75% at 80°C). Furthermore, interesting to note that at highest investigated temperature a small amount of other CO_2-derivated products was detected (*Figure 7.13*) (i.e. formate (FE_{HCOO^-} : ~ 3% at T = 80°C), acetate (FE_{CH3COO^-} : ~ 2% at T = 40 – 80 °C) and a presence of H_2 was observed (EF_{H_2}= 10%).

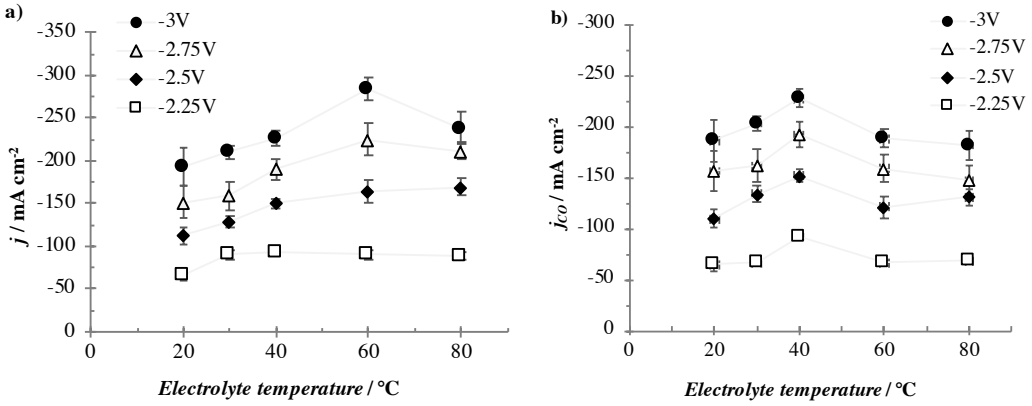

Figure 7.12 Effect of electrolyte temperature on the (a) total current density and (b) CO partial current density. Electrolyses were performed at Ag-GDE (1 mg_{Ag} cm^{-2}) in aqueous electrolyte of KOH (1 M) using a flow electrolyzer cell. Cell potential range: 1.6 - 3 V. Anode: IrO_2 (3 mg cm^{-2}). CO_2 flow rate: 17 mL min^{-1}. Electrolyte flow rate: 1 mL min^{-1}. System IV. Error bars refer to the difference in three injections.

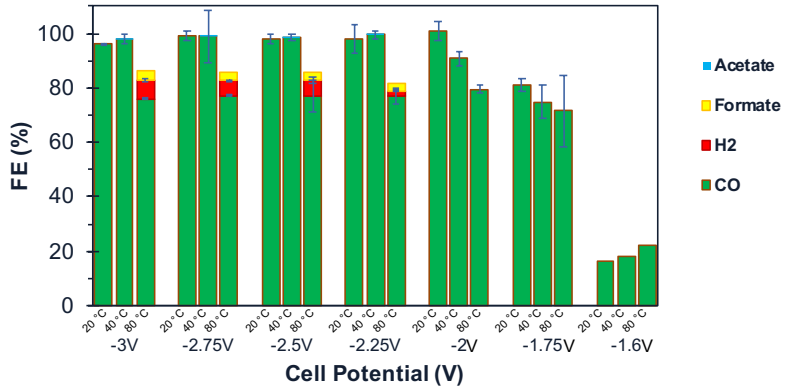

Figure 7.13 Effect of temperature on products distribution at different cell potential.

Several studies pointed out that the temperature could improve the performances of the process by affecting the energetic efficiency. Hence, in order to highlighted how the temperature influences the EE of the process, a series of electrolyses was performed in amperostatic mode (5 – 230 mA cm^{-2}) using an Ag-GDE (1 mg_{Ag} cm^{-2}), 1 M KOH at 0.5 mL min^{-1}. *Figure 7.14a* reports the cell potential as a function of the applied current density at different electrolyte temperature (20, 40, 60, 80°C). At all the temperature, as expected, the cell potential increases proportionally by enhancing the current density. Furthermore, as shown in *Figure 7.14a*, at very low current density, the temperature did not seem affect the cell potential; however, at higher current densities, an increase of the temperature gave rise to lower cell potentials, probably due to the high conductivity of the solution at higher temperature. For example, at 170 mA cm^{-2}, an increase of the temperature from 20 to 80°C resulted in a reduction of the cell potential of about 600 mV (cell potential 3.15 vs 2.50 V at 20 vs 80°C). Also in this case, an increase of the temperature decrease the selectivity for CO; indeed, FE_{CO} close to 100% at 20 - 40°C, 92% at 60°C and 73% at 80°C were achieved. An increase of the temperature is expected to upgrade the conductivity of the electrolytic solution, reducing the cell potential and, consequently, increase the EE.

However, as shown in *Figure 7.14b*, the EE_{CO} reached a maximum at 40°C at all the current densities, even if the cell potential decrease with the temperature at each current density;

this is due to the fact that the temperature favors more the kinetic of the HER with respect the CO_2 reduction, determining losses in selectivity toward CO.

Secondly, the remaining part of the drop-in cell potential could be due to a decrease in the anode potential and a drop in the ohmic resistances of the electrolyte. The electrolyte conductivity should increase as the temperature increases and the produced gas bubbles become smaller, and this leads to a lower shielding effect of the electrodes and to better contact with the electrolyte.

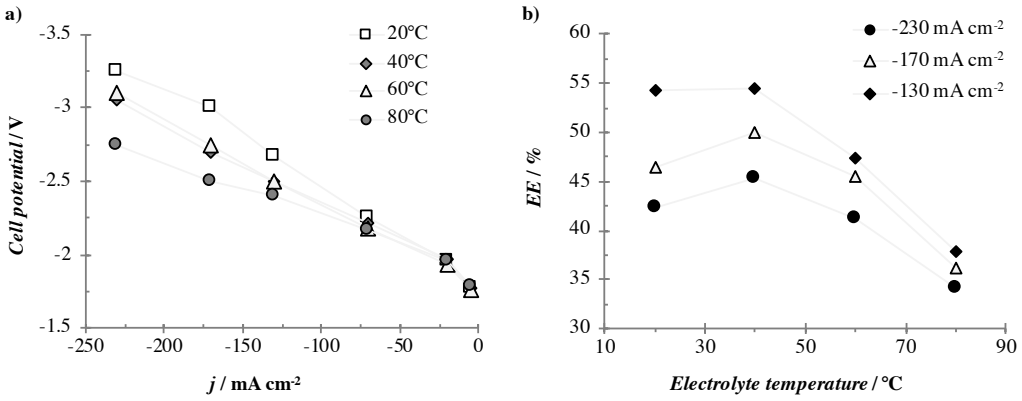

Figure 7.14 Effect of the temperature on the (a) cell potential and (b) energy efficiency at different current densities: 5- 230 mA cm^{-2}. Electrolyses were performed at Ag-GDE (1 mg_{Ag} cm^{-2}) in aqueous electrolyte of KOH (1 M) using a flow electrolyzer cell. Anode: IrO_2 (3 mg cm^{-2}). CO_2 flow rate: 17 mL min^{-1}. Electrolyte flow rate: 0.5 mL min^{-1}. System IV.

Conclusions

Conclusions

The electrochemical conversion of CO_2 is an interesting but challenging route in the perspectives of an utilization on the applicative scale; in particular, several obstacles are still to be overcome due to low CO_2 solubility in water (0.033M), low stability and high overall costs, for example, related to high energetic consumption and to costs of catalysts and membranes. In this work, electrochemical processes for the conversion of carbon dioxide to formic acid and carbon monoxide at Sn and Ag cathodes, respectively, in aqueous electrolyte, were studied using a simple and cheaper undivided pressurized electrochemical cell, to avoid the penalties given by the presence of the separator, in order to improve the performances of the processes (in terms of current density, faradaic efficiency, concentration of the liquid product, in the case of formic acid, and stability with the time).

Formic acid is the simplest carboxylic acid used in several industrial fields, i.e. pharmaceuticals, chemicals, and agriculture, with a global demand of 0.95 Mton/year. According to literature, if properly optimized, the electrochemical production of HCOOH could be a cheaper and more ecofriendly alternative with respect to the traditional ways for its synthesis. In particular, to be suitable for the large-scale industry, the process should present simultaneously high values of current density, faradaic efficiency and concentration of HCOOH as well as good stability. However, up to our knowledges on the literature of CO_2 reduction to HCOOH, nowadays, we are far to reach this goal. Indeed, most studies are characterized by high faradaic efficiency of HCOOH in a wide range of CO_2 reduction rate (~ 5 - 400 mA cm^{-2}), but they don't report long test analysis on the performances of the process (time < 4 h); conversely, the few stability analyses reported in literature are coupled with quite high faradaic efficiency of HCOOH, but really low conversion rate (< 20 mA cm^{-2}) which is no appealing for the applicative scale. An exception is given by the results reported by Kaczur that report high current density (140 mA cm^{-2}), faradaic efficiency (85%) and time (140 h); however, the high overall costs of

this configuration setup make it less suitable from an applicative point of view. In this framework, gas diffusion electrodes (GDEs) and pressurized CO_2 systems were implemented to overcome the mass transport limitation due to the low CO_2 solubility.

In this work, to achieve information on reaction mechanism and evaluate the kinetic of the process, electrochemical conversion of CO_2 to formic acid in aqueous electrolyte of Na_2SO_4 was investigated by both polarizations and electrolyses in a wide range of CO_2 pressure, using an undivided cell under pressurized conditions equipped with a simple and cheap Sn foil cathode. It was found that the reduction of pressurized CO_2 at a tin cathode can be described by a simple reaction mechanism, which involves the following key stages: (i) mass transfer of CO_2 to the cathode; (ii) its adsorption described by a Langmuir equation; (iii) cathodic reduction of adsorbed CO_2 to adsorbed $CO_2^{-\cdot}$; (iv) cathodic reduction of adsorbed $CO_2^{-\cdot}$ to HCOOH. In particular, according to our results and the proposed reaction mechanism, the pressurized CO_2 reduction process at tin cathode is under mixed kinetic control of mass transport and reduction of adsorbed CO_2; more in detail, it is more limited by mass transfer for lower values of CO_2 pressure and by the reduction stages for higher values of CO_2 pressure.

It was observed that the utilization of pressure can change drastically the performances of the process; in particular, according to the literature, for sufficiently high current density, the increase of pressure resulted in a dramatic enhancement of the final concentration of formic acid. As an example, a faradaic efficiency of about 60% coupled with a generation of formic acid of 426 mM was achieved at 30 bar and 75 mA cm^{-2}. According to these interesting results in the perspective of practical utilization of this synthetic route, the electrochemical conversion of CO_2 to formic acid at a tin cathode was attempted in an undivided pressurized filter-press cell with a continuous recirculation of the solution (0.9 L). The effect of several operating parameters on the performances of the process was investigated. It was found that the system is stable with the time and it allows the generation of high concentrations of HCOOH (up to about 0.4 M) using relatively high carbon dioxide pressures (such as 23 bar) and current densities (such as 50 mA cm^{-2}). Furthermore, the results achieved in the adopted system are similar or slightly better than that achieved in a batch pressurized cell with a small volume (0.05 L), thus showing that the scale-up of the

process did not worse the performances of the system allowing to reach faradaic efficiency of 75%.

Eventually, according to the presented mechanism reaction and the relative rate determining steps, a simple theoretical model was developed based on the cathodic conversion of pressurized CO_2 to HCOOH and on its anodic oxidation, in order to describe the process and to evaluate the effect of operative parameters by using an undivided cell. The theoretical model was in good agreement with experimental results collected and well described the effect of several operative parameters, including current density and pressure, time passed, kind of reactor and flow-dynamic.

Carbon monoxide is one of the main C_1-building blocks and a key carbon intermediate used in large industrial processes, such as the synthesis of hydrocarbons by the Fischer-Tropsch process. The electrochemical *via* for the CO production could be a valid strategy to both reuse waste-CO_2 obtaining an added-value product and develop a new and safer alternative CO generation to be integrated with a follow-up CO utilization for organic synthesis, overcoming the transportation issues linked to its usage as toxic reagent. To date, carbon monoxide production via electrochemical pathway is mainly studied using GDEs allowing to achieve high current densities coupled with quantitative FE for a short time. Here, the electrochemical conversion of CO_2 to CO was studied at both simple silver electrodes under pressurized conditions (1 – 30 bar) and at GDE at 1 bar with the aim of evaluate the nature of the supporting electrolyte using an aqueous solution and an undivided and simple cell by carrying out both polarizations, pseudo-polarizations and electrolyses. It was found that the utilization of pressure has a strong effect on the CO_2 reduction with all the adopted supporting electrolytes, enhancing the faradaic efficiencies of CO. For example, at silver plate electrode and 12 mA cm^{-2}, FE_{CO} dramatically increased from really low values (< 4%) at 1 bar to 67% at 30 bars or 44% at 15 bars by using an aqueous electrolyte of K_2SO_4 or KCl, respectively. Moreover, at high pressure, there is a very important effect of the nature of the supporting electrolyte; indeed, at 15 bars, a higher production of CO with a quite high current efficiency of about 65% was reached by

replacing K_2SO_4 or KCl (both FE_{CO} ~ 40%) with KOH at silver plate cathode and 12 mA cm^{-2}.

To improve the performances, the effect of the surface of the electrode was analyzed, showing that it strongly depends on the adopted CO_2 pressure. At 1 bar the increase of the surface allows to improve the performances of the process; as an example, the replacement of the plate Ag electrode with a high surface one allows to increase the FE_{CO} from 8 to 24% at 36 mA cm^{-2}. However, at 20 bar the effect of the surface is reduced; indeed, the replacement gave rise to a quite small improvement of the faradaic efficiency for CO from 50 to 57% at plate and high surface Ag electrode, respectively, at 36 mA cm^{-2}, thus showing that the productivity of the system can be increased, by enhancing the current density, i) using high pressure of CO_2 or ii) high surface electrodes. It is worth to mention that, under particular operative conditions, the reduction of pressurized CO_2 gave rise to the formation of CH_4 even if with low current efficiency (4%). Eventually, the stability of the process was reported. It was shown that the stability highly depends on the adopted operating conditions for both pressurized system at silver plate electrode. In particular, at least for the utilization of KOH as supporting electrolyte, the process was stable with the time maintaining a quite high current efficiency for CO of about 70% for 10 h using relatively high pressure (15 bar) and a simple plate silver electrode.

In order to evaluate the implementation of GDE electrodes, during a research stage at the *Chemical and Biomolecular Engineering Department*, *University of Illinois at Urbana-Champaign*, Illinois, *USA*, the effect of different operative parameters, including nature of the supporting electrolyte (NaOH, KOH, CsOH), catalyst cathode loading, electrolyte flow rate and concentration, on the performances of the CO_2 reduction to CO was investigated using an electrolyzer flow cell equipped with an Ag based gas diffusion electrode. It was found that the highest performances were guaranteed by the utilization of CsOH as supporting electrolyte and the higher was the concentration, the higher were the performances. Furthermore, the reduction rate of CO_2 at Ag-GDE increased by enhancing the electrolyte flow rate; indeed, an increase of the flow rate up to 5 mL min^{-1} allowed to reach 890 mA cm^{-2} coupled with a faradaic efficiency for CO of 98% using CsOH based

electrolyte at -3V (cell potential), becoming the highest partial current density of CO reported in the literature at ambient condition.

In conclusion, the results collected during the PhD thesis demonstrate that the reduction of carbon dioxide to formic acid or carbon monoxide can be carried out in simple undivided cells equipped with plate electrodes, avoiding the additional costs of membranes and more complex electrodes, using mild pressures (10-20 bar) that are not expensive on an applicative scale. Further studies will be useful in the future to better evaluate the stability with the time and the economics of the developed processes.

Bibliographic references

[1] A.S. Reis Machado, M. Nunes da Ponte, CO_2 capture and electrochemical conversion, Curr. Opin. Green Sustain. Chem. 11 (2018) 86–90. doi:10.1016/j.cogsc.2018.05.009.

[2] W. Zhang, Y. Hu, L. Ma, G. Zhu, Y. Wang, X. Xue, Progress and Perspective of Electrocatalytic CO_2 Reduction for Renewable Carbonaceous Fuels and Chemicals, Adv. Sci. 5 (2018) 1700275. doi:10.1002/advs.201700275.

[3] O.S. Bushuyev, P. De Luna, C.T. Dinh, L. Tao, G. Saur, J. Van De Lagemaat, S.O. Kelley, E.H. Sargent, What Should We Make with CO_2 and How Can We Make It ?, Joule. 2 (2018) 1–8. doi:10.1016/j.joule.2017.09.003.

[4] S. Zhao, S. Li, T. Guo, S. Zhang, J. Wang, Y. Wu, Advances in Sn-Based Catalysts for Electrochemical - CO_2 Reduction, Nano-Micro Lett. 11 (2019) 62. doi:10.1007/s40820-019-0293-x.

[5] P.R. Yaashikaa, P.S. Kumar, S.J. Varjani, A. Saravanan, A review on photochemical , biochemical and electrochemical transformation of CO_2 into value-added products, J. CO_2 Util. 33 (2019) 131–147. doi:10.1016/j.jcou.2019.05.017.

[6] J.S. Yoo, R. Christensen, T. Vegge, J.K. Nørskov, F. Studt, Theoretical Insight into the Trends that Guide the Electrochemical Reduction of Carbon Dioxide to Formic Acid, ChemSusChem. 9 (2016) 358–363. doi:10.1002/cssc.201501197.

[7] W. Lv, R. Zhang, P. Gao, L. Lei, Studies on the faradaic efficiency for electrochemical reduction of carbon dioxide to formate on tin electrode, J. Power Sources. 253 (2014) 276–281. doi:10.1016/j.jpowsour.2013.12.063.

[8] A.S. Agarwal, Y. Zhai, D. Hill, N. Sridhar, The electrochemical reduction of carbon dioxide to formate/formic acid: Engineering and economic feasibility, ChemSusChem. 4 (2011) 1301–1310. doi:10.1002/cssc.201100220.

[9] H.R.M. Jhong, S. Ma, P.J. Kenis, Electrochemical conversion of CO_2 to useful chemicals: Current status, remaining challenges, and future opportunities, Curr. Opin. Chem. Eng. 2 (2013) 191–199. doi:10.1016/j.coche.2013.03.005.

[10] M.R. Singh, E.L. Clark, A.T. Bell, Effects of electrolyte, catalyst, and membrane composition and operating conditions on the performance of solar-driven electrochemical reduction of carbon dioxide, Phys. Chem. Chem. Phys. 17 (2015) 18924–18936. doi:10.1039/C5CP03283K.

[11] V.S.K. Yadav, M.K. Purkait, Solar cell driven electrochemical process for the reduction of CO_2 to HCOOH on Zn and Sn electrocatalysts, Sol. Energy. 124 (2016) 177–183. doi:10.1016/j.solener.2015.11.037.

[12] S. Sabatino, A. Galia, G. Saracco, O. Scialdone, Development of an Electrochemical Process for the Simultaneous Treatment of Wastewater and the Conversion of Carbon Dioxide to Higher Value Products, ChemElectroChem. 4 (2017) 150–159. doi:10.1002/celc.201600475.

[13] T.E. Lister, E.J. Dufek, Chlor-syngas: Coupling of electrochemical technologies for production of commodity chemicals, Energy and Fuels. 27 (2013) 4244–4249. doi:10.1021/ef302033j.

[14] N. Sridhar, A. Agarwal, E. Rode, Electrochemical Production of Chemicals, (2012).

[15] A. Dominguez-Ramos, B. Singh, X. Zhang, E.G. Hertwich, A. Irabien, Global warming footprint of the electrochemical reduction of carbon dioxide to formate, J. Clean. Prod. 104 (2015) 148–155. doi:10.1016/j.jclepro.2013.11.046.
[16] H. Li, C. Oloman, Development of a continuous reactor for the electro-reduction of carbon dioxide to formate – Part 2 : Scale-up, J. Appl. Electrochem. 37 (2007) 1107–1117. doi:10.1007/s10800-007-9371-8.
[17] A.J. Martín, G.O. Larrazábal, J. Pérez-Ramírez, Towards sustainable fuels and chemicals through the electrochemical reduction of CO_2: Lessons from water electrolysis, Green Chem. 17 (2015) 5114–5130. doi:10.1039/c5gc01893e.
[18] A.S.R. Machado, A.V.M. Nunes, M.N. da Ponte, Carbon dioxide utilization—Electrochemical reduction to fuels and synthesis of polycarbonates, J. Supercrit. Fluids. 134 (2018) 150–156. doi:10.1016/j.supflu.2017.12.023.
[19] D. Du, R. Lan, J. Humphreys, S. Tao, Progress in inorganic cathode catalysts for electrochemical conversion of carbon dioxide into formate or formic acid, J. Appl. Electrochem. 47 (2017) 661–678. doi:10.1007/s10800-017-1078-x.
[20] J. Qiao, Y. Liu, F. Hong, J. Zhang, A review of catalysts for the electroreduction of carbon dioxide to produce low-carbon fuels, Chem. Soc. Rev. 43 (2014) 631–675. doi:10.1039/c3cs60323g.
[21] M. Jitaru, D. a. Lowy, M. Toma, B.C. Toma, L. Oniciu, Electrochemical reduction of carbon dioxide on flat metallic cathodes, J. Appl. Electrochem. 27 (1997) 875–889. doi:10.1023/1018441316386.
[22] Y. Zheng, W. Zhang, Y. Li, J. Chen, B. Yu, J. Wang, L. Zhang, J. Zhang, Energy related CO_2 conversion and utilization: Advanced materials/nanomaterials, reaction mechanisms and technologies, Nano Energy. 40 (2017) 512–539. doi:10.1016/j.nanoen.2017.08.049.
[23] C. Zhao, J. Wang, Electrochemical reduction of CO_2 to formate in aqueous solution using electro-deposited Sn catalysts, Chem. Eng. J. 293 (2016) 161–170. doi:10.1016/j.cej.2016.02.084.
[24] J. Durst, A. Rudnev, A. Dutta, Y. Fu, J. Herranz, V. Kaliginedi, A. Kuzume, A.A. Permyakova, Y. Paratcha, P. Broekmann, T.J. Schmidt, Electrochemical CO_2 Reduction – A Critical View on Fundamentals, Materials and Applications, Chim. Int. J. Chem. 69 (2015) 769–776. doi:10.2533/chimia.2015.769.
[25] L.M. Chiacchiarelli, N. Scientific, G.S. Frankel, Cathodic degradation mechanisms of pure Sn electrocatalyst in a nitrogen atmosphere Cathodic degradation mechanisms of pure Sn electrocatalyst in a nitrogen atmosphere, J. Appl. Electrochem. 42 (2012) 21–29. doi:10.1007/s10800-011-0367-z.
[26] S. Hernández, M.A. Farkhondehfal, F. Sastre, M. Makkee, G. Saracco, N. Russo, Syngas Production from Electrochemical Reduction of CO_2: Current Status and Prospective Implementation, Green Chem. 19 (2017) 2326–2346. doi:10.1039/C7GC00398F.
[27] J. Turner, G. Sverdrup, M.K. Mann, P. Maness, B. Kroposki, M. Ghirardi, R.J. Evans, D. Blake, Renewable hydrogen production, Int. J. Energy Res. 32 (2008) 379–407. doi:10.1002/er.1372.
[28] P. Millet, D. Dragoe, S. Grigoriev, V. Fateev, C. Etievant, R. De Nozay, GenHyPEM : A research program on PEM water electrolysis supported by the European Commission, Int. J. Hydrogen Energy. 34 (2009) 4974–4982.

doi:10.1016/j.ijhydene.2008.11.114.
[29] L.M. Gandı, R. Oroz, A. Ursu, P. Sanchis, P.M. Die, Renewable Hydrogen Production: Performance of an Alkaline Water Electrolyzer Working under Emulated Wind Conditions, Energy & Fuels. 21 (2007) 1699–1706. doi:10.1021/ef060491u.
[30] D. Kopljar, A. Inan, P. Vindayer, N. Wagner, E. Klemm, Electrochemical reduction of CO_2 to formate at high current density using gas diffusion electrodes, J. Appl. Electrochem. 44 (2014) 1107–1116. doi:10.1007/s10800-014-0731-x.
[31] M. Alvarez-Guerra, A. Del Castillo, A. Irabien, Continuous electrochemical reduction of carbon dioxide into formate using a tin cathode: Comparison with lead cathode, Chem. Eng. Res. Des. 92 (2014) 692–701. doi:10.1016/j.cherd.2013.11.002.
[32] E. Alper, O.Y. Orhan, CO_2 utilization : Developments in conversion processes, Petroleum. 3 (2017) 109–126. doi:10.1016/j.petlm.2016.11.003.
[33] E. Irtem, T. Andreu, A. Parra, M.D. Hernández-Alonso, S. García-Rodríguez, J.M. Riesco-García, G. Penelas-Pérez, J.R. Morante, Low-energy formate production from CO_2 electroreduction using electrodeposited tin on GDE, J. Mater. Chem. A. 4 (2016) 13582–13588. doi:10.1039/C6TA04432H.
[34] O. Scialdone, A. Galia, G. Lo Nero, F. Proietto, S. Sabatino, B. Schiavo, Electrochemical reduction of carbon dioxide to formic acid at a tin cathode in divided and undivided cells: Effect of carbon dioxide pressure and other operating parameters, Electrochim. Acta. 199 (2015) 332–341. doi:10.1016/j.electacta.2016.02.079.
[35] A. Martin, U. Armbruster, I. Gandarias, P.L. Arias, Glycerol hydrogenolysis into propanediols using in situ generated hydrogen – A critical review, Eur. J. Lipid Sci. Technol. 115 (2013) 9–27. doi:10.1002/ejlt.201200207.
[36] D.A. Bulushev, J.R.H. Ross, Vapour phase hydrogenation of olefins by formic acid over a Pd/C catalyst, Catal. Today. 163 (2011) 42–46. doi:10.1016/j.cattod.2010.01.055.
[37] I. Ganesh, Conversion of carbon dioxide into methanol - A potential liquid fuel: Fundamental challenges and opportunities (a review), Renew. Sustain. Energy Rev. 31 (2014) 221–257. doi:10.1016/j.rser.2013.11.045.
[38] H.-Y. Kim, I. Choi, S.H. Ahn, S.J. Hwang, S.J. Yoo, J. Han, J. Kim, H. Park, J.H. Jang, S.-K. Kim, Analysis on the effect of operating conditions on electrochemical conversion of carbon dioxide to formic acid, Int. J. Hydrogen Energy. 39 (2014) 16506–16512. doi:10.1016/j.ijhydene.2014.03.145.
[39] M. Rumayor, A. Dominguez-Ramos, A. Irabien, Formic Acid Manufacture: Carbon Dioxide Utilization Alternatives, Appl. Sci. 8 (2018) 914. doi:10.3390/app8060914.
[40] S. Sharma, D.S. Patle, A. Premkumar, S. Pandit, D. Manca, G.S. Nirmala, Intensification and performance assessment of the formic acid production process through a dividing wall reactive distillation column with vapor recompression, Chem. Eng. Process. Process Intensif. 123 (2018) 204–213. doi:10.1016/j.cep.2017.11.016.
[41] S. Verma, B. Kim, H.R.M. Jhong, S. Ma, P.J.A. Kenis, A Gross-Margin Model for Defining Technoeconomic Benchmarks in the Electroreduction of CO_2, ChemSusChem. 9 (2016) 1972-1979. doi:10.1002/cssc.201600394.

[42] Y. Hori, H. Wakabe, T. Tsukamoto, O. Koga, Electrocatalytic process of CO selectively in electrochemical reduction of CO_2 at metal electrodes in aqueous media, Electrochim. Acta. 39 (1994) 1833–1839. doi:10.1016/0013-4686(94)85172-7.

[43] M. Azuma, K. Hashimoto, M. Watanabe, T. Sakata, Electrochemical reduction of carbon dioxide to higher hydrocarbons in a $KHCO_3$ aqueous solution, J. Electroanal. Chem. 294 (1990) 299–303.

[44] Y. Hori, K. Kikuchi, S. Suzuki, Production of CO and CH_4 in electrochemical reduction of CO_2 at metal electrodes in aqueous hydrogencarbonate solution, Chem. Lett. 14 (1985) 1695–1698.

[45] F. Köleli, T. Atilan, N. Palamut, A. Gizir, Electrochemical reduction of CO2 at Pb- and Sn-electrodes in a fixed-bed reactor in aqueous K_2CO_3 and $KHCO_3$ media, J. Appl. Electrochem. 33 (2003) 447–450. doi:10.1023/A:1024471513136.

[46] J.T. Feaster, C. Shi, E.R. Cave, T. Hatsukade, D.N. Abram, K.P. Kuhl, C. Hahn, J.K. Nørskov, T.F. Jaramillo, Understanding Selectivity for the Electrochemical Reduction of Carbon Dioxide to Formic Acid and Carbon Monoxide on Metal Electrodes, ACS Catal. 7 (2017) 4822–4827. doi:10.1021/acscatal.7b00687.

[47] S. Verma, B. Kim, H.R.M. Jhong, S. Ma, P.J.A. Kenis, A gross-margin model for defining technoeconomic benchmarks in the electroreduction of CO_2, ChemSusChem. 9 (2016) 1972–1979. doi:10.1002/cssc.201600394.

[48] Anawati, G.S. Frankel, A. Agarwal, N. Sridhar, Degradation and deactivation of Sn catalyst used for CO_2 reduction as function of overpotential, Electrochim. Acta. 133 (2014) 188–196. doi:10.1016/j.electacta.2014.04.057.

[49] S. Verma, X. Lu, S. Ma, R.I. Masel, P.J.A. Kenis, The effect of electrolyte composition on the electroreduction of CO_2 to CO on Ag based gas diffusion electrodes, Phys. Chem. Chem. Phys. 18 (2016) 7075–7084. doi:10.1039/C5CP05665A.

[50] D. Kopljar, N. Wagner, E. Klemm, Transferring Electrochemical CO_2 Reduction from Semi-Batch into Continuous Operation Mode Using Gas Diffusion Electrodes, Chem. Eng. Technol. 39 (2016) 2042–2050. doi:10.1002/ceat.201600198.

[51] J. Wu, F.G. Risalvato, F. Ke, P.J. Pellechia, X. Zhou, Electrochemical Reduction of Carbon Dioxide I. Effects of the Electrolyte on the Selectivity and Activity with Sn Electrode, J. Electrochem. Soc. 159 (2012) 353–359. doi:10.1149/2.049207jes.

[52] Y. Chen, M.W. Kanan, Tin Oxide Dependence of the CO_2 Reduction Efficiency on Tin Electrodes and Enhanced Activity for Tin/Tin Oxide Thin-Film Catalysts, J. Am. Chem. Soc. 134 (2012) 1986–1989.

[53] R. Daiyan, X. Lu, Y.H. Ng, R. Amal, Surface engineered tin foil for electrocatalytic reduction of carbon dioxide to formate, Catal. Sci. Technol. 7 (2017) 2542–2550. doi:10.1039/C7CY00246G.

[54] S. Rasul, A. Pugnant, H. Xiang, J. Fontmorin, E.H. Yu, Low cost and efficient alloy electrocatalysts for CO_2 reduction to formate, J. CO_2 Util. 32 (2019) 1–10. doi:10.1016/j.jcou.2019.03.016.

[55] B. Kumar, V. Atla, J.P. Brian, S. Kumari, T.Q. Nguyen, M. Sunkara, J.M. Spurgeon, Reduced SnO_2 Porous Nanowires with a High Density of Grain Boundaries as Catalysts for Efficient Electrochemical CO_2-into-HCOOH Conversion, Angew. Chemie - Int. Ed. 56 (2017) 1–6. doi:10.1002/anie.201612194.

[56] M.F. Baruch, J.E.P. Iii, J.L. White, A.B. Bocarsly, Mechanistic Insights into the Reduction of CO_2 on Tin Electrodes using in Situ ATR-IR Spectroscopy, ACS Catal. 5 (2015) 3148–3156. doi:10.1021/acscatal.5b00402.

[57] R. Zhang, W. Lv, L. Lei, Role of the oxide layer on Sn electrode in electrochemical reduction of CO_2 to formate, Appl. Surf. Sci. 356 (2015) 24–29. doi:10.1016/j.apsusc.2015.08.006.

[58] H. Ge, Z. Gu, P. Han, H. Shen, A.M. Al-enizi, L. Zhang, G. Zheng, Mesoporous tin oxide for electrocatalytic CO_2 reduction, J. Colloid Interface Sci. 531 (2018) 564–569. doi:10.1016/j.jcis.2018.07.066.

[59] S. Sen, S.M. Brown, M. Leonard, F.R. Brushett, Electroreduction of carbon dioxide to formate at high current densities using tin and tin oxide gas diffusion electrodes, J. Appl. Electrochem. 49 (2019) 917–928. doi:10.1007/s10800-019-01332-z.

[60] S. Zhang, P. Kang, T.J. Meyer, Nanostructured tin catalysts for selective electrochemical reduction of carbon dioxide to formate, J. Am. Chem. Soc. 136 (2014) 1734–1737. doi:10.1021/ja4113885.

[61] X. Hu, H. Yang, M. Guo, M. Gao, E. Zhang, H. Tian, Synthesis and Characterization of (Cu,S) Co-doped SnO_2 for Electrocatalytic Reduction of CO_2 to Formate at Low Overpotential, ChemElectroChem. 5 (2018) 1330–1335. doi:10.1002/celc.201800104.

[62] S. Mu, J. Wu, Q. Shi, F. Zhang, Electrocatalytic Reduction of Carbon Dioxide on Nanosized Fluorine Doped Tin Oxide in the Solution of Extremely Low Supporting Electrolyte Concentration: Low Reduction Potentials, ACS Appl. Energy Mater. 1 (2018) 1680–1687. doi:10.1021/acsaem.8b00146.

[63] A. Dutta, A. Kuzume, M. Rahaman, S. Vesztergom, P. Broekmann, Monitoring the Chemical State of Catalysts for CO_2 Electroreduction: An In Operando Study, ACS Catal. 5 (2015) 7498−7502. doi:10.1021/acscatal.5b02322.

[64] E. Csapo, A.M. Ismail, G.F. Samu, Composition-Dependent Electrocatalytic Behavior of Au−Sn Bimetallic Nanoparticles in Carbon Dioxide Reduction´, ACS Energy Lett. 4 (2019) 48–53. doi:10.1021/acsenergylett.8b01996.

[65] I. Choi, H.-Y. Kim, S.H. Ahn, S.J. Hwang, S.J. Yoo, H.Y. Kim, J. Choi, H.J. Park, J.H. Jang, S.-K. Kim, Electrochemical Conversion of Carbon Dioxide to Formic Acid on Sn–Zn Alloy Catalysts Prepared by Electrodeposition, J. Nanosci. Nanotechnol. 16 (2016) 10470–10474. doi:10.1166/jnn.2016.13179.

[66] H. Kim, H. Lee, T. Lim, S.H. Ahn, Facile fabrication of porous Sn-based catalysts for electrochemical CO_2 reduction to HCOOH and syngas, J. Ind. Eng. Chem. 66 (2018) 248–253. doi:10.1016/j.jiec.2018.05.036.

[67] Q. Lai, N. Yang, G. Yuan, Highly efficient In – Sn alloy catalysts for electrochemical reduction of CO_2 to formate, Electrochem. Commun. 83 (2017) 24–27. doi:10.1016/j.elecom.2017.08.015.

[68] D. Gao, H. Zhou, F. Cai, D. Wang, Y. Hu, B. Jiang, W. Cai, X. Chen, R. Si, F. Yang, S. Miao, J. Wang, G. Wang, X. Bao, Switchable CO_2 electroreduction via engineering active phases of Pd nanoparticles, Nano Res. 10 (2017) 2181–2191. doi:10.1007/s12274-017-1514-6.

[69] R. Kortlever, I. Peters, S. Koper, M.T.M. Koper, Electrochemical CO_2 Reduction to Formic Acid at Low Overpotential and with High Faradaic Efficiency on Carbon-Supported Bimetallic Pd−Pt Nanoparticles, ACS Catal. 5 (2015) 3916–3923.

doi:10.1021/acscatal.5b00602.
[70] C. Oloman, H. Li, Electrochemical processing of carbon dioxide., ChemSusChem. 1 (2008) 385–391. doi:10.1002/cssc.200800015.
[71] O. Scialdone, F. Proietto, A. Galia, Electrochemical conversion of CO_2 to HCOOH at tin cathode: development of a theoretical model and comparison with experimental results, ChemElectroChem. 6 (2019) 162–172. doi:10.1002/celc.201801067.
[72] D.H. Won, C.H. Choi, J. Chung, M.W. Chung, E.H. Kim, S.I. Woo, Rational Design of a Hierarchical Tin Dendrite Electrode for Efficient Electrochemical Reduction of CO_2, ChemSusChem. 8 (2015) 3092–3098. doi:10.1002/cssc.201500694.
[73] V.S.K. Yadav, Y. Noh, H. Han, W.B. Kim, Synthesis of Sn catalysts by solar electro-deposition method for electrochemical CO_2 reduction reaction to HCOOH, Catal. Today. 303 (2018) 276–281. doi:10.1016/j.cattod.2017.09.015.
[74] W. Lv, J. Zhou, F. Kong, H. Fang, W. Wang, Porous tin-based film deposited on copper foil for electrochemical reduction of carbon dioxide to formate, Int. J. Hydrogen Energy. 41 (2015) 1585–1591. doi:10.1016/j.ijhydene.2015.11.100.
[75] S. Liu, F. Pang, Q. Zhang, R. Guo, Z. Wang, Y. Wang, W. Zhang, J. Ou, Stable nanoporous Sn/SnO_2 composites for efficient electroreduction of CO_2 to formate over wide potential range, Appl. Mater. Today. 13 (2018) 135–143. doi:10.1016/j.apmt.2018.08.014.
[76] P. Bumroongsakulsawat, G.H. Kelsall, Tinned graphite felt cathodes for scale-up of electrochemical reduction of aqueous CO_2, Electrochim. Acta. 159 (2015) 242–251. doi:10.1016/j.electacta.2015.01.209.
[77] D.T. Whipple, E.C. Finke, P.J.A. Kenis, Microfluidic Reactor for the Electrochemical Reduction of Carbon Dioxide: The Effect of pH, Electrochem. Solid-State Lett. 13 (2010) B109. doi:10.1149/1.3456590.
[78] A. Del Castillo, M. Alvarez-Guerra, J. Solla-Gullón, A. Sáez, V. Montiel, A. Irabien, Sn nanoparticles on gas diffusion electrodes: Synthesis, characterization and use for continuous CO_2 electroreduction to formate, J. CO_2 Util. 18 (2017) 222–228. doi:10.1016/j.jcou.2017.01.021.
[79] A. Del Castillo, M. Alvarez-guerra, J. Solla-gullón, A. Sáez, V. Montiel, A. Irabien, Electrocatalytic reduction of CO_2 to formate using particulate Sn electrodes: Effect of metal loading and particle size, Appl. Energy. 157 (2015) 165–173. doi:10.1016/j.apenergy.2015.08.012.
[80] Q. Wang, H. Dong, H. Yu, Development of rolling tin gas diffusion electrode for carbon dioxide electrochemical reduction to produce formate in aqueous electrolyte, J. Power Sources. 271 (2014) 278–284. doi:10.1016/j.jpowsour.2014.08.017.
[81] Y. Fu, Y. Li, X. Zhang, Y. Liu, X. Zhou, J. Qiao, Electrochemical CO_2 reduction to formic acid on crystalline SnO_2 nanosphere catalyst with high selectivity and stability, Chinese J. Catal. 37 (2016) 1081–1088. doi:10.1016/S1872-2067(15)61048-8.
[82] S. Sen, B. Skinn, T. Hall, M. Inman, E.J. Taylor, F.R. Brushett, Pulsed Electrodeposition of Tin Electrocatalysts onto Gas Diffusion Layers for Carbon Dioxide Reduction to Formate, MRS Adv. 2 (2017) 451–458. doi:10.1557/adv.2016.652.

[83] G.K.S. Prakash, F.A. Viva, G.A. Olah, Electrochemical reduction of CO_2 over Sn-Nafion coated electrode for a fuel-cell-like device, J. Power Sources. 223 (2013) 68–73. doi:10.1016/j.jpowsour.2012.09.036.

[84] Q. Wang, H. Dong, H. Yu, H. Yu, Enhanced performance of gas diffusion electrode for electrochemical reduction of carbon dioxide to formate by adding polytetrafluoroethylene into catalyst layer, J. Power Sources. 279 (2015) 1–5. doi:10.1016/j.jpowsour.2014.12.118.

[85] P. Jeanty, C. Scherer, E. Magori, K. Wiesner-Fleischer, O. Hinrichsen, M. Fleischer, Upscaling and continuous operation of electrochemical CO_2 to CO conversion in aqueous solutions on silver gas diffusion electrodes, J. CO_2 Util. 24 (2018) 454–462. doi:10.1016/j.jcou.2018.01.011.

[86] J. Wu, S.G. Sun, X.D. Zhou, Origin of the performance degradation and implementation of stable tin electrodes for the conversion of CO_2 to fuels, Nano Energy. 27 (2016) 225–229. doi:10.1016/j.nanoen.2016.06.028.

[87] Y. Hori, H. Konishi, T. Futamura, A. Murata, O. Koga, H. Sakurai, K. Oguma, "Deactivation of copper electrode" in electrochemical reduction of CO_2, Electrochim. Acta. 50 (2005) 5354–5369. doi:10.1016/j.electacta.2005.03.015.

[88] J.J. Kaczur, H. Yang, Z. Liu, S.D. Sajjad, R.I. Masel, Carbon Dioxide and Water Electrolysis Using New Alkaline Stable Anion Membranes, Front. Chem. 6 (2018) 1–16. doi:10.3389/fchem.2018.00263.

[89] D.U. Nielsen, X.M. Hu, K. Daasbjerg, T. Skrydstrup, Chemically and electrochemically catalysed conversion of CO_2 to CO with follow-up utilization to value-added chemicals, Nat. Catal. 1 (2018) 244–254. doi:10.1038/s41929-018-0051-3.

[90] M.T. Jensen, M.H. Rønne, A.K. Ravn, R.W. Juhl, D.U. Nielsen, S.U. Pedersen, K. Daasbjerg, T. Skrydstrup, X. Hu, Scalable carbon dioxide electroreduction coupled to carbonylation chemistry, Nat. Commun. 8 (2017) 1–8. doi:10.1038/s41467-017-00559-8.

[91] K. Sun, L. Wu, W. Qin, J. Zhou, Y. Hu, Z. Jiang, B. Shen, Z. Wang, Enhanced electrochemical reduction of CO_2 to CO on Ag electrocatalysts with increased unoccupied density of states, J. Mater. Chem. A. 4 (2016) 12616–12623. doi:10.1039/c6ta04325a.

[92] Y.-C. Hsieh, S.D. Senanayake, Y. Zhang, W. Xu, D.E. Polyansky, Effect of Chloride Anions on the Synthesis and Enhanced Catalytic Activity of Silver Nanocoral Electrodes for CO_2 Electroreduction, ACS Catal. 5 (2015) 5349–5356. doi:10.1021/acscatal.5b01235.

[93] M.R. Thorson, K.I. Siil, P.J. a. Kenis, Effect of Cations on the Electrochemical Conversion of CO_2 to CO, J. Electrochem. Soc. 160 (2013) F69–F74. doi:10.1149/2.052301jes.

[94] M. Ko, J. Vaes, E. Klemm, D. Pant, Solvents and Supporting Electrolytes in the Electrocatalytic Reduction of CO_2, IScience. 19 (2019) 135–160. doi:10.1016/j.isci.2019.07.014.

[95] B. Kim, S. Ma, H.R. Molly Jhong, P.J.A. Kenis, Influence of dilute feed and pH on electrochemical reduction of CO_2 to CO on Ag in a continuous flow electrolyzer, Electrochim. Acta. 166 (2015) 271–276. doi:10.1016/j.electacta.2015.03.064.

[96] S. Ma, R. Luo, J.I. Gold, A.Z. Yu, B. Kim, P.J.A. Kenis, Carbon nanotube

containing Ag catalyst layers for efficient and selective reduction of carbon dioxide, J. Mater. Chem. A. 4 (2016) 8573–8578. doi:10.1039/c6ta00427j.
[97] A. Salehi-Khojin, H.R.M. Jhong, B.A. Rosen, W. Zhu, S. Ma, P.J.A. Kenis, R.I. Masel, Nanoparticle silver catalysts that show enhanced activity for carbon dioxide electrolysis, J. Phys. Chem. C. 117 (2013) 1627–1632. doi:10.1021/jp310509z.
[98] Q. Lu, J. Rosen, Y. Zhou, G.S. Hutchings, Y.C. Kimmel, J.G. Chen, F. Jiao, A selective and efficient electrocatalyst for carbon dioxide reduction., Nat. Commun. 5 (2014) 1–6. doi:10.1038/ncomms4242.
[99] S. Ma, J. Liu, K. Sasaki, S.M. Lyth, P.J.A. Kenis, Carbon Foam Decorated with Silver Nanoparticles for Electrochemical CO_2 Conversion, Energy Technol. 5 (2017) 861–863. doi:10.1002/ente.201600576.
[100] Y. Chen, C.W. Li, M.W. Kanan, Aqueous CO_2 Reduction at Very Low Overpotential on Oxide-Derived Au Nanoparticles, J. Am. Chem. Soc. 134 (2012) 19969–19972. doi:10.1021/ja309317u.
[101] C.W. Li, M.W. Kanan, CO_2 reduction at low overpotential on Cu electrodes resulting from the reduction of thick Cu_2O films, J. Am. Chem. Soc. 134 (2012) 7231–7234. doi:10.1021/ja3010978.
[102] M.A. Farkhondehfal, S. Hernández, M. Rattalino, M. Makkee, A. Lamberti, A. Chiodoni, K. Bejtka, A. Sacco, F.C. Pirri, N. Russo, Syngas production by electrocatalytic reduction of CO_2 using Ag-decorated TiO2 nanotubes, Int. J. Hydrogen Energy. (2019). doi:10.1016/j.ijhydene.2019.04.180.
[103] M. Ma, B.J. Trześniewski, J. Xie, W.A. Smith, Selective and Efficient Reduction of Carbon Dioxide to Carbon Monoxide on Oxide-Derived Nanostructured Silver Electrocatalysts, Angew. Chemie - Int. Ed. 55 (2016) 9748–9752. doi:10.1002/anie.201604654.
[104] M.G. Kibria, J.P. Edwards, C.M. Gabardo, C. Dinh, A. Seifitokaldani, D. Sinton, E.H. Sargent, Electrochemical CO_2 Reduction into Chemical Feedstocks: From Mechanistic Electrocatalysis Models to System Design, Adv. Mater. 31 (2019) 1807166. doi:10.1002/adma.201807166.
[105] Q. Lu, F. Jiao, Electrochemical CO2reduction: Electrocatalyst, reaction mechanism, and process engineering, Nano Energy. 29 (2016) 439–456. doi:10.1016/j.nanoen.2016.04.009.
[106] R. Perry, D. Green, Perry's chemical engineers' handbook, 2008.
[107] B. Endrodi, G. Bencsik, F. Darvas, R. Jones, K. Rajeshwar, C. Janaàky, Continuous-flow electroreduction of carbon dioxide, Prog. Energy Combust. Sci. 62 (2017) 133–154. doi:10.1016/j.pecs.2017.05.005.
[108] D. Giovanelli, N.S. Lawrence, R.G. Compton, Electrochemistry at High Pressures: A Review, Electroanalysis. 16 (2004) 789–810. doi:10.1002/elan.200302958.
[109] F. Proietto, B. Schiavo, A. Galia, O. Scialdone, Electrochemical conversion of CO2 to HCOOH at tin cathode in a pressurized undivided filter-press cell, Electrochim. Acta. 277 (2018) 30–40. doi:10.1016/j.electacta.2018.04.159.
[110] K. Hara, A. Kudo, T. Sakata, Electrochemical Reduction of Carbon Dioxide under High Pressure on Various Electrodes in an Aqueous Electrolyte, J. Electroanal. Chem. 391 (1995) 141–147. doi:10.1016/0022-0728(95)03935-A.
[111] K. Hara, a. Kudo, T. Sakata, Electrochemical CO_2 reduction on a glassy carbon electrode under high pressure, J. Electroanal. Chem. 421 (1997) 1–4.

doi:10.1016/S0022-0728(96)01028-5.
[112] K. Hara, A. Tsuneto, A. Kudo, T. Sakata, Electrochemical Reduction of CO_2 on a Cu Electrode under High Pressure: Factors that Determine the Product Selectivity, J. Electrochem. Soc. 141 (1994) 2097–2103. doi:10.1149/1.2055067.
[113] M. Todoroki, K. Hara, A. Kudo, T. Sakata, Electrochemical reduction of high pressure CO_2 at Pb, Hg and In electrodes in an aqueous $KHCO_3$ solution, J. Electroanal. Chem. 394 (1995) 199–203. doi:10.1016/0022-0728(95)04010-L.
[114] K. Hara, A. Kudo, T. Sakata, Electrochemical reduction of high pressure carbon dioxide on Fe electrodes at large current density, J. Electroanal. Chem. 386 (1995) 257–260.
[115] A. Kudo, S. Nakagawa, A. Tsuneto, T. Sakata, Electrochemical Reduction of High Pressure CO_2 on Ni Electrodes, J. Electrochem. Soc. 140 (1993) 1541. doi:10.1149/1.2221599.
[116] T. Mizuno, K. Ohta, A. Sasaki, T. Akai, M. Hirano, A. Kawabe, Effect of Temperature on Electrochemical Reduction of High-Pressure CO_2 with In, Sn, and Pb Electrodes, Energy Sources. 17 (1995) 503–508. doi:10.1080/00908312.
[117] F. Köleli, T. Yesilkaynak, D. Balum, High pressure-high temperature CO_2 electro-reduction on Sn granules in a fixed-bed reactor, Fresenius Enviromental Bull. 12 (2003) 1202–1206.
[118] F. Köleli, D. Balun, Reduction of CO_2 under high pressure and high temperature on Pb-granule electrodes in a fixed-bed reactor in aqueous medium, Appl. Catal. A Gen. 274 (2004) 237–242. doi:10.1016/j.apcata.2004.07.006.
[119] M. Ramdin, A.R.T. Morrison, M. de Groen, R. van Haperen, R. De Kler, L.J.P. van den Broeke, J.P.M. Trusler, W. de Jong, T.J.H. Vlugt, High Pressure Electrochemical Reduction of CO_2 to Formic Acid/Formate: A Comparison between Bipolar Membranes and Cation Exchange Membranes, Ind. Eng. Chem. Res. 58 (2019) 1834–1847. doi:10.1021/acs.iecr.8b04944.
[120] E.J. Dufek, T.E. Lister, S.G. Stone, M.E. McIlwain, Operation of a Pressurized System for Continuous Reduction of CO_2, J. Electrochem. Soc. 159 (2012) F514–F517. doi:10.1149/2.011209jes.
[121] E.J. Dufek, T.E. Lister, S.G. Stone, Sampling dynamics for pressurized electrochemical cells, J. Appl. Electrochem. 44 (2014) 849–855. doi:10.1007/s10800-014-0693-z.
[122] C.M. Gabardo, A. Seifitokaldani, J.P. Edwards, C. Dinh, T. Burdyny, G. Kibria, C.P.O. Brien, E.H. Sargent, D. Sinton, Combined high alkalinity and pressurization enable efficient CO_2 electroreduction to CO, Energy Environ. Sci. 11 (2018) 2531–2539. doi:10.1039/c8ee01684d.
[123] H.R.Q. Jhong, F.R. Brushett, P.J.A. Kenis, The effects of catalyst layer deposition methodology on electrode performance, Adv. Energy Mater. 3 (2013) 589–599. doi:10.1002/aenm.201200759.
[124] A. Tamimi, E.B. Rinker, O.C. Sandall, Diffusion Coefficients for Hydrogen Sulfide, Carbon Dioxide, and Nitrous Oxide in Water over the Temperature Range 293–368 K, J. Chem. Eng. Data. 39 (1994) 330–332. doi:10.1021/je00014a031.
[125] A.A. Wragg, A.A. Leontaritis, Local mass transfer and current distribution in baffled and unbaffled parallel plate electrochemical reactors, Chem. Eng. J. 66 (1997) 1–10. doi:10.1016/S1385-8947(96)03148-8.

[126] C.A. Martínez-Huitle, S. Ferro, A. De Battisti, Electrochemical incineration of oxalic acid: Reactivity and engineering parameters, J. Appl. Electrochem. 35 (2005) 1087–1093. doi:10.1007/s10800-005-9003-0.
[127] W. Paik, T.N. Andersen, H. Eyring, Kinetic studies of the electrolytic reduction of carbon dioxide on the mercury electrode, Electrochim. Acta. 14 (1969) 1217–1232. doi:10.1016/0013-4686(69)87019-2.
[128] O. Azizi, M. Jafarian, F. Gobal, H. Heli, M.G. Mahjani, The investigation of the kinetics and mechanism of hydrogen evolution reaction on tin, Internatinal J. Hydrog. Energy. 32 (2007) 1755–1761. doi:10.1016/j.ijhydene.2006.08.043.
[129] Y.B. Vassiliev, V.S. Bagotsky, N.V. Osetrova, O.A. Khazova, N.A. Mayorova, Electroreduction of carbon dioxide: Part I. The mechanism and kinetics of electroreduction of CO_2 in aqueous solutions on metals with high and moderate hydrogen overvoltages, J. Electroanal. Chem. Interfacial Electrochem. 189 (1985) 271–294. doi:10.1016/0368-1874(85)80073-3.
[130] K. Subramanian, K. Asokan, D. Jeevarathinam, M. Chandrasekaran, Electrochemical membrane reactor for the reduction of carbondioxide to formate, J. Appl. Electrochem. 37 (2007) 255–260. doi:10.1007/s10800-006-9252-6.
[131] O. Scialdone, Electrochemical oxidation of organic pollutants in water at metal oxide electrodes: A simple theoretical model including direct and indirect oxidation processes at the anodic surface, Electrochim. Acta. 54 (2009) 6140–6147. doi:10.1016/j.electacta.2009.05.066.
[132] J. Rosen, G.S. Hutchings, Mechanistic Insights into the Electrochemical reduction of CO_2 to CO on Nanostructured Ag Surfaces, ACS. 5 (2016) 4293–4299.
[133] Y. Hori, H. Ito, K. Okano, K. Nagasu, S. Sato, Silver-coated ion exchange membrane electrode applied to electrochemical reduction of carbon dioxide, Electrochim. Acta. 48 (2003) 2651–2657. doi:10.1016/S0013-4686(03)00311-6.
[134] E.J. Dufek, T.E. Lister, M.E. McIlwain, Bench-scale electrochemical system for generation of CO and syn-gas, J. Appl. Electrochem. 41 (2011) 623–631. doi:10.1007/s10800-011-0271-6.
[135] Z. He, T. Liu, J. Tang, C. Zhou, L. Wen, J. Chen, S. Song, Highly active, selective and stable electroreduction of carbon dioxide to carbon monoxide on a silver catalyst with truncated hexagonal bipyramidal shape, Electrochim. Acta. 222 (2016) 1234–1242. doi:10.1016/j.electacta.2016.11.097.
[136] K.P. Kuhl, T. Hatsukade, E.R. Cave, D.N. Abram, J. Kibsgaard, T.F. Jaramillo, Electrocatalytic Conversion of Carbon Dioxide to Methane and Methanol on Transition Metal Surfaces, J. Am. Chem. Soc. 136 (2014) 14107–14113. doi:10.1021/ja505791r.
[137] B.A. Rosen, A. Salehi-Khojin, M.R. Thorson, W. Zhu, D.T. Whipple, P.J.A. Kenis, R.I. Masel, Ionic liquid-mediated selective conversion of CO_2 to CO at low overpotentials, Science. 334 (2011) 643–644. doi:10.1126/science.1209786.
[138] Y. Hori, K. Kikuchi, A. Murata, S. Suzuki, Production of Methane and Ethylene in Electrochemical Reduction of Carbon Dioxide At Copper Electrode in Aqueous Hydrogencarbonate Solution, Chem. Lett. 15 (1986) 897–898. doi:10.1246/cl.1986.897.
[139] W. Zhu, B.A. Rosen, A. Salehi-Khojin, R.I. Masel, Monolayers of choline chloride can enhance desired electrochemical reactions and inhibit undesirable ones,

Electrochim. Acta. 96 (2013) 18–22. doi:10.1016/j.electacta.2013.02.061.
[140] T.E. Lister, E.J. Dufek, S.G. Stone, Electrochemical Systems for Production of Syngas and Co-Products, ECS Trans. 58 (2013) 125–137. doi:10.1149/05802.0125ecst.

Scientific dissemination

PUBLICATIONS

1. F. Proietto, A. Galia, & O. Scialdone (2019). Electrochemical Conversion of CO_2 to HCOOH at Tin Cathode: Development of a Theoretical Model and Comparison with Experimental Results. ChemElectroChem, 6(1), 162-172.

2. F. Proietto, B. Schiavo, A. Galia, & O. Scialdone (2018). Electrochemical conversion of CO_2 to HCOOH at tin cathode in a pressurized undivided filter-press cell. Electrochimica Acta, 277, 30-40.

3. A.H. Ltaïef, S. Sabatino, F. Proietto, S. Ammar, A. Gadri, A. Galia, & O. Scialdone, (2018). Electrochemical treatment of aqueous solutions of organic pollutants by electro-Fenton with natural heterogeneous catalysts under pressure using Ti/IrO_2-Ta_2O_5 or BDD anodes. Chemosphere, 202, 111-118.

4. N. Klidi, F. Proietto, F. Vicari, A. Galia, S. Ammar, A. Gadri, & O. Scialdone, (2019). Electrochemical treatment of paper mill wastewater by electro-Fenton process. Journal of Electroanalytical Chemistry, 841, 166-171.

5. O. Scialdone, A. Galia, G. Lo Nero, F. Proietto, S. Sabatino, & B. Schiavo, (2016). Electrochemical reduction of carbon dioxide to formic acid at a tin cathode in divided and undivided cells: effect of carbon dioxide pressure and other operating parameters. Electrochimica Acta, 199, 332-341

SUBMITTED PAPER

1. F. Proietto, A. Galia, & O. Scialdone, (2019). Electrochemical conversion of CO_2 to CO at silver based cathodes: effect of pressure, supporting electrolyte and other operative parameters on the performances of the process.

2. S. Bhargava, F. Proietto, D. Azmoodeh, E. Cofell, D. Henckel, S. Verma, C. Brooks, A. Gewirth, & P. Kenis, (2019) System Design Rules for Intensifying the Electrochemical Reduction of CO_2 to CO on Ag Nanoparticles

COMMUNICATIONS

National

1. Electrochemical conversion of carbon dioxide in pressurized electrochemical cells. Onofrio Scialdone, Alessandro Galia, Federica Proietto; GEI2019 – Giornate dell'Elettrochimica Italiana, 09/2019, Padova, Italia - 09/2019

2. Electrochemical conversion of carbon dioxide to formic acid at Sn and BDD cathodes. Federica Proietto, Alessandro Galia, Onofrio Scialdone; GEI2019 – Giornate dell'Elettrochimica Italiana, Padova, Italia - 09/2019

3. Liquefazione idrotermica di fanghi di depurazione dalle acque reflue in presenza di acido formico come co-solvente. Claudia Prestigiacomo, Vito Armando Laudicina Federica Proietto, Alessandro Galia, Onofrio Scialdone; Convegno GRICU2019, Palermo-Mondello (PA), Italia – 07/2019

4. Electrochemical conversion of Carbon Dioxide to formic acid: on the road to applicative scale. Federica Proietto, Benedetto Schiavo, Alessandro Galia, Onofrio Scialdone; Winter GEI 2018- Giornate dell'Elettrochimica Italiane, Sestriere (TO), Italy - 01/2018

5. Premio di Laurea "Ametek Scientific Instruments": Electrochemical Conversion of Carbon Dioxide to Formic Acid. Study of the Effect of the Operating Parameters. Federica Proietto, Alessandro Galia, Onofrio Scialdone; XXVI Congresso Nazionale della Società Chimica Italiana, Centro Congressi Hotel Ariston, Paestum (SA), Italy - 09/2017

6. Electrochemical conversion of carbon dioxide: effect of the cell and of the operating parameters on the performances of the process. Federica Proietto, Simona Sabatino, Benedetto Schiavo, Alessandro Galia, Onofrio Scialdone; XXVI Congresso Nazionale della Società Chimica Italiana, Centro Congressi Hotel Ariston, Paestum (SA), Italy - 09/2017

7. Effect of Pressure on the Electrochemical Conversion of CO_2 to CO. Federica Proietto, Alessandro Galia, Onofrio Scialdone; XXVI Congresso Nazionale della Società Chimica Italiana, Centro Congressi Hotel Ariston, Paestum (SA), Italy - 09/2017

International

1. Effect of the air pressure on electro-Fenton process. Onofrio Scialdone, Alessandro Galia, Aziz Ltaïef, Federica Proietto, José Pérez, Manuel Andrés Rodrigo, Simona Sabatino; ISE 25th Topical Meeting, New electrochemical processes for energy and the environment, Toledo, Spain - 05/2019

2. Pressurized CO_2 Electrochemical Conversion to Formic Acid: From Theoretical Model to Experimental Results. Onofrio Scialdone, Alessandro Galia, Federica Proietto; ISE 25th Topical Meeting, New electrochemical processes for energy and the environment, Toledo, Spain - 05/2019

3. Intensifying the CO_2 Electrolysis Process. Saket Bhargava, Federica Proietto, Daniel Azmoodeh, Stephanie Chen, Danielle Henckel, Emiliana Cofell, Sumit Verma, Andrew A. Gewirth, Paul J. A. Kenis, John Pigos, Christopher Brooks; 235th ECS Meeting, Dallas, Texas USA - 05/2019

4. Electrochemical conversion of Carbon Dioxide: effect of operating parameters and of the reactor on the performances of the process. Federica Proietto, Simona Sabatino, Benedetto Schiavo, Alessandro Galia, Onofrio Scialdone; 10th World Congress of Chemical Engineering, Barcellona, Spain - 10/2017

5. Reduction of Carbon dioxide to formic acid in various kinds of electrochemical devices. Onofrio Scialdone, Simona Sabatino, Benedetto Schiavo, Adriana D'Angelo, Fabrizio Vicari Federica Proietto, Alessandro Galia; The 67rd Annual Meeting of the International Society of Electrochemistry, The Hague, Netherlands - 08/2016

6. Electrochemical reduction of carbon dioxide to formic acid at tin cathode in divided and undivided cells: Effect of operating parameters. O. Scialdone, A. Galia, F. Proietto, G. Lo Nero. S. Sabatino. The 66rd Annual Meeting of the International Society of Electrochemistry, 4-9 October 2015, Taipei, Taiwan

Acknowledgments

"They say the first sentence in any speech is always the hardest. Well, that one's behind me, anyway. But I have a feeling that the sentences to come – the third, the sixth, the tenth, and so on, up to the final line – will be just as hard since I'm supposed to talk about poetry." *Wislawa Szymborska - Nobel Lecture*, *December 7, 1996*.
She was so right. I think that whether it is talking about poetry or fashion style, science or other ordinary things, the first sentence is always the hardest.
Anyway, now I am far from it… few lines after… However, it is still difficult, not because I have no idea who exactly I would like to thanks… but because it is hard to put down in the paper some words which can explain how important have been a few people I have met during this wonderful Ph.D. experience. To be honest, these words will not be enough in any case.

At the beginning of the Ph.D., I read a social network's post where it was written: "Carefully choose your advisor before to get in a Ph.D. program!" … To date, I can understand these words! I was so lucky to be under the supervision of professor Onofrio Scialdone, known as Nuccio, and professor Alessandro Galia. Thanks to them, I had professional and personal growth due to their way to be. They shared with me their indisputable scientific knowledges and life experiences, being for me an example of generosity, humility, determination, love and passion for the science, and team working. Nuccio was always a leader, not a boss… even if invisible! His playfulness, passion for the research, empathy, our laughs and comical acts, his enormous as well as cutes "*Pipponi"* allowed me to go easily ahead through my Ph.D. thesis. I enjoyed Alessandro for his team spirit, his marvelous art of patience and meticulousness, his doggedness as well as our funny and lovely coffee breaks (*Vi va una dose di caffeina?! cit.*)!
I appreciated your trust, even if I was a clown most of the time! … "*Che crasta*!" (*A. Galia - Most of coffee-breaks*)

Friendship is the hardest thing in the world to explain and to talk about. It is not something you learn at school. During this experience, I had the possibility to meet Claudia… what can I say? I think a real friend is one who walks in when the rest of the world walks out… Thanks for getting in! Her patience, calm, silences, shyness, smiles, her "delay-time" make her a special need in my life! "*Tattiche*!" (*C. Prestigiacomo - Almost always*).

Elisa. She is braver than she believes, stronger than she seems, and smarter than she thinks. I would like to tell her that we don't have to be perfect for everyone, it is enough to be special for someone…Thanks for being special to me. She understands my past, believes

in my future and accepts myself just the way I am. She has just a huge defect... She loves Philosophy.

Averlo come amico un calore… Of course, my worst friend and best enemy… He has been an unexpected and indescribable discovery… when also the silence is comfortable, friendship is true.… a mix of powerfulness, loyalty, dependability, and loveliness... When he looks at me it seems he overlooks the broken fence and admires wonderful flowers in a garden.
Wavelengths make us unique. Thanks, thanks for being in my life.
"…Conforta il desiderio di rivederlo se lontano, di evocarlo per sentirlo vicino, quasi per udire la sua voce e continuare colloqui mai finiti." D. M. Tulordo.

Mom, thanks for being my mother, whatever it means…Thanks! Love you.

All of you have made my Ph.D. a wonderful experience.

Federica
November 10th, 2019